GROWTH INHIBITORY EFFECTS OF 3'-HYDROXYPTEROSTILBENE IN HUMAN PROSTATE CANCER CELLS AND XENOGRAFT MICE

By

HUI-YUN TSAI

A dissertation submitted to the

Graduate School-New Brunswick

Rutgers, The State University of New Jersey

In partial fulfillment of the requirements

For the degree of

Doctor of Philosophy

Graduate Program in Food Science

Written under the direction of

Dr. Chi-Tang Ho

And approved by

_____

_____

_____

_____

_____

New Brunswick, New Jersey

January, 2016

ABSTRACT OF THE DISSERTATION

Growth Inhibitory Effects of 3'-Hydroxypterostilbene in Human Prostate Cancer Cells and Xenograft Mice

by HUI-YUN TSAI

Dissertation Director:

Dr. Chi-Tang Ho

Prostate cancer is the second highest cause of cancer-related death among men in the United States. Most of these deaths are caused by invasive and metastatic spread of the prostate cancer. Therefore, more efforts should be dedicated to the development of preventive strategies to reduce prostate cancer prevalence and impact. Pterostilbene (Pt) is a natural antioxidant compound predominantly found in blueberries, grapes and a tree wood, *Pterocarpus marsupium*. 3'-Hydroxypterostilbene (OHPt), one of hydroxyl analogs of pterostilbene, can be isolated from whole plant of the herb *Sphaerophysa salsula*, a shrub widely distributed in central Asia and northwest China. The objective of this study was to investigate the growth inhibitory effects of 3'-hydroxypterostilbene on human

prostate cancer cells *in vitro* and *in vivo*. The results showed that OHPt significantly decreased cell viability of PC-3 and LNCaP cells in a dose- and time-dependent manner. However, OHPt showed much stronger inhibitory effects on the growth of the prostate cancer cells in comparison with its parent compound Pt, suggesting that addition of an OH group to the 3'-position of Pt ameliorated its anti-cancer cell proliferative activity. Next, we further elucidated the molecular mechanisms of anti-proliferation of human prostate cancer cells by OHPt. Treatment with OHPt induced apoptosis via disruption of mitochondrial membrane integrity and activation of caspase-8, caspase-9 and caspase-3 in both PC-3 and LNCaP cells. Moreover, OHPt increased the ratio of proapototic protein Bax to anti-apoptotic protein Bcl-xL. These findings suggested that OHPt had a strong growth inhibitory effect on PC-3 and LNCaP cells through induction of intrinsic and extrinsic apoptotic pathway. Besides, OHPt induced autophagic cell death by upregulating the expression of Beclin-1, LC3 proteins and autophagosome formation. Furthermore, *in vivo* study, OHPt showed potent anti-tumor effects in PC-3 xenograft nude mice. Treatment of mice with OHPt efficiently inhibited the tumor volume and tumor weight. Taken together, the findings of this research provide insights that OHPt might have significant chemotherapeutic applications for the future management of prostate cancer.

ACKNOWLEDGEMENTS

I would like to express my deepest gratitude towards my Ph.D. dissertation advisor, Dr. Chi-Tang Ho, for his guidance, support and continuous encouragement throughout my Ph.D. study at Rutgers University.

I am also grateful to my committee members, Dr. Tung-Ching Lee, Dr. Qingrong Huang, Dr. Qing-Li Wu, and Dr. Shiming Li, for offering many valuable suggestions and the help on this project. I thank Dr. Chi-Chen Lin and Dr. Min-Hsiung Pan for their help and suggestions for my research. My research could not have been completed without their generous help. I deeply appreciate Dr. Lucy Sun Hwang for her warm-hearted help on my career development and research work. Also thanks to my labmates and friends, Pei-Hsuan Hsieh, Tzu-Min Wang, Yen-Chen Tung, Wenping Wang, Siyu Wang, Siyu Liu, Wan Ling Chuang, Tsai-Wei Yang, Jenny Wu, who assist and support me whenever I need and make my life productive, enjoyable and happiness.

Most importantly, I would like to express my deep appreciation to my beloved families, my husband, Yu-Kuo Chen, and my son, Jeremy, for their continuous encouragement and support. Without their generous love, I could not have finished my research and had the opportunity for such a wonderful graduate life in the United States.

CONTENTS

LIST OF ILLUSTRATIONS

LIST OF TABLES

CHAPTER 1. INTRODUCTION

Prostate cancer is the most frequently diagnosed form of cancer and the second leading cause of cancer-related death among men in the United States (*1*). Despite the fact that prostate cancer is highly treatable in its early stage by hormones therapy, chemotherapy or radical prostatectomy, many patients present locally advanced or metastatic cancers, eventually leading to death (*2, 3*) Thus, the perspectives of developing more effective therapeutic agents that can cure localized and advanced metastatic prostate cancers are extremely necessary.

Two distinct programmed cell death (PCD) processes, apoptosis (‘self-killing’) and autophagy (‘self-eating’) play essential roles in the pathogenesis of carcinogenesis (*4-7*). Dysfunctional PCD leads to various diseases such as cancer, neurodegeneration, and aging. (*8, 9*). Apoptosis, type I PCD, is the most common form of PCD, naturally occurring process in the body. When the cells are superfluous, damaged or abnormal, they may need to be removed to ensure proper development (*10*). Autophagic cell death is second type of PCD which is a cellular lysosomal degradation pathway. During the induction of autophagy, targeted cytoplasmic constituents, misfolded proteins and damaged organelles are sequestered within the isolation membrane and eventually mature

into double-membraned vesicle, autophagosome. The autophagosome then fuses with lysosome to form autolysosome, and the dysfunctional constituents are digested and recycled (*11-13*). Cumulative examples in literature demonstrated that hyperactivation of autophagy lead the cancer cell death and might be a new and useful strategy for cancer treatment. (*14-16*).

Cancer chemoprevention is defined as the use of chemical agents to prevent, inhibit, reverse or retard carcinogenesis (*17*). Thus, based on the principles of cancer chemoprevention, using phytochemicals for inhibition of carcinogenesis will be beneficial for preventive strategy. Pterostilbene (trans-3,5-dimethoxy- 4'-hydroxystilbene), dimethylated analogue of resveratrol, is a stilbenoid phytochemical compound predominantly found in blueberries, grapes and a tree wood, *Pterocarpus marsupium* (*18-21*). The relationship between pterostilbene and the prevention of prostate cancer has been reported previously (*22-24*). A study conducted by Wang *et al.* demonstrated that treatment of human prostate cancer LNCaP cell with pterostilbene could inhibit cell viability and induce cell cycle arrest at G1/S phase (*22*). Besides, Chakraborty *et al.* indicated that pterostilbene induced apoptosis via upregulation of cellular ROS, caspase-3 and the ratio of Bax to Bcl-2 protein in PC-3 human prostate cancer cells (*23*). Moreover, pterostilbene inhibited the proliferation of prostate cancer cell through activation of

AMPK activity and suppression of lipogenesis by decreasing the expression of fatty acid synthase and acetyl-CoA carboxylase (*24*).

3'-Hydroxypterostilbene (trans-3,5-dimethoxy-3',4'-dihydroxystilbene), one of hydroxyl structural analogs of pterostilbene, which can be isolated from whole plant of the herb *Sphaerophysa salsula*, a shrub widely distributed in central Asia and northwest China (*20, 25*). From chemical structure point of view, the difference between 3'-hydroxypterostilbene and pterostilbene is that 3'-hydroxypterostilbene contains a catechol group at B-phenyl ring, while pterostilbene contains a phenol group. Multiple catechol-related compounds have been reported to have anti-cancer activities (*26, 27*). However, there is a paucity of published studies involving biological activities of 3'-hydroxypterostilbene so far. In a study conducted by Tolomeo *et al.* reported that 3'-hydroxypterostilbene induced apoptosis in sensitive and resistant leukemia cells (*25*). Recently, 3'-hydroxypterostilbene was demonstrated to have anti-proliferation effect on human colon cancer cells (*28*). However, to our knowledge, the anti-carcinogenic effects of 3'-hydroxypterostilbene on human prostate cancer remain unknown.

The aims of this study are (i) to evaluate the chemotherapeutic effect of 3'-hydroxypterostilbene against LNCaP and PC-3 human prostate cancer cells and to further investigate the cell death molecular mechanisms induced by OHPt. (ii) To further

evaluate the anti-tumor effect of OHPt *in vivo* by using PC-3 xenograft nude mice model.

CHAPTER 2. LITERATURE REVIEW

2.1 Prostate Cancer

Prostate cancer is the most common malignancy in males in the United State. The American Cancer Society (ACS) estimates that 241,740 men will be diagnosed with prostate cancer, and 28,170 men will die from prostate cancer in 2012 (*29*). Therefore, more efforts should be dedicated to the development of preventive strategies to reduce prostate cancer prevalence and impact.

2.1.1 TNM staging of prostate cancer

The TMN classification system is widely used for staging prostate cancer which is maintained by the American Joint Committee on Cancer (AJCC) and International Union for Cancer Control (IUCC) (*30-32*). Determining the stage of prostate cancer is important for selecting the most appropriate treatment for patients. The TNM classification system divides prostate cancer into three main categories: T categories (primary tumor), N categories (nodes), and M categories (metastasis) (*30, 31*). T categories refer to the size

and the extent of the primary tumor within prostate gland; N categories describe whether the cancer has spread to the nearby the lymph nodes (regional); and M categories describe whether the cancer has metastasized to the distant parts of the body (*30*). The TMN classification of prostate cancer is shown as Table 1. After determining the T, N, and M categories, this information is usually combined with the Gleason score (based on prostate biopsy) and prostate-specific antigen (PSA) level to predict the overall stage of the prostate cancer (*33*-*35*).

Table 1. TNM classification of prostate cancer (*30*)

Primary Tumor (T)	
T0	No evidence of primary tumor.
T1	Clinically unapparent tumor, neither palpable nor visible by imaging.
T2	Palpable or visible carcinoma confined to the prostate gland.
T3	The tumor extends through the prostate capsule and may have grown into seminal vesicles.
T4	The tumor has grown into adjacent structures other than seminal vesicles, such as bladder, rectum, the wall of pelvis.
Regional Lymph Nodes (N)	
N0	The tumor has not spread to the nearby lymph nodes.
N1	The tumor has not spread to the regional lymph nodes of pelvis.
Distant metastasis (M)	
M0	No distance metastasis.
M1	The tumor has metastasized into other sites of the body.

2.1.2 Androgen and the Progression of Prostate Cancer

Androgen plays an important role in the development of normal prostate epithelial cells, but are also involved the pathogenesis of prostate cancer (*36*, *37*). The early-stage prostate cancer relies on androgens for growth, differentiation and survival, which is called “androgen-dependent” or “androgen-sensitive” prostate cancer. Current therapy used for prostate cancer is primarily based on androgen deprivation (*3, 38*). The aim of androgen deprivation therapies is lower the androgen levels which are able to inhibit the prostate cancer cells proliferation and prevent them from progressing into advanced prostate cancer (*39*, *40*). However, if the prostate cancers are not cured by hormone therapy, chemotherapy or surgery, finally become highly aggressive androgen independent cancers. These cells do not depend on androgen for growth and survival which render the effective androgen deprivation therapy useless (*3, 39*). Such cancer is clinically defined as hormone refractory prostate cancer (*3*). The development of hormone refractory prostate cancer may due to the missense mutations in androgen receptor gene that lower the specificity of ligand binding and inappropriately activated by several non-androgen steroids, androgen antagonists and peptide growth factors such as corticosteroids, flutamide and insulin-like growth factor-1 (IGF-1) (*3, 40*). Moreover, the overexpression of oncoprotein Bcl-2 and the mutations of p53 tumor suppressor gene are

commonly found in hormone-refractory prostate cancer, indicating that these alterations may be involved in the progression of prostate cancer to advanced androgen-independent state (*40-42*). Once the prostate cancer progress into hormone refractory prostate cancer, the advanced cancer cells will highly metastasize into other tissues or organs, eventually leading to deaths (*37*). Thus, the perspectives of developing more effective therapeutic agents that can cure localized and advanced metastatic prostate cancers are extremely necessary.

2.1.3. Cell and Animal Models in Prostate Cancer Research

LNCaP and PC-3 cell lines are commonly used for prostate cancer studies. LNCaP cell line is androgen-dependent, p53 wild type human prostate cancer cell, derived from lymph node metastasis of prostatic adenocarcinoma from a 50-year-old Caucasian male in 1977 (*43-45*); PC-3 cell line is androgen-independent, p53 null type, advanced human prostate adenocarcinoma cell line, derived from bone metastasis in a 62-year-old Caucasian male in 1979 (*45, 46*). Besides, PC-3 cells have high metastatic potential compared to LNCaP cells which have low metastatic potential (*46, 47*). These cells provide useful and convenient tools for screening anti-prostate cancer therapeutic agents and also can be used to investigate the biochemical changes and molecular mechanisms

in prostate cancer cells (*24, 45, 46*). Moreover, they can be used in prostate xenograft models to create subcutaneous tumors in athymic nude mice in order to study the biology of prostate cancer, tumor progression and the molecular mechanisms *in vivo* (*46, 48*).

2.2 Programmed Cell Death (PCD)

Programmed cell death is an important physiological process required for the normal development and maintenance of tissue homeostasis, such as delete unneeded structures, adjust the number of cells and eliminate abnormal, misplaced, useless or harmful cells (*49*). Two distinct programmed cell death processes, apoptosis ('self-killing') and autophagy ('self-eating') play essential roles in the pathogenesis of carcinogenesis (*4-7*). These two forms of PCD can jointly decide the fate of cancer cells (*50, 51*). Thus, understanding the molecular pathways and regulatory mechanisms underlying these cellular processes may be crucial in cancer therapies.

2.3 Apoptosis

Apoptosis is the most common form of PCD, naturally occurring process in the body. When the cells are superfluous, damaged or abnormal, they may need to be removed to ensure proper development. One way to remove these cells without causing damage to

other cells is through apoptosis (*52*). Aberrant regulation of the apoptosis can lead to either abnormal cell accumulation or improper cell loss, which results in various diseases, including cancer, autoimmune diseases, ischemia and neurodegenerative disorders (*53, 54*).

2.3.1 Morphological Features of Apoptosis

Apoptotic cells can be characterized by morphological appearance changes include the cell shrinkage, cytoplasm condensed, chromatin condensation (pyknosis), nuclear fragmentation (karyorrhexis), and plasma membrane blebbing which lead to apoptotic bodies formation (*10, 49, 53, 55*). Biochemical changes associated with apoptosis include oligonucleosomal DNA fragments, phosphatidylserine externalization, mitochondrial outer membrane permeabilization, activation of the effector caspases and a number of intracellular substrate proteolytic cleavages (*52, 55, 56*). These morphological manifestations and biochemical changes contribute to detect apoptosis easily.

The apoptotic bodies consisting of cytoplasm with the condensed chromatin and organelles are fragmented into compact membrane-enclosed structures during the processes of blebbing or budding. These bodies are subsequently engulfed by phagocytic cells and degraded within phagolysosomes without triggering inflammatory response (*16,*

27). No inflammation reaction associated with apoptosis because of the intact membrane of apoptotic bodies isolate the cellular constituents which prevent it from releasing into surrounding tissue to cause damage (*10, 52, 57*) (Figure 1). Apoptosis is different from the necrotic cell death in which case the cells suffer a significant damage, resulting in a loss of membrane integrity, swelling and rupture of the cells. The loss of the membrane integrity results in the release of the cytoplasmic contents uncontrolled into the surrounding tissue, sending chemotactic signals which subsequently recruit inflammatory cells and cause strong inflammatory response (*10, 50, 52*) (Figure 1).

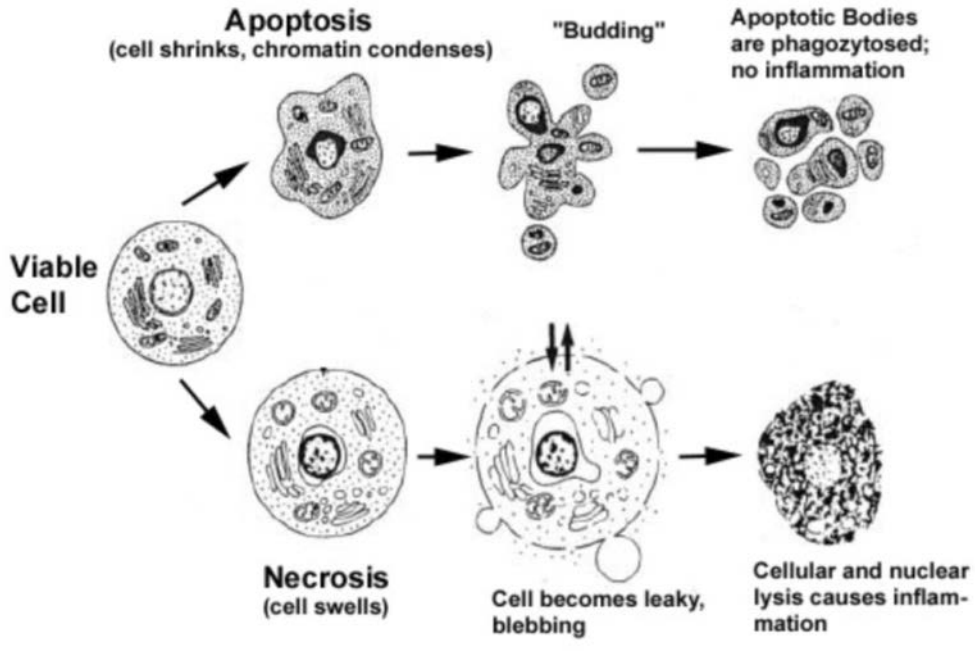

Figure 1. Hallmarks of the apoptotic and necrotic cell death process (*10*).

2.3.2. Molecular Mechanisms of Apoptosis Signaling Pathways

Apoptosis is the most important form of cell death and its molecular signaling pathway has been well-studied. Research indicates that there are two mainly apoptotic signaling pathways, which are known as the intrinsic and extrinsic pathways (*8*).

The intrinsic pathway also called mitochondrial apoptotic pathway. Most apoptotic stimuli transmit death signals to the mitochondria and increase the mitochondrial outer membrane permeabilization (MOMP), which leads to the release of apoptogenic proteins, such as cytochrome c, Smac/DIABLO and Omi/HtrA2, into the cytoplasm from the mitochondria (*58, 59*). After its release, cytochrome c binds with apoptotic protease activating factor-1 (Apaf-1) and procaspase-9, forming a death inducing protein platform called apoptosome, which in turn activates the caspase 3 to execute apoptotic cell death (*60, 61*). Smac and Omi promote apoptosis by inhibiting X-linked inhibitor of apoptosis protein (XIAP) that function as endogenous caspase inhibitors (*62, 63*). Mitochondrial outer membrane permeability is primarily controlled through interactions between pro-and anti-apoptotic members of Bcl-2 family (*63*). The anti-apoptotic members include Bcl-2, Bcl-xL and Mcl-1 which are typically overexpressed in tumor tissues. The pro-apoptotic group is divided in multi-domain proteins (Bax and Bak) and the BH3-only proteins (Bim, Bid, Bad, Bik, Bmf, Puma and Noxa) which have only the BH3 domain in

common (*10, 64*). In a non-apoptotic cell, the pro-apoptotic proteins are neutralized and sequestered by the anti-apoptotic Bcl-2 family members (*10*). In response to an apoptosis stimulus, activated BH3-only proteins disrupt the multi-domain pro-apoptotic proteins (Bax and Bak) antagonism by anti-apoptotic Bcl-2 members, allowing them to be activated via oligomerization. Moreover, Bax and Bak oligomers insert into mitochondrial outer membrane which provoke membrane permeabilization and release of apoptogenic proteins (i.e., cytochrome c) into cytosol that commits to apoptotic cell death (*65, 66*) (Figure 2). Besides, the tumor suppressor protein p53 can induce Bax and Bak oligomerization and antagonize the Bcl-2 and Bcl-xL anti-apoptotic effect, resulting in disruption of mitochondrial membranes and subsequent release apoptogenic factors to cause apoptosis (*67*).

The extrinsic apoptotic pathway is mediated by the activation of death receptors belonging to the tumor necrosis factor-α receptor (TNF-R) family, such as FAS/CD95, TNFR and TRAIL, directly activates caspase-8 (*68, 69*). Once caspase-8 is activated, the execution phase of apoptosis is triggered that activates downstream caspases, such as caspase-3 or caspase-7, which leads to apoptotic cell death (*70*). Besides this direct route to death through caspase-8 and caspase-3, there is another detour towards mitochondria to promote the cell death signal. An additional target of caspase-8 is BH3-only protein

Bid and after cleavage of Bid, the product of which truncated Bid (tBid) directly translocates to the outer mitochondrial membrane and activate mitochondrial (intrinsic) apoptotic cell death (*71*, *72*).

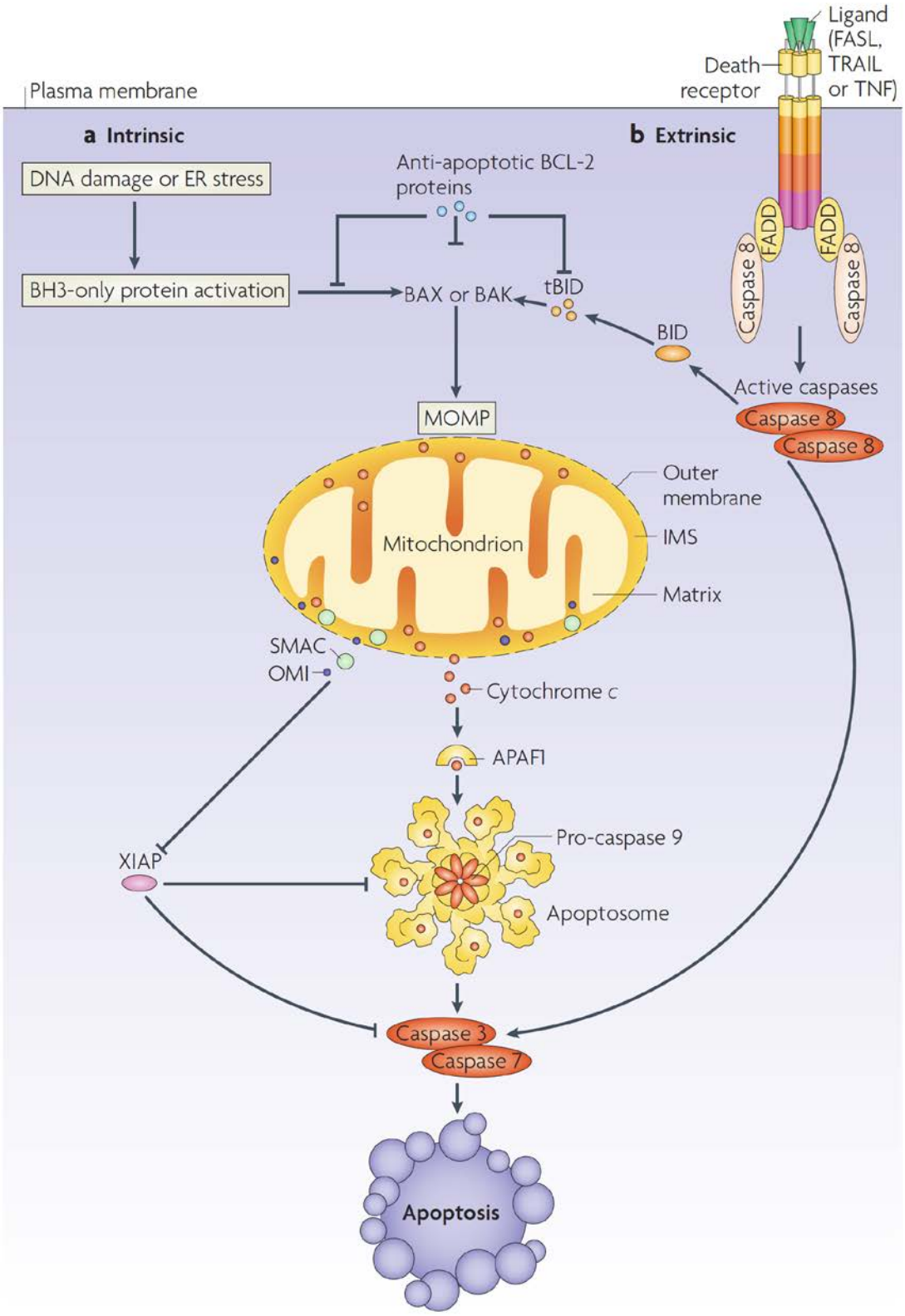

Figure 2. Intrinsic and extrinsic pathways of apoptosis (*63*)

2.4 Autophagy

Autophagy is the process of self-eating, which has essential roles in cellular basal homeostasis, development and survival. Recently, its roles in human health and disease has become widespread (*73*). Autophagy is the basis catabolic mechanism that facilitates the degradation and recycling of unnecessary or dysfunctional cellular components through the actions of lysosomes (*8, 12, 74*) . It is accelerated by various cellular stressors such as nutrient depletion, ATP shortage, DNA damage, and organelle damage (*8*). This self-digestion not only provides nutrients to promote cellular survival during starvation but also can degrade the superfluous or misfolded proteins, damaged organelles, and invasive microbes (*73*). Although autophagy is the mainly protective process for the cell, it can also play a role in cell death. Autophagic dysfunction is involved in many diseases such as cancer, neurodegeneration, microbial infection and ageing (*75*). Interestingly, self-digestion by autophagy which is induced by starvation is now emerging as a crucial biological pathway to promote health (*8, 11, 12*).

2.4.1 Molecular Mechanisms of Autophagic Pathway

Autophagy is a cellular lysosomal degradation pathway shown in figure 3. During the induction of autophagy, targeted cytoplasmic constituents, misfolded proteins and

damaged organelles are sequestered within the isolation membrane called phagophore (*73*). The expanding phagophore eventually mature into double-membraned vesicle known as autophagosome. The autophagosome then fuses with lysosome to form autolysosome, and its cargo is digested and recycled (*11-13*).

One of the key regulators of autophagy is the target of mammalian (mechanistic) target of rapamycin complex 1 (mTORC1), which is the major inhibitory signal that suppress autophagy (*73*). The mTORC1 consists of mTOR, the regulatory-associated protein of mTOR (Raptor), DEP-domain containing mTOR-interacting protein (Deptor), G-protein beta-subunit-like protein (GβL), and proline-rich AKT substrate 40 kDa (PRAS40), which in turn negatively regulates the ULK protein kinase complex, consisting of Unc-51-like kinases 1/2 (ULK1/2) Atg13, and focal adhesion kinase family interacting protein of 200 kDa (FIP200) (*76-78*). Inhibition of mTORC1 strongly induces autophagy by regulating the activity of the ULK protein kinase complex that is required for the initiate generation of isolated membrane (phagophore) (*79*). Class I phosphatidylinositol-3-kinase (PI3K)-Akt activates mTORC1 in response to insulin-like and other growth factor signaling, acting as a negative regulator of autophagy (*80*) Besides, Class I PI3K-Akt can negatively regulate autophagy by suppressing Beclin 1–associated Vps34 activity (*81*)

Class III phosphatidylinositol 3-kinase (PI3K) is also needed to regulate autophagy, which is a component of a multi-protein complex that includes Beclin1(Atg6), Atg14, Vps34, and Vps15. Stimulation of this complex generates phosphatidylinositol-3-phosphate (PI3P), which promotes the initiation of phagophore (*82*). The autophagy capability of the Class III PI3K complex is activated by UVRAG, Ambra-1, and Bif-1 and inhibited by Rubicon, Bcl-2 and Bcl-xL (*83*).

Subsequent elongation and closure of isolated membrane are mediated by two ubiquitin-like conjugation systems, Atg5–Atg12 system and the microtubule-associated protein 1 light chain 3 (LC3, Atg8) system (*84, 85*). The first conjugation system, ubiquitin-like protein Atg12 is conjugated to Atg5 that requires Atg7 (E1-like) and Atg10 (E2-like) enzymes (*86*). The Atg5–Atg12 conjugate then interact with Atg16 to form a large complex, which involved in the elongation of the autophagic membrane (*87, 88*). A second conjugation system requires the ubiquitin-like protein LC3. LC3 is cleaved by protease Atg4 to generate the cytosolic LC3-I form. LC3-I is subsequently conjugated to phosphatidylethanolamine (PE) at the C-terminal glycine residue which is required Atg7 (E1-like) and Atg3 (E2-like) enzymes (*89, 90*). The PE-conjugated form of LC3 (LC3-II) is attached to the autophagosomal membrane and forms autophagosome (*90*). Finally, the autophagosome fuses with lysosome in which the cytosolic cargo is breakdown and

degraded (*91*).

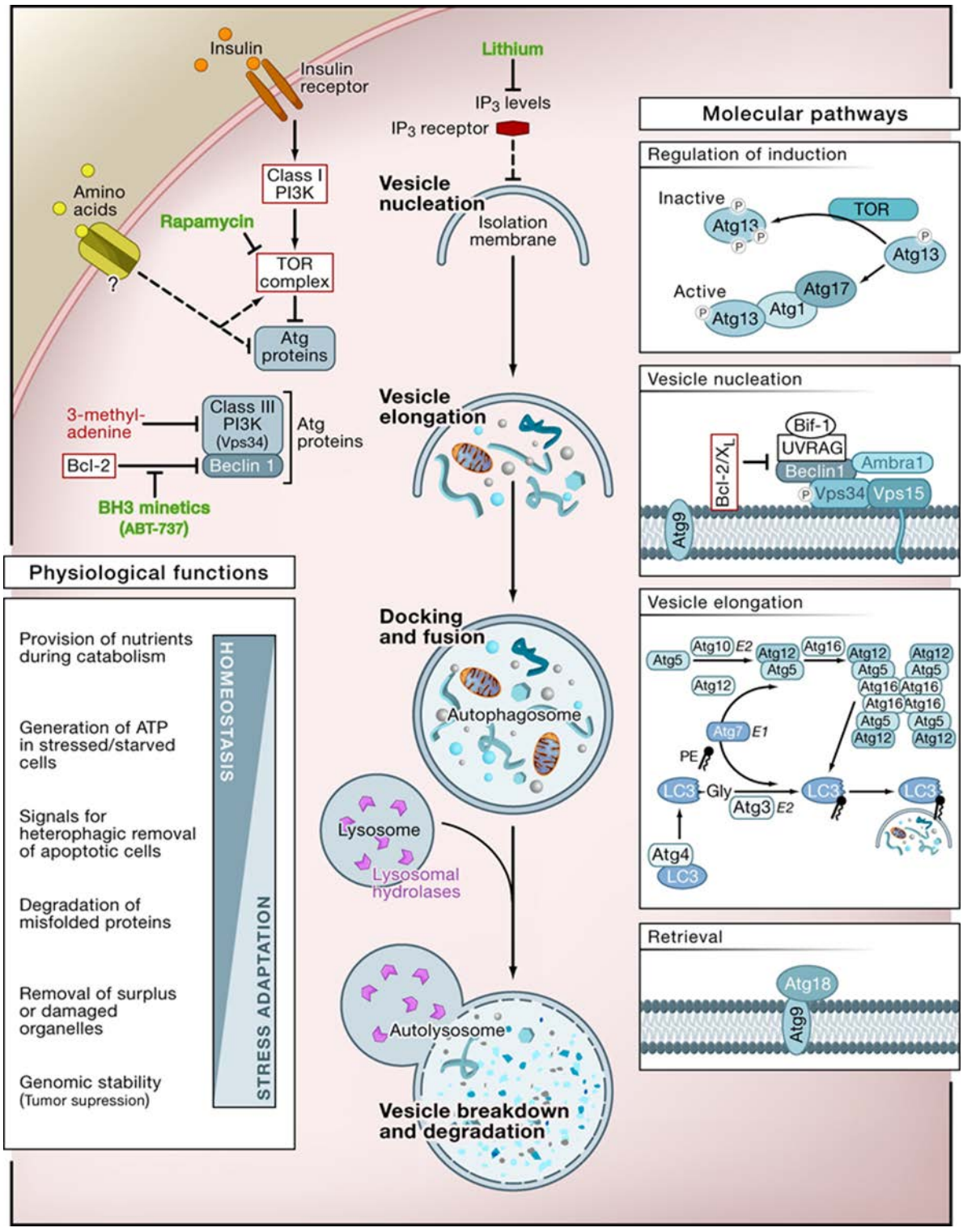

Figure 3. Regulation of the autophagic pathway (*73*)

2.5 Crosstalk between Apoptosis and Autophagy

In recent years, the continuously growing number of researchers dedicated to work on the crosstalk between apoptosis and autophagy. Some key proteins which are initially thought to be anti-apoptotic proteins are newly found to regulate autophagy. Similarly, some autophagy-related proteins are now discovered that they are also involved in apoptosis. These new evidences suggested that apoptosis and autophagy share certain signaling pathways and proteins, communicating with each other to determine cell fate. (*92-96*). However, the extensive crosstalk between apoptosis and autophagy are extremely complex, the mechanisms by which interaction occur have not yet been fully understood. To date, some key molecular are clearly demonstrated that play essential roles in linking together between apoptosis and autophagy, such as Bcl-2 family proteins, Beclin-1, Atg5 and p53. (*95, 97, 98*).

2.5.1 Bcl-2 Family Proteins

Bcl-2 family proteins are key regulators of mitochondrial apoptotic pathway that have also been identified to regulate autophagy (Figure 4) (*51, 95, 96*). The pro-apoptotic proteins, Bax and Bak, play an important role in inducing mitochondrial outer membrane permeabilization (MOMP), increasing the release of cytochrome c and subsequently

activate the apoptotic caspase cascades (*58, 63, 96, 99*). The anti-apoptotic Bcl-2 family proteins, Bcl-2, Bcl-xL and Mcl-1, can antagonize pro-apoptotic proteins (Bax and Bak) and inhibit the activator BH3-only protein (Bid, Puma and Bim), thus prevent apoptosis (*58, 63, 96, 99*). Moreover, recent studies indicated that the anti-apoptotic Bcl-2 family proteins can also inhibit autophagic function by interacting with Beclin-1 which can sequester Beclin-1 from binding to Vps34 (*96, 100*). Thus, the dual function of anti-apoptotic proteins, Bcl-2 and Bcl-xL, in inhibiting both apoptosis and autophagy makes them as ideal targets for chemotherapy.

2.5.2 Beclin-1

Beclin-1 is an important initiator of autophagy during the autophagosome nucleation and cleavage of Beclin-1 is another regulatory mechanism involved in apoptosis (Figure 4) (*97*). The apoptotic caspases can cleave the Beclin-1 into fragment which fails to induce autophagy. However, the cleavage product of Beclin-1, C-terminal of Beclin-1 fragment (Beclin-1-C) can translocate into mitochondrial membrane and increase the mitochondrial membrane permeability to cause apoptosis (*96-98, 100*). Moreover, Wirawan *et al*. (2010) reported that recombining Beclin-1-C protein into isolated mitochondria from murine were able to release pro-apoptotic factors such as HtrA2/Omi

and cytochrome c (*101*). These findings demonstrated that caspase-mediated cleavage of Beclin-1 creates an amplifying loop that can enhance apoptotic cell death. In contrast, full-length Beclin-1 can induce autophagy which can counteract apoptosis by mediating the autophagic degradation of caspase 8 (*98*). Therefore, Beclin-1 is able to participate in both autophagy and apoptosis depending on the appearance of full length or cleaved form.

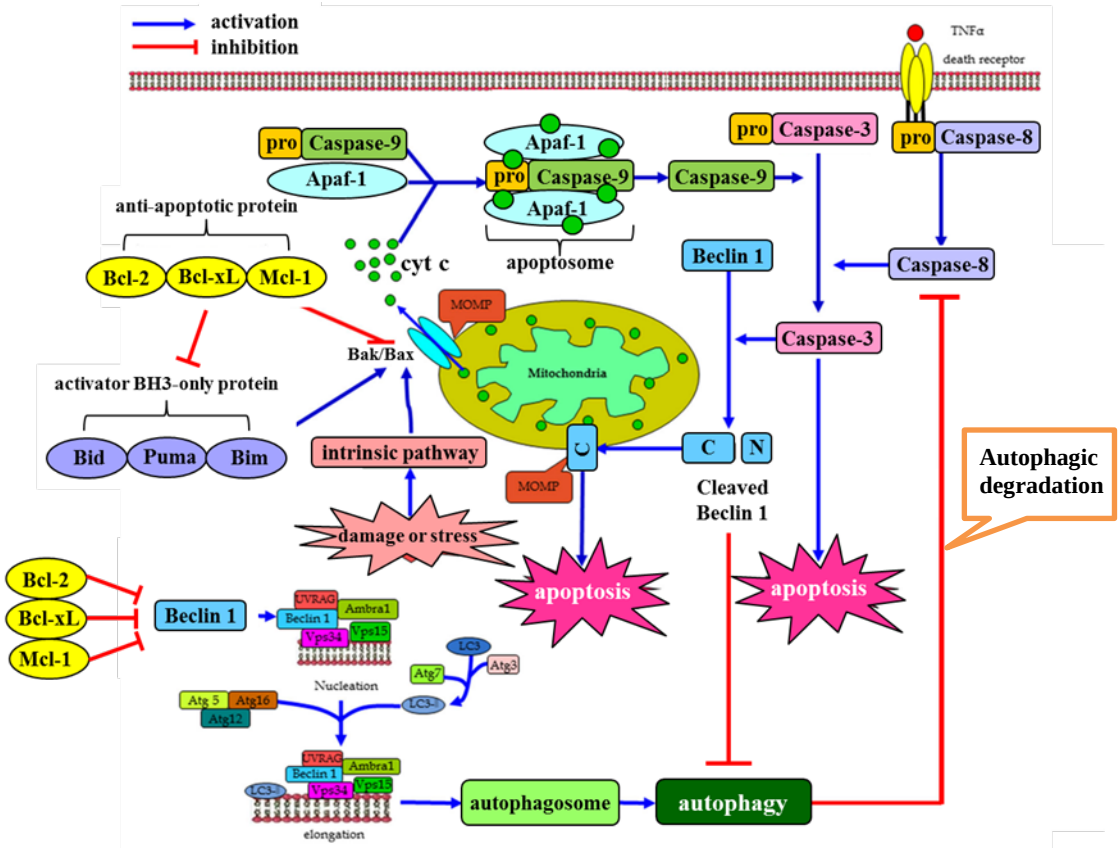

Figure 4. The crosstalk between autophagy and apoptosis is through Bcl-2 family proteins and Beclin 1 network (*96*).

2.5.3 Atg5

Atg5 plays critical role in autophagy during the elongation of autophagosomes (*102*). In addition to regulating autophagy, recent studies demonstrated that the cleavage form of Atg5 is an important regulator of apoptosis (*96, 102, 103*). When the full-length Atg5 is cleaved by calcium-dependent calpain 1 and calpain 2 into its 24-kDa truncated form, the proautophagic functions of Atg5 is failed; however, the truncated Atg5 can translocate from cytosol into the mitochondria, associate with the anti-apoptotic protein Bcl-xL, antagonize Bcl-xL anti-apoptotic effect and induce apoptotic cell death by releasing cytochrome c and activating caspases (*92, 95, 97, 103*). Thus, similar to that of Beclin-1, calpain-mediated Atg5 cleavage may also amplify the apoptotic cell death (*92, 97*). Taken together, Atg5 represents a key molecular in linking together between autophagy and apoptosis.

2.5.4 p53

The tumor suppressor p53 regulates the expression of genes involved in apoptosis and autophagy (Figure 5) (*104*). p53 gene mutation is one of the most common genetic instabilities occurring in human cancer (*105*). When cells are exposed to DNA damage, oncogenic stress, nucleotide depletion or other cellular stress, activation of p53 will lead

to apoptosis through both transcription-independent and -dependent pathways (*67, 96, 104*). In the cytoplasm, p53 mediates transcriptional-independent oncosuppressing function which directly induces pro-apoptotic proteins Bax and Bak oligomerization at mitochondria to cause mitochondrial outer membrane permeabilization and release cytochrome c into cytosol that triggers apoptosis (*96, 106*). In the nucleaus, active p53 functions as transcription factor, which can bind to the promoter regions of the target genes and induce the expression of pro-apoptotic members, such as Bax, Bak, PUMA, and Noxa. Activation of the pro-apoptotic members leads to apoptotic cell death and antagonizes the Bcl-2 and Bcl-xL anti-apoptotic effect (*104, 106*). Besides, nuclear p53 elevates the expression of PUMA can displace cytoplasmic p53 from the Bcl-xL, thereby allowing cytoplasmic p53 directly activate Bax and cause mitochondria membrane permeabilization to execute apoptosis (*107*).

Furthermore, p53 has recently been found to regulate autophagy in dual role, which can induce or repress autophagy depending on its subcellular localization (Figure 5) (*96, 106, 108*). Generally, in the absence of stress signals, the basal levels of p53 present in the cytoplasm to inhibit autophagy, but translocate to the nucleus to induce autophagy in response to DNA damage or genotoxic stress (*109-111*). In the cytoplasm, cytosolic p53 inhibits autophagy by downregulating the autophagy protein FIP200, thereby obstructing

the activation of the ULK1 complex (comprising ULK1/2–Atg13–FIP200–Atg101), ultimately suppressing autophagosome formation (*109, 112*). In the nucleus, p53 promotes autophagy through transcription-dependent and transcription-independent mechanisms. Nuclear p53 induce autophagy by transcriptionally upregulating several autophagy-related genes, including sestrins 1 and 2, DRAM (damage-regulated autophagy modulator) and ULK1 (*96, 106, 109*). Moreover, nuclear p53 can directly activate AMPK (AMP-activated protein kinase) by transcription-independent function, which in turn activates the tuberous sclerosis complex (TSC) proteins TSC1 and TSC2, thus downregulating the negative regulator of autophagy mTOR and facilitating autophagy (*96, 106*). Taken together, the localization of p53 is the key regulator of p53-induced apoptosis and autophagy. On the one hand, nuclear p53 functions as transcription factor which induces cellular autophagy and apoptosis. On the other hand, cytoplasmic p53 induces apoptosis and represses autophagy.

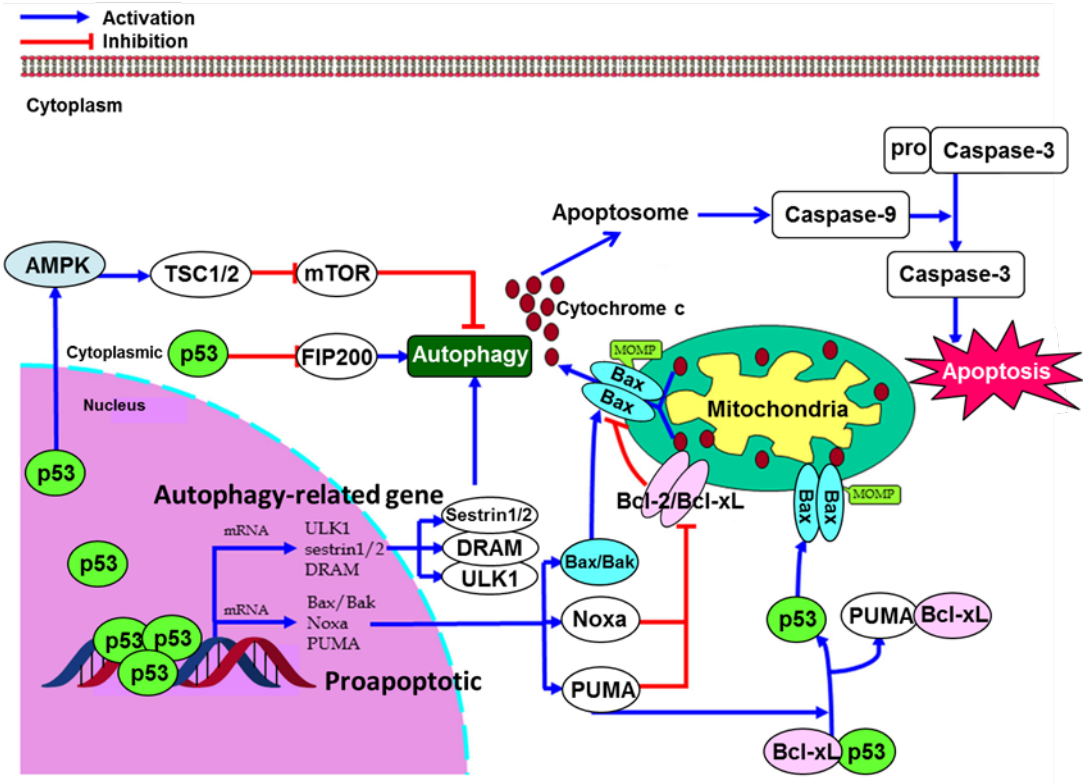

Figure 5. p53 modulated both autophagy and apoptosis (*96*).

2.6 Pterostilbene

Pterostilbene (trans-3,5-dimethoxy-4'-hydroxystilbene) (Figure 6 (B)), natural dimethylated analogue of resveratrol (3,5,4'-trihydroxy-trans-stilbene) (Figure. 6 (A)), is a stilbenoid phytochemical compound primarily found in blueberries, grapes and a tree wood, *Pterocarpus marsupium* (*18-21*). Pterostilbene content varies from different type of berries. *Vaccinium ashei* (rabbiteye blueberry) contains 99 ng/g dry sample while *Vaccinium stamineum* (deerberry) contains 560 ng/g dry sample (*113, 114*).

(A)

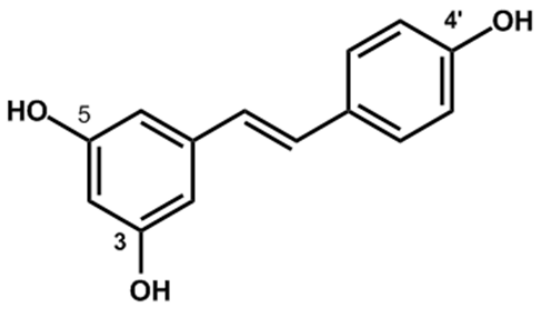

Resveratrol

(B)

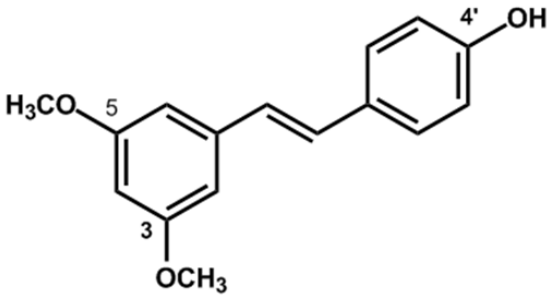

Pterostilbene

Figure 6. Chemical structures of resveratrol and pterostilbene (Pt).

2.6.1 Biological Actions of Pterostilbene

Substantial studies demonstrate that pterostilbene have diverse pharmacological activities for the prevention and treatment of diseases including cancer, inflammation, diabetes, dyslipidemia and cardiovascular disease (*21*, *115-120*). In a study conducted by Hsu *et al*. showed that pterostilbene exhibited strong inflammatory inhibitory effects in

3T3-L1 adipocytes and RAW264.7 macrophages coculture. The results of this study showed that pterostilbene inhibited IL-6 and TNF-α secretion and proinflammatory mRNA expression including COX-2, iNOS, MCP-1 and PAI-1, and also decreased the migratory ability of macrophages toward adipocytes (*121*). Moreover, pterostilbene has been reported to have powerful growth inhibitory effects on different types of cancer cell lines, including bladder cancer, breast cancer, colon cancer, leukemia, liver cancer, lung, cancer, melanoma, pancreas cancer, prostate cancer and stomach cancer (Table 2) (*24, 122-130*). In these researches, pterostilbene was shown to be an effective apoptotic and autophagic agent on various cancer cell lines which are able to inhibit cancer cell viability, induce cell cycle arrest, alter apoptosis expression gene, promote autophagy-related proteins and inhibit cancer cells metastasize (Table 2) (*24, 122-130*).

Table 2. Pterostilbene and cancer-related studies

Cancer Cell Type	Pterostilbene-induced Growth Inhibitory Mechanisms on Cancer Cells			Reference
	Apoptosis	Autophagy	Anti-metastasis	
Bladder	√	√		Wang *et al*., 2010
Breast			√	Pan *et al*., 2011
	√	√		Wang *et al*., 2012
		√		Chakraborty *et al*., 2012
Colon	√			Nutakul *et al*., 2011
	√	√		Pan *et al*., 2014
Leukemia	√			Tolomeo *et al*, 2005
Liver	√		√	Pan *et al*., 2009
	√			Remsberg *et al*., 2008
Lung	√			Schneider *et al*., 2010
Melanoma	√			Schneider *et al*., 2009
Pancreas	√			McCormack *et al*., 2011
Prostate	√			Wang *et al*., 2010
	√		√	Chakraborty *et al*., 2010
	√			Lin *et al*., 2012
Stomach	√			Pan *et al*., 2007

In breast cancer, Chakraborty *et al*. found that pterostilbene induced cytotoxic effects by generating reactive oxygen species (ROS) in MCF-7 breast cancer cells (*23*). Treated MCF-7 cells with pterostilbene could trigger apoptosis via increasing the levels of caspase-3 and apoptotic protein Bax, and decreasing the anti-apoptotic protein Bcl-2 levels and mitochondrial membrane potential (*23*). In 2012, the same research group further demonstrated that pterostilbene caused autophagy by upregulating the expression of autophagy-related proteins, Beclin-1 and LC3 II in MCF-7 cells (*131*). Furthermore, Wang *et al*. also indicated that pterostilbene could simultaneously stimulate apoptosis, cell cycle arrest, and autophagy in MCF-7 and Bcap-37 cells (*123*).

In prostate cancer researches, Wang *et al.* reported that treatment of p53 wild type human prostate cancer LNCaP cell with 25 μM pterostilbene could inhibit cell viability and induce cell cycle arrest at G1/S phase by increasing the cyclin-depedent kinase inhibitor CDNK1A and CDNK1B (*22*). Furthermore, pterostilbene treatment had strong inhibitory effect on prostate-specific antigen (PSA) expression. Besides, Chakraborty *et al.* treated p53 null type human prostate cancer PC-3 cell with pterostilbene and found that pterostilbene induced apoptosis by increasing the cellular ROS, caspase-3 and apoptotic protein Bax and decreasing anti-apoptotic protein Bcl-2 (*23*). Pterostilbene also inhibited matrix metalloproteinase 9 (MMP9) and α -methylacyl-CoA recemase

(AMACR), two notable metastasis activators. Other study conducted by Lin *et al.* (2012) indicated the same results as previous studies. Pterostilbene treatment induced differential effects in p53 positive and negative human prostate cancer cell which could upregulate cell cycle arrest at G1 phase in LNCaP cells, while caused the PC-3 cells undergo apoptosis (*24*). Moreover, Lin *et al.* discovered that pterostilbene inhibited prostate cancer cell growth and proliferation through activation of AMPK activity and suppression of lipogenesis by decreasing the expression of fatty acid synthase and acetyl-CoA carboxylase (*24*).

Table 3. The anticarcinogenic mechanisms of pterostilbene against prostate cancer.

	Cell Type	Mechanism	Reference
Pterostilbene	LNCaP (p53 wild type)	**G1 phase arrest** **− Caspase-3** ↑ CDNK1A ↑ CDNK1B (cyclin-depedent kinase inhibitor)	Wang *et al*., 2010
Pterostilbene	PC-3 (p53 null type)	**Apoptosis** ↑ Caspase-3 ↑ Bax ↓ Bcl-2 ↑ ROS generation ↓ MMP ↑ AMCAR	Chakraborty *et al*., 2010
Pterostilbene	LNCaP (p53 wild type)	**G1 phase arrest** ↑ p53 ↑ p21 ↑ AMPK ↓ Fatty acid synthase ↓ Acetyl CoA carboxylase	Lin *et al*., 2012
	PC-3 (p53 null type)	**Apoptosis** ↑ Caspase-3 ↑ Caspase-9 ↑ AMPK ↓ Fatty acid synthase ↓ Acetyl CoA carboxylase	

In colon cancer, the anticarcinogenic effects of pterostilbene have been demonstrated in human colon cancer COLO205, HCT-116 and HT-29 cells and COLO205 xenograft tumors (*28*). Pterostilbene induced apoptosis by down regulating mammalian target of rapamycin (mTOR), phosphatidylinositol 3-kinase (PI3K)/Akt and mitogen-activated protein kinases (MAPKs) signaling pathways. Besides, pterostilbene also caused autophagy via increasing the production of Beclin-1 and LC3 II in human colorectal carcinoma COLO 205 cells (*28*). Moreover, *in vivo* experiments, treatment with pterostilbene was able to inhibit colorectal aberrant crypt foci and colon carcinogenesis via suppressing the inflammatory signal transduction pathway (*118*). Other research group indicates that pterostilbene decreased mucosal levels of the proinflammatory cytokines, tumor necrosis factor-α, interleukin (IL)-1β and IL-4 and inhibited colon tumorigenesis by regulating the Wnt/β-catenin-signaling pathway and inflammatory responses in rats (*117*).

Regarding to antidiabetic activity, pterostilbene was demonstrated to have cytoprotective effects on pancreatic beta-cells, as it was found to eliminate oxidative stress by mediating the Nrf2 downstream target genes expression including heme oxygenase 1 (HO1), superoxide dismutase (SOD), catalase (CAT), and glutathione peroxidase (GPx) (*132*). Also, pterostilbene increased the expression of anti-apoptotic

protein, Bcl-2 and down-regulated the pro-apoptotic Bax and caspase-3 expression, which protects pancreatic beta-cells from apoptosis in diabetes (*132*). Additionally, pterostilbene significantly lower blood glucose and glycosylated hemoglobin concentration in diabetic rats (*120*). Treatment with pterostilbene significantly increased the expression of glycolysis enzyme, hexokinase, and decreased the expression of gluconeogenesis enzyme, glucose-6-phosphatase and fructose-1,6-bisphosphatase, which regulates glucose homeostasis (*120*). Recently, Gómez-Zorita *et al*. demonstrated that pterostilbene improves glycaemic control *(133)*. In this study, pterostilbene was shown to decrease insulin resistance index (HOMA-IR) and increase GLUT4 protein expression, phosphorylated-Akt/total Akt ratio, cardiotrophin-1, and glucokinase activity in insulin resistance rats induced by obesogenic diet (*133*).

Finally, pterostilbene possess significant hypolipidemic activity. Satheesh and Pari indicated that pterostilbene could effectively modify the dyslipidemia, as it can decrease low density lipoprotein cholesterol (LDL-C) and very low density lipoprotein cholesterol (VLDL-C) and increase the high density lipoprotein cholesterol (HDL-C) in streptozotocin-nicotinamide induced diabetic rats (*134*). Besides, pterostilbene significantly reduced the levels of serum and tissue triglycerides, free fatty acids and phospholipids (*134*). Moreover, Gómez-Zorita *et al*. evaluated the hypolipidemic effects

of pterostilbene in wistar rats which were fed commercial obesogenic diet with or without pterostilbene for 6 weeks (*135*). The findings of this study showed that pterostilbene significantly reduced total adipose tissue weights including perirenal, mesenteric and subcutaneous fat mass. The activities of lipogenic enzymes, malic enzyme (ME), fatty acid synthase (FAS), acetyl-CoA carboxylase (ACC) were significantly reduced in white adipose tissue. The glucose-6-phosphate dehydrogenase (G6PDH) and malic enzyme (ME) involved in liver lipogenesis were also reduced. Moreover, the activities of fatty acid oxidation enzymes, carnitine palmitoyltransferase 1a (CPT-1a) and acyl-CoA oxidase, were markedly increased in liver. Thus, the proposed mechanisms for reducing body fat by pterostilbene are reduction of lipogenesis in adipose tissue and liver and induction of fatty acid oxidation in liver. Furthermore, a recent study performed by Rimando *et al*. provided insight that pterostilbene acts as a peroxisome proliferator activated receptor α (PPARα) ligand, which regulates fatty acid *β*-oxidation (*136*). Pterostilbene markedly increased PPARα gene expression in a dose dependent manner in H4IIEC3 rat hepatoma cells. Moreover, the activation of PPARα gene expression of pterostilbene at 10 μmol/L was greater than that of fenofibrate at 100 and 200 μmol/L, which is a clinical drug used to treat high cholesterol levels (*136*).

2.6.2 Bioavailability of Pterostilbene

Pterostilbene shares many pharmacological similarities with resveratrol such as antioxidant, anti-inflammation and anti-cancer activity; however, pterostilbene exhibits much better bioavailability and more biologically active than resveratrol (*115, 118, 124, 137-140*). Based on the chemical structure, pterostilbene could possess better bioavailability as it contains two methoxy groups and one hydroxyl group while resveratrol has three hydroxyl groups. The two methoxy groups cause pterostilbene to have relatively higher lipophilicity, which may enhance the cell membrane permeability and increase oral absorption (*21*). One study conducted by Nutakul *et al*. indicated that the amount of intracellular pterostilbene were 2-4 folds higher than those of resveratrol following treatments of each compound at the same concentration (*141*). In the same study, pterostilbene showed much stronger anti-proliferation and apoptotic effects than those of resveratrol. Moreover, Chiou *et al.* demonstrated that pterostilbene was more potent than resveratrol in preventing colon tumorigenesis via activation of the NF-E2-related factor 2 (Nrf2)-mediated antioxidant signaling pathway (*140*). Other research group indicated that pterostilbene was more effective than resveratrol as an anti-inflammatory agent for inhibition of colon carcinogenesis in HT-29 human adenocarcinoma cell line (*124*). Thus, The biological activities of pterostilbene were

usually found to be more potent than resveratrol may due to its higher bioavailability. Moreover, in a pharmacokinetic study, pterostilbene was shown to have 80% oral bioavailability compared to only 20% for resveratrol, making it as an ideal chemotherapeutic compound (*137*).

2.7 3'-Hydroxypterostilbene

3'-Hydroxypterostilbene (trans-3,5-dimethoxy-3',4'-dihydroxystilbene) (Figure 7), one of hydroxyl structural analogs of pterostilbene, can be isolated from whole plant of the herb *Sphaerophysa salsula*, a shrub widely distributed in central Asia and northwest China (*142*). The physicochemical properties of 3’-hydroxypterostilbene are colorless and needle-shaped crystals (*20, 143*). There is a paucity of published studies involving biological activities of 3’-hydroxypterostilbene so far.

In a study conducted by Tolomeo *et al.* reported that 3'-hydroxypterostilbene exerted cytotoxicity in five different human leukemia cell lines which included HL60, K562, HUT78, HL60-R and K562-ADR, but showed low toxicity in normal hemopoietic stem cells (*25*). The proposed mechanism of anti-proliferation potential of 3'-hydroxypterostilbene in leukemia cells was due to intrinsic apoptotic cell death by disrupting mitochondrial membrane potential (*25*). Recently, 3'-hydroxypterostilbene was

demonstrated to have anti-proliferation effect in human COLO 205, HCT-116 and HT-29 colon cancer cells (*28*). The results of the study showed that 3'-hydroxypterostilbene induced apoptosis and autophagy by increasing the activities of caspase-3, -8 and -9 and inhibiting mTOR/p70S6K, PI3K/Akt and MAPKs signaling pathways. In the same study, further experiments were conducted to evaluate anti-tumor effect of 3'-hydroxypterostilbene *in vivo* using COLO 205 xenograft nude mice model. The findings suggested that 3'-hydroxypterostilbene significantly inhibited the tumor volume and tumor weight via down-regulating the protein expressions of cyclooxygenase (COX-2), matrix metallopeptidase-9 (MMP-9), vascular endothelial growth factor (VEGF) and cyclin D1. Moreover, the anti-cancer effects of 3'-hydroxypterostilbene were more potent than that of pterostilbene in human colon cancer cells and xenograft nude mice (*28*).

In addition, the other study conducted by Takemoto and Davies focused on pharmacokinetics characterization of 3'-hydroxypterostilbene in rats. Following intravenous administration of 3'-hydroxypterostilbene, the pharmacokinetic parameter, mean half-life ($t_{1/2}$), in serum was ~0.45 h and in urine was ~1.02 h and the mainly form excreted in urine is the 3'-hydroxypterostilbene glucuronide (*143*).

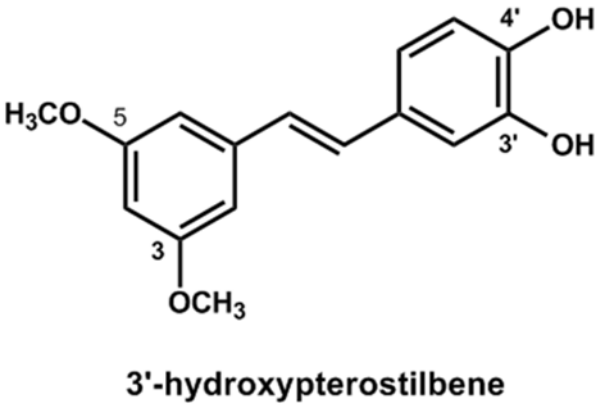

Figure 7. Chemical structure of 3'-hydroxypterostilbene (OHPt).

CHAPTER 3. HYPOTHESIS AND RESEARCH OBJECTIVES

3.1 Hypothesis

Numerous evidences in literature demonstrated that pterostilbene could possess growth inhibitory effects on human prostate cancer cells. However, there is a paucity of published studies involving in its hydroxyl analog, 3’-hydroxypterostilbene, and there are no previous studies that have examined 3’-hydroxypterostilbene on the effect of human prostate cancer cells. Thus, in this study, we are highly interested in 3’-hydroxypterostilbene. From the chemical structure point of view, the difference between 3'-hydroxypterostilbene and pterostilbene is that 3'-hydroxypterostilbene contains a catechol group, while pterostilbene contains a phenol group. Multiple catechol and phenol based compounds have been reported to have antioxidant and anti-cancer activities. Moreover, the analogs of trans-resveratrol containing catechol group had significantly higher apoptotic activities than those of the other analogs containing phenol. Based on these previous findings, we are wondering whether 3’-hydroxypterostilbene containing catechol group has anti-prostate cancer activity or has better biological activity than pterostilbene. Therefore, we hypothesize that 3’-hydroxypterostilbene has capability to inhibit human prostate cancer cell growth and

even has more potent anti-prostate cancer activity than pterostilbene.

3.2 Research Objectives

(1) The objective of the present study is to examine the cell growth inhibitory effects of 3'-hydroxypterostilbene and pterostilbene on PC-3 and LNCaP human prostate cancer cells. Additionally, to further investigate molecular mechanisms of the anti-prostate cancer cell growth by 3'-hydroxypterostilbene, including cell cycle distribution, apoptotic cell death and autophagic cell death mechanisms.

(2) To further evaluate the anti-tumor effect of 3'-hydroxypterostilbene *in vivo* by using xenograft nude mice model. Basically, PC-3 human prostate cancer cells will be transplanted into nude mice, and the mice will be treated with various dosages of 3'-hydroxypterostilbene. Determination of tumor volume and tumor weight will be performed to evaluate the anti-tumor activity of 3'-hydroxypterostilbene *in vivo*.

CHAPTER 4. EXPERIMENTAL DESIGN

4.1 Human Prostate Cancer Cell Lines PC-3 Experiment

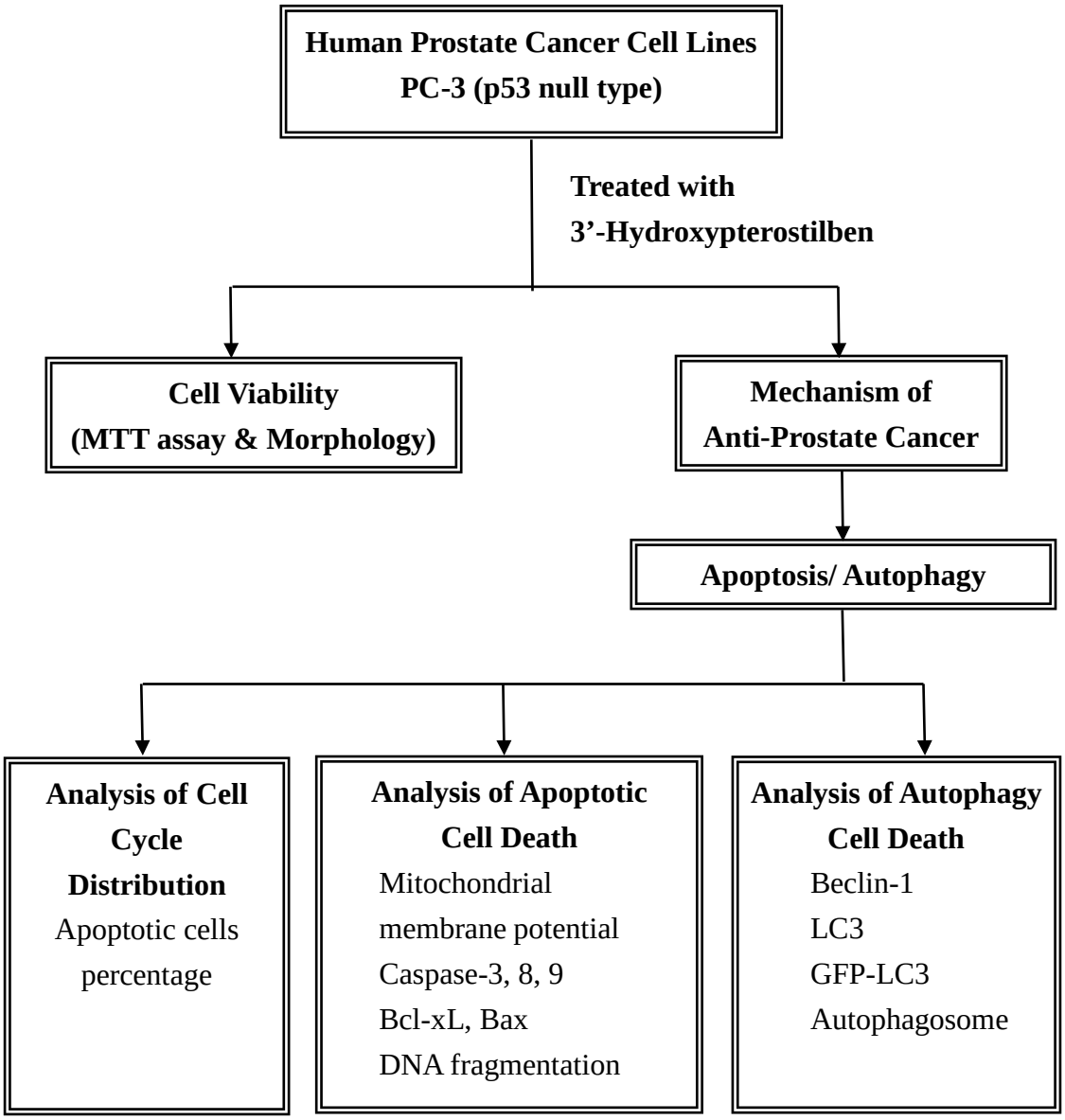

4.2 Human Prostate Cancer Cell Lines LNCaP Experiment

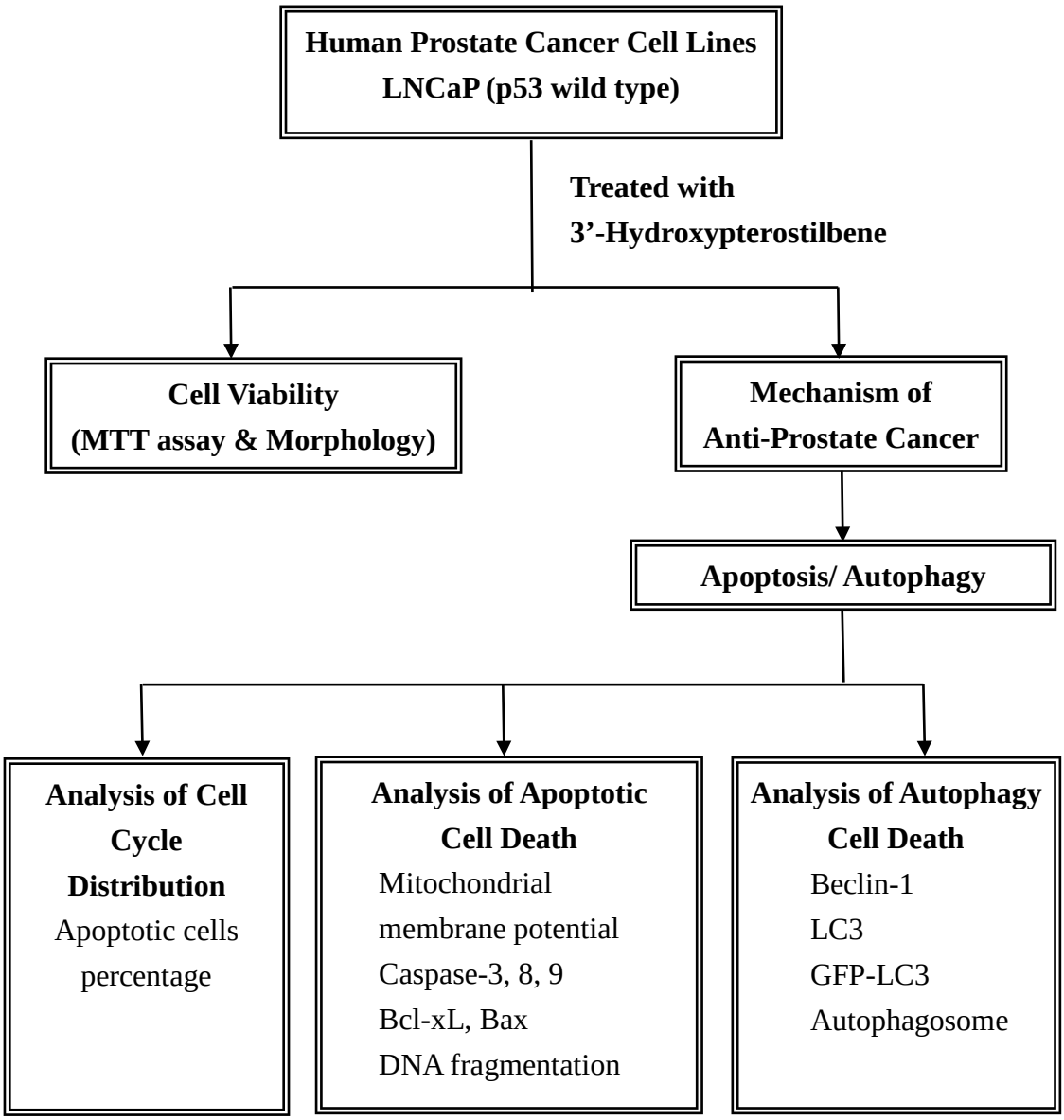

4.3 PC-3 Xenograft Nude Mice Model

4.3.1 Human Prostate Cancer PC-3 Cells Inoculation

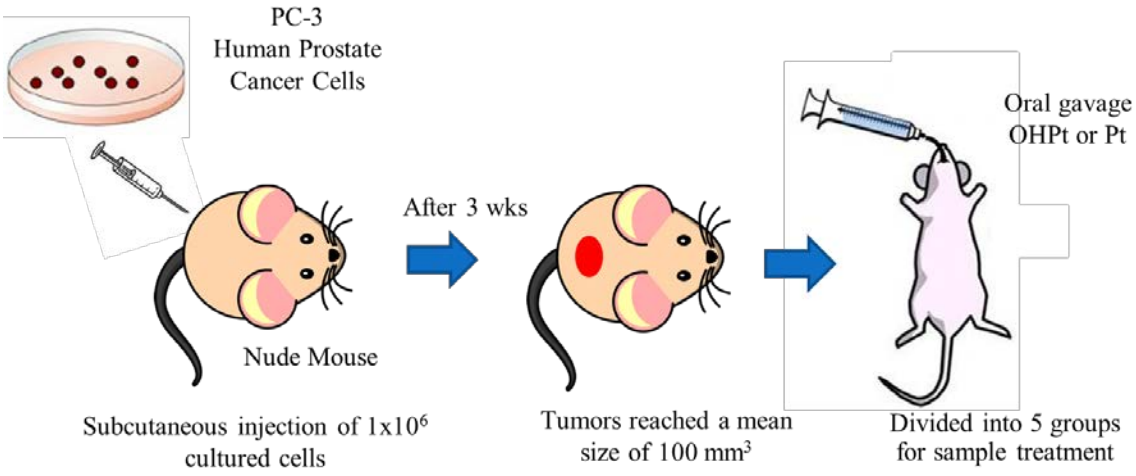

4.3.2 Study Design

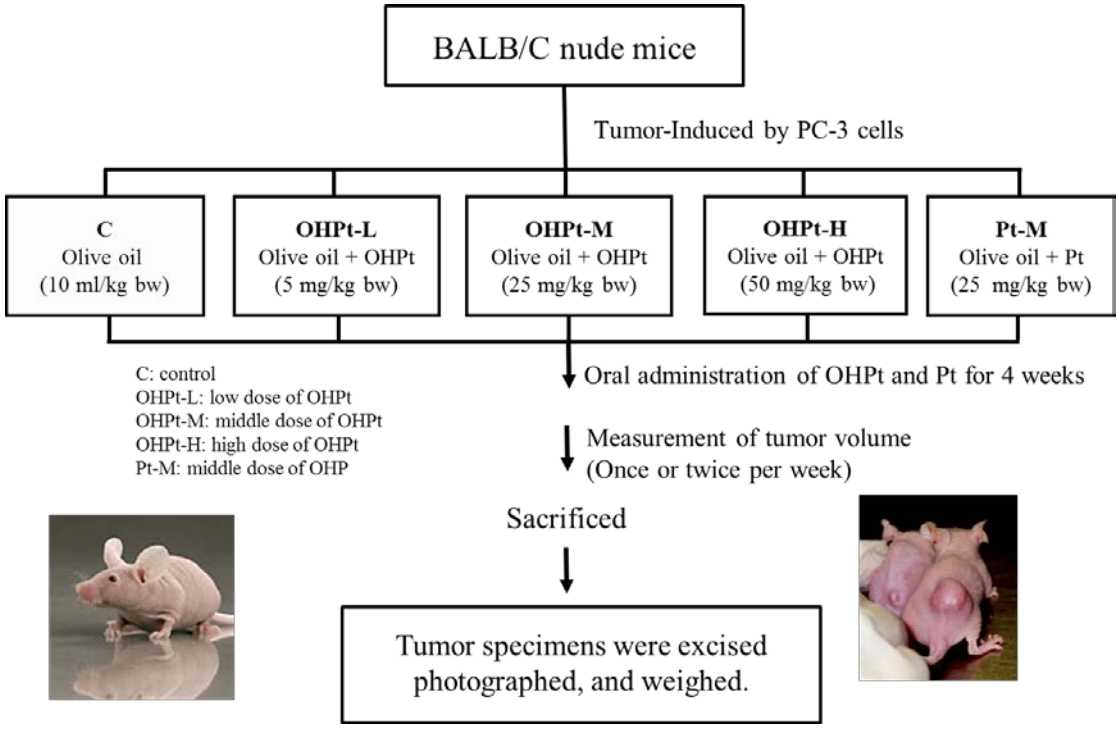

CHAPTER 5. MATERIALS AND METHODS

5.1 PC-3 and LNCaP Experiments

5.1.1 Materials and Chemicals

RPMI-1640, fetal bovine serum (FBS), penicillin−streptomycin, and 40,6-diamidino-2-phenylindole (DAPI) were purchased from Gibco (Grand Island, NY). Ethanol (95%) was purchased from EchoChemical (Taipei, Taiwan). A QIAamp DNA Mini Kit was purchased from Qiagen (Hilden, Germany). 3-(4,5-Dimethylthiazol-2-yl)-2,5-diphenyltetrazolium bromide (MTT), dimethyl sulfoxide (DMSO), trypsin-ethylenediaminetetraacetic acid (EDTA) sodiumdodecylsulfate (SDS), propidiumiodide (PI), and all other chemicals were obtained from Sigma Chemical Co. (St. Louis, MO). CaspGLOW™ Fluorescein Staining Kit for Caspase-3, -8, and -9 were purchased from eBioscience (San Diego, CA). Coomassie (Bradford) Protein Assay Kit was purchased from Thermo Scientific (Rockford. IL). 3,3'-Dihexyloxacarbocyanine Iodide was obtained from Life Technologies (Grand Island, NY). Pterostilbene and 3’-hydroxypterostilbene was provided by the Sabinsa Corporation® (Piscataway, NJ, USA)

5.1.2 Cell Culture

Human prostate cells, and PC-3 (p53 null type) and LNCaP (p53 wild type) cell lines, were grown in RPMI-1640 media supplemented with 10% FBS and 1% penicillin−streptomycin at 37°C in a humidified atmosphere of 5% CO_2. Upon reaching 70 to 80% confluence in full medium, cells were subcultured at 1:4 or higher ratio using 1 mL of trypsin-EDTA solution and were fed fresh growth medium.

5.1.3 Cell Viability Assay

PC-3 and LNCaP cells were seeded at a density of 5×10^3 cells/100 μL RPMI/well in 96-well plates. After incubated for 24 h to allow the cells to adhere to the bottom of the culture plate, the medium was replaced by 100 μL of serum-free RPMI containing different concentrations of OHPt of Pt for 24, 48, or 72 h of treatment, each in triplicate. The OHPt and Pt samples were dissolved in DMSO, and the final ratio of DMSO in the medium was 0.2%. At the end of the treatment, the medium was discarded, and 25 μL of MTT solution and 100 μL of serum free RPMI were added to each well and then incubated at 37°C for 4 h. Subsequently, MTT-containing medium were removed and 100 μL of DMSO was added to each well to dissolve the formazan converted from tetrazolium salt. Then, the absorbance at 570 nm was measured using an enzyme linked

immunosorbent assay plate reader (Anthos 2001, Salzburg). Inhibition of cell viability was represented as a percentage of growth of DMSO-treated cells (control), and the concentration of sample required to inhibit 50% of cell growth (IC_{50}) was determined by interpolation from the dose response.

5.1.4 Cell Morphology Observation

PC-3 cells and LNCaP (3×10^5 cells /well) were seeded in 6-well plates for 24 h and then incubated with various concentrations of OHPt at 37°C, 5% CO_2, and 95% air for 48 h. The shrinkage and floating of the cells were examined and photographed by phase-contrast microscopy for the examination of morphological changes.

5.1.5 Cell Cycle Distribution Assay

Cell cycle distribution was analyzed by FACScan flow cytometer (Becton Dickinson, San Jose, CA) with ModFit LT Ver. 2.0 (Verity Software House, Topsham,ME). Briefly, PC-3 and LNCaP cells (3×10^5 cells /well) were plated on a 6-well plate and treated with various concentrations of OHPt (2.5, 5, 10, and 20 μM) for 48 h. The cells were then harvested by trypsinization, washed with ice-cold phosphate-buffered saline (PBS), and gently fixed in 70% ice-cold ethanol at -20°C for at least 24 h. The cells were then

collected by centrifugation and resuspended in PBS containing 40 μg/mL propidium iodide (PI), 0.1 mg/mL RNase A, and 0.1% TritonX-100 in a dark room at room temperature for 30 min. Subsequently, cells were filtered before they were analyzed with FACScan flow cytometer, and the results were analyzed by ModFit LT Ver. 3.0 software. The proportion of sub-G1 hypodiploid cells was quantitated and represented as a percentage of apoptotic cells.

5.1.6 DNA Fragmentation Assay

PC-3 and LNCaP cells were treated with OHPt at different concentrations (2.5, 5, 10, and 20 μM). Two days after treatment, adherent cells were harvested by trypsinization and were washed with cold PBS and pelleted by centrifugation. DNA was extracted from cell pellets using QIAamp DNA mini kit, and then, the DNA fragmentation pattern was analyzed by electrophoresis in a 2% agarose gel at 50 V. The agarose gel was stained with ethidium bromide (1 μg/mL) and photographed after electrophoresis.

5.1.7 Caspase-3, 8, 9 Activities Determination

PC-3 and LNCaP cells (3×10^5 cells /well) were seeded in 6-well plates. After 24 h, cells were treated with various concentrations of OHPt and 10 μM of Pt for another 48 h.

The cells were then harvested by trypsinization, washed with ice-cold PBS and incubated with caspase-3, -8, or -9 kit for 30 minutes in a 37°C incubator with 5% CO_2. After incubation, centrifuge cells at 3000 rpm for 5 min and remove supernatant, and then wash cells with 0.5 mL of wash buffer provided from the kit and repeat the wash procedure twice. The activities of caspase-3, -8, and -9 were evaluated by flow cytometry.

5.1.8 Mitochondrial Membrane Potential Determination

The mitochondrial membrane potential ($\triangle\Psi$) was measured by flow cytometry after staining the cells with the cationic lipophilic fluorochrome $DiOC_6$. PC-3 cells and LNCaP (3×10^5 cells /well) were treated with various concentrations of sample for 48 h, and the cells were incubated at 37°C for 30 min in the presence of $DiOC_6$ (40 nM). The analysis of fluorochrome incorporation was performed using a Becton Dickinson flow cytometer.

5.1.9 Western blot

PC-3 and LNCaP cells (1×10^6 cells) were seeded in 10 cm dishes. After 24 h, cells were treated with 10 μM OHPt at different time intervals 0, 3, 6, 12, 24, 48 h. The cells were harvested by trypsinization, washed with PBS and then added the lysis buffer (10% glycerol, 1% Triton X-100, 1 mM PMSF, 10 μg/mL leupeptin, 1 mM sodium

orthovanadate, 1 mM EGTA, 10 mM NaF, 1 mM sodium pyrophosphate, 100 mM β-glycerophosphate, 20 mM Tris-HCl, 137 mM NaCl, 5 mM EDTA, 0.1% sodium dodecyl sulfate and 10 μg/mL aprotinin, and adjunct pH to 7.9). To take the suspension solution after the cell lysates were centrifuged, and using the Bio-Rad protein assay kit (Bio-Red Laboratories) to determine the protein content. Taken 25 μg proteins to resolve by SDS-PAGE, and transferred to PVDF membrane (polyvinylidene Fluoride Transfer Membrane) (BioTrace, UK.). Membrane blocked by blocking buffer (non-fat milk (5%), NaN_3 (0.2%) and Tween 20 (0.2%, v/v) in TBS). Then the PVDF membrane was incubated with primary antibodies Bax, Bcl-xL, Beclin-1 and LC3 followed by incubation with horseradish peroxidase-conjugated goat anti-mouse antibody (1:2500 dilution, Roche Applied Science, Indianapolis, IN). Reactive bands were visualized with an enhanced chemiluminescence system (Amersham Biosciences, Arlington Heights, IL). The intensity of the bands was scanned and quantified with Image J software.

5.1.10 GFP-LC3 Plasmid Transfection

PC-3 and LNCaP cells (3×10^5 cells/well) were seeded on the slide in 6-well plates. After incubated for 24 h to allow the cells to adhere on the slide, cells were transfected with GFP-LC3 plasmid using a Lipofectamine 2000 transfection reagent for 24 h and

then treated with or without OHPt for 18 h. The cells on the slide were then fixed with 4% formaldehyde for 30 min and then washed twice in PBS. Cell nuclei were stained with DAPI. All samples were imaged using a Leica SP5 confocal laser-scanning microscope.

5.1.11 Statistical analysis

All experiments were performed in triplicate and presented as means ± standard deviations (SDs). Statistical analyses were performed using one-way analysis of variance and Duncan's multiple comparison tests (SAS Institute Inc., Cary, NC) to determine significant differences among means ($P < 0.05$).

5.2 PC-3 Xenograft Nude Mice Model

5.2.1 Animals and Study Design

Male Balb/c nude mice weighing 16-18 g (3~4 weeks old) were obtained from the BioLASCO Experimental Animal Center (BioLASCO, Taipei, Taiwan). All animals were kept in pathogen-free sterile environment and in an air-conditioned room (25 ± 1 ˚C at 50-70% relative humidity) with a 12-hour light/12 hour dark cycle according to institutional guidelines. Animals were fed with standard laboratory rodent diet 5001 and

all food, water, cages, cage tops, water bottles and bedding were sterilized before use. Animals were given ad libitum access to food and water at all times. All animal experimental protocol was conducted and approved by Institutional Animal Care and Use Committee of the National Pingtung University of Science and Technology. After 1 week of acclimation, 1×10^6 PC-3 cells were injected subcutaneously into the dorsal flank of each mouse. After transplantation, tumor dimensions were measured using calipers, and tumor volume (mm^3) was calculated by following ellipsoidal mathematical formula: Volume = $(\text{shortest diameter})^2 \times (\text{longest diameter}) \times 0.52$. When xenografted tumor volume reached around 100 mm^3, mice were randomly divided into five groups. Each group consisted of 6 animals. Mice were orally administrated with daily doses of 3'-hydroxypterostilbene (5, 25 and 50 mg/kg/d) and pterostilbene (25 mg/kg/d) for 4 weeks; while control group was orally administrated with olive oil only. During the experiment, the tumor volume was determined and recorded once or twice per week using caliper measurements. At the end of the experiment, animals were sacrificed by CO_2 asphyxiation and the individual organs (liver, lung, kidneys and spleen) and solid tumors were excised immediately and weighed.

5.2.2 Statistical Analysis

Data were presented as means ± standard deviations (SDs). Statistical analyses were performed using one-way analysis of variance and Student's t test to determine significant differences between two groups. p value < 0.05 was considered to be statistically significant.

CHAPTER 6. RESULTS

6.1 Human Prostate Cancer PC-3 Cell Line Experiment

Pterostilbene is well known for its anti-cancer effects in human prostate cancer cells (*22-24*). In this study, we are highly interested in its hydroxyl structural analogue, 3'-hydroxypterostilbene, on prostate cancer treatment. Our preliminary MTT results showed that Pt and OHPt treatments significantly decreased cell viability of PC-3 human prostate cancer cells in a dose-dependent manner. After 48 h treatment, the IC_{50} of Pt and OHPt for PC-3 cells are >20 μM and 5 μM, respectively (Figure 8 and Table 4). OHPt showed much stronger inhibitory effects on the growth of the prostate cancer cells in comparison with its parent compound Pt. This result suggested that the extra hydroxyl group at 3’-position of Pt showed a better anti-cancer property. Therefore, in the following part of the experiment, we further elucidate the molecular mechanisms of anti-proliferation of prostate cancer cells induced by 3'-hydroxypterostilbene.

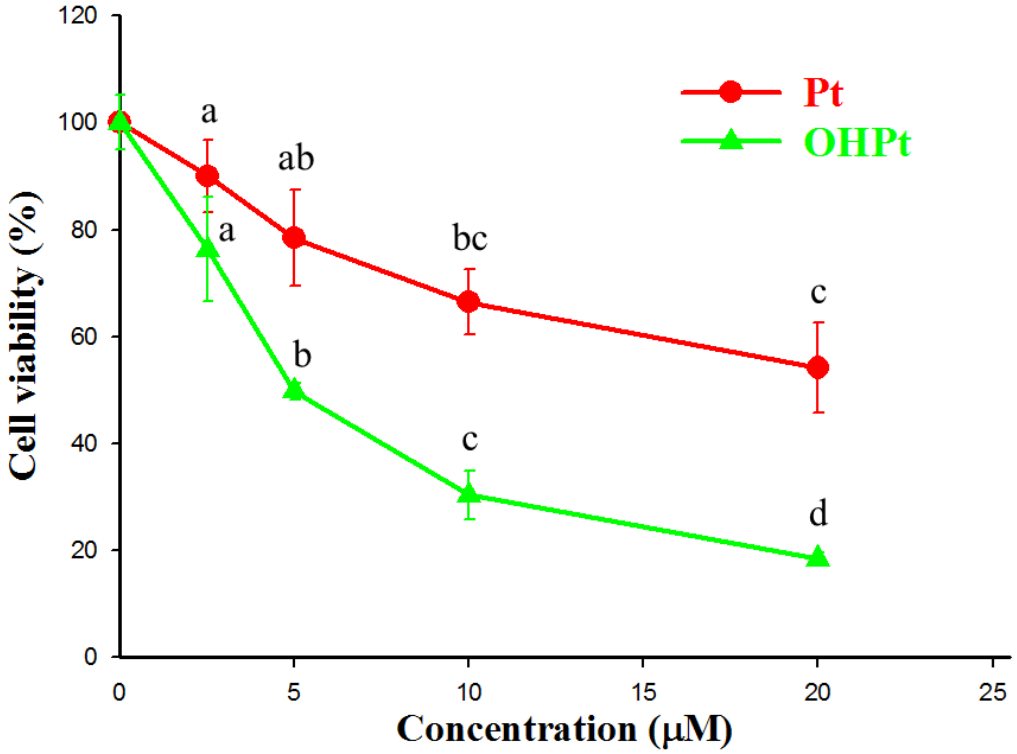

Figure 8. Effects of Pt and OHPt on the cell viability of PC-3 cells. Cells were treated various concentrations of Pt and OHPt for 48 h.

Table 4. Effect of pterostilbene and 3'-hyroxypterostilbene on the cell viability of human prostate cancer PC-3 cells

Concentration	Cell viability (% of control)[1,2,3]	
(μM)	Pterostilbene	3'-hyroxypterostilbene
2.5	90.0 ± 6.7 [a]	76.3 ± 9.7 [a]
5	78.4 ± 9.1 [ab]	49.8 ± 1.6 [b]
10	66.5 ± 6.1 [bc]	30.3 ± 4.6 [c]
20	54.2 ± 8.4 [c]	18.4 ± 1.2 [d]
IC_{50}	>20	5.0

[1]PC-3 cells were treated with pterostilbene or 3'-hyroxypterostilbene for 48 hours.

[2] Each data represents mean ± SD (n=3).

[3] Data with different superscripts in the column were significantly different (p<0.05).

6.1.1 *Effects of OHPt on the Cell Viability*

Figure 9 shows the effect of OHPt on the growth of PC-3 human prostate cancer cells. PC-3 cells were treated with various concentrations (2.5, 5, 10, and 20 μM) of OHPt for 24, 48, and 72 h, and the results indicated that OHPt markedly reduced the cell viability of PC-3 in a dose-dependent manner. Besides, a time-dependent decrease in the cell viability of PC-3 was also determined, and the IC_{50} values of OHPt against PC-3 cells treated for 24, 48, and 72 h were 8.0, 5.0, and 3.4 μM, respectively (Table 5). Moreover, we also treated the OHPt on normal peripheral blood mononuclear cells. As shown in Figure 10B, OHPt showed slight cytotoxic effect on the normal peripheral blood mononuclear cells. This result indicated that OHPt could specifically kill the prostate cancer cell but slightly influence normal cells (Figure 10).

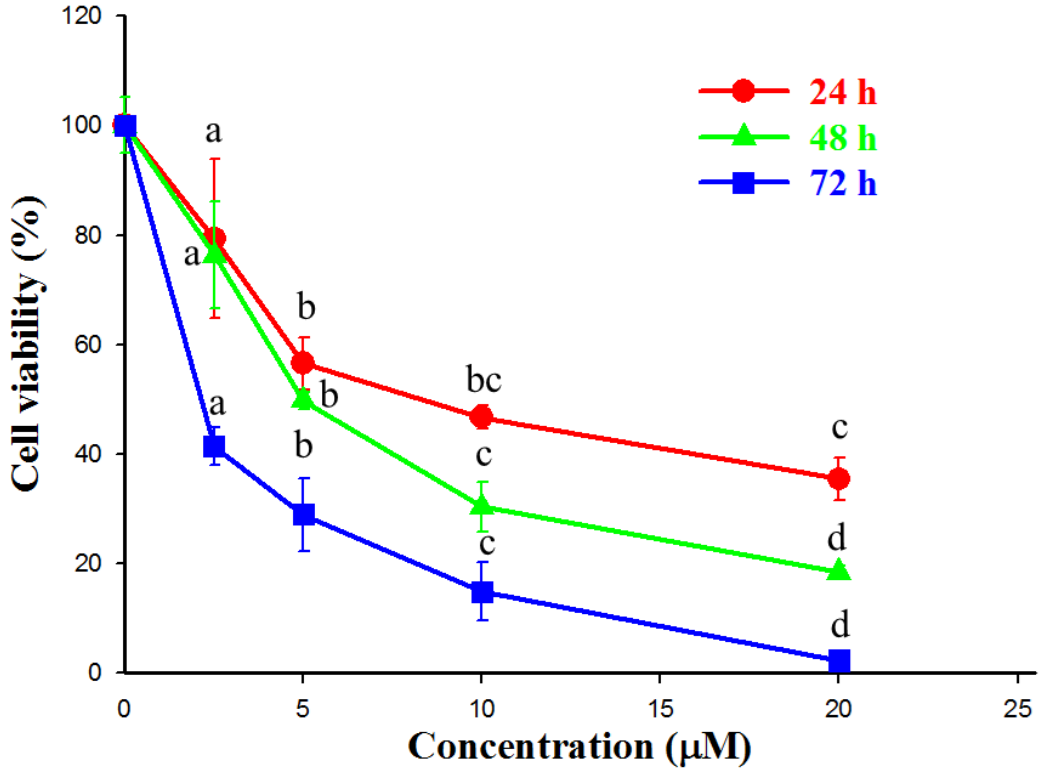

Figure 9. Effect of OHPt on the cell viability of PC-3 cells. Cells were treated various concentrations of OHPt for 24, 48, and 72 h.

Table 5. Effect of 3'-hyroxypterostilbene on the cell viability of human prostate cancer PC-3 cells

Concentration	Cell viability (% of control)[1,2,3]		
(μM)	24	48	72
2.5	79.3 ± 14.5 [a]	76.3 ± 9.7 [a]	41.4 ± 3.5 [a]
5	56.5 ± 4.8 [b]	49.8 ± 1.6 [b]	28.9 ± 6.7 [b]
10	46.7 ± 2.1 [bc]	30.3 ± 4.6 [c]	14.9 ± 5.2 [c]
20	35.4 ± 3.8 [c]	18.4 ± 1.2 [d]	2.2 ± 1.4 [d]
IC_{50}	8.0	5.0	3.4

[1]PC-3 cells were treated with 3'-hyroxypterostilbene for 24, 48, or 72 hours.

[2] Each data represents mean ± SD (n=3).

[3] Data with different superscripts in the column were significantly different (p<0.05).

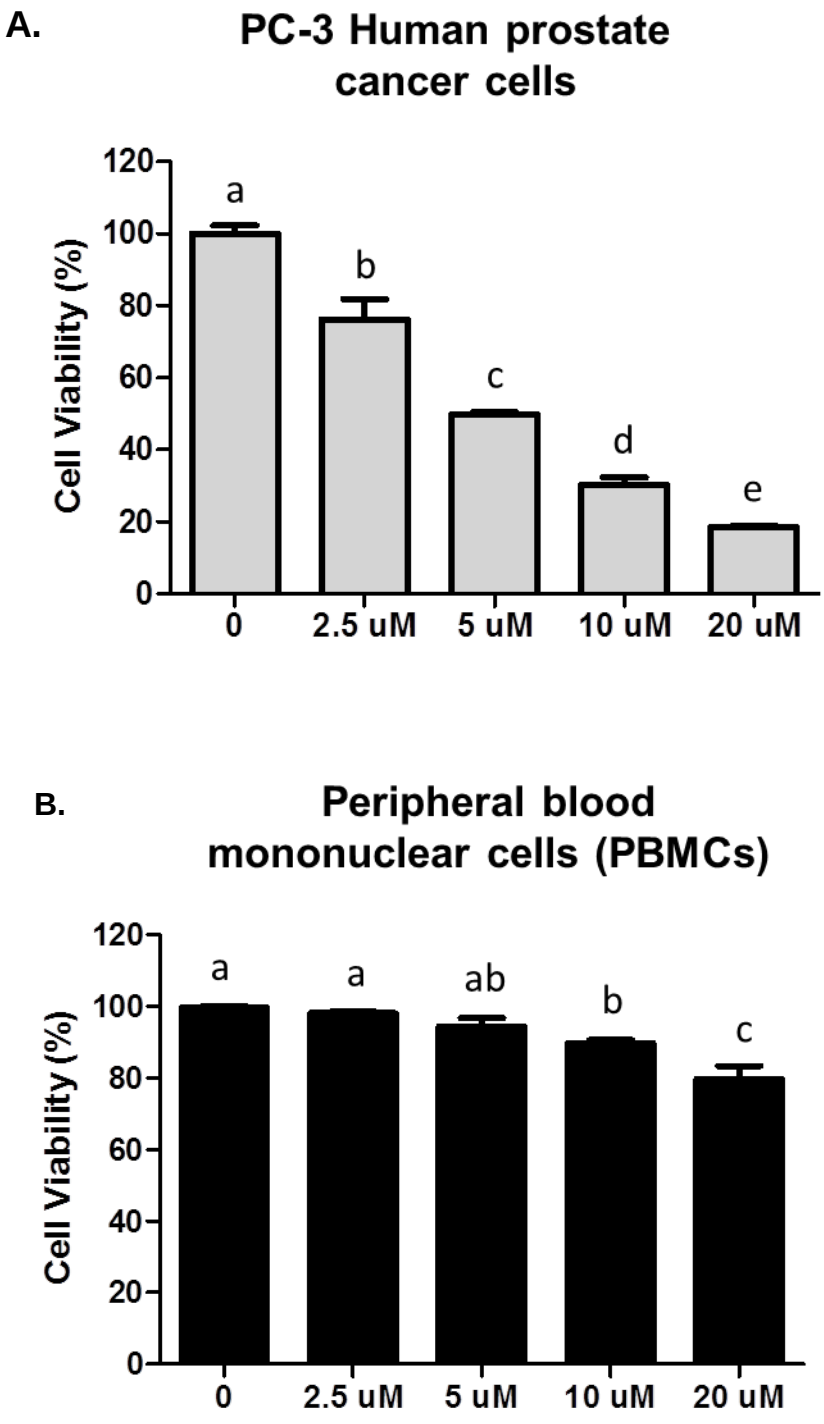

Figure 10. Effects of OHPt on the cell viability of PC-3 cells and Peripheral blood mononuclear cells (PBMCs). Cells were treated various concentrations of OHPt for 48 h.

6.1.2 Effects of OHPt on Morphology Changes

OHPt-induced morphological changes in PC-3 cells which was observed under a phase-contrast microscope. Control group without treated sample, the prostate cancer cell was spindle-shaped and attached on the plate very well (Figure 11A). After treated with various concentrations (2.5, 5, 10, and 20 μM) of OHPt, the PC-3 cells were shrinkage with much smaller size and floated up in the medium in a dose-dependent manner (Figure 11B-E).

6.1.3 Effect of OHPt on Cell Cycle Distribution

Cell cycle is a key process in cell proliferation. Toward this, we used flow cytometry to study the regulation of the cell cycle distribution in PC-3 cells after 48 h treatment of OHPt. As shown in Figure 12, it was quite evident that the percentage of sub-G1 phase distribution (DNA content less than 2N) had markedly increased by OHPt treatment with 5, 10 and 20 μM in a dose-dependent manner, indicating OHPt induced DNA genome destruction in PC-3 cells significantly. These results indicated that OHPt clearly induced apoptosis in human prostate cancer PC-3 cells.

A. Control

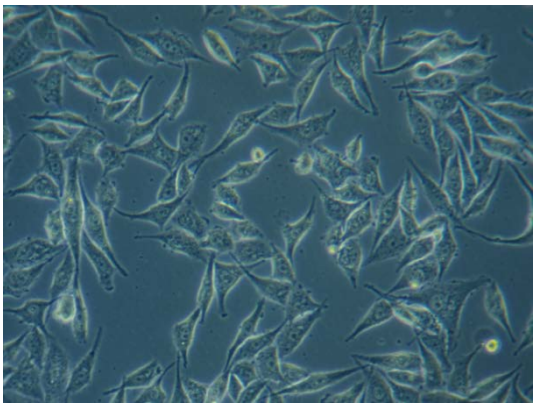

B. OHPt 2.5 µM

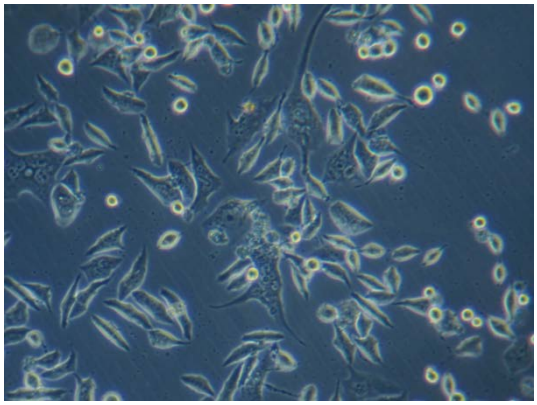

C. OHPt 5 µM

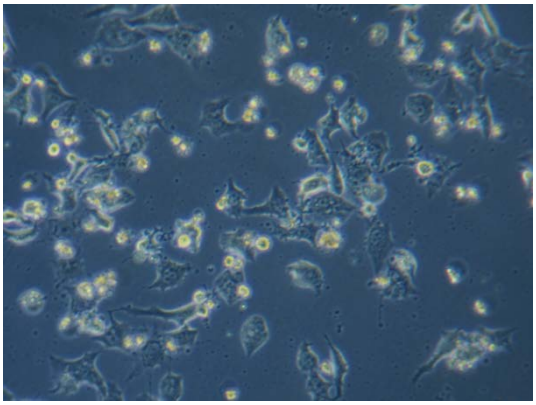

D. OHPt 10 µM

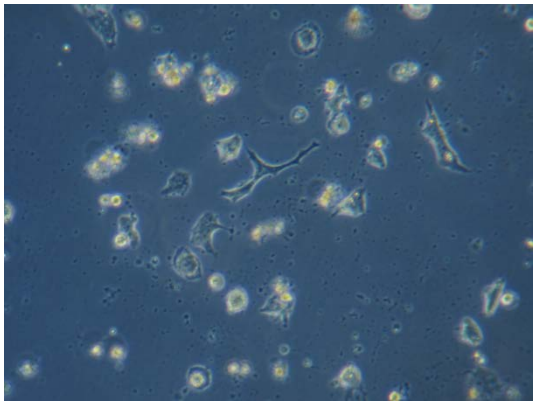

E. OHPt 20 µM

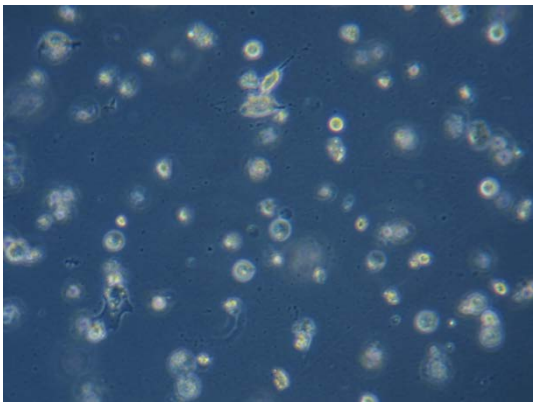

Figure 11. Morphology changes of PC-3 cells treated with various concentrations of OHPt for 48 hr. (100X under inverted stage microscope equipped with phase contrast)

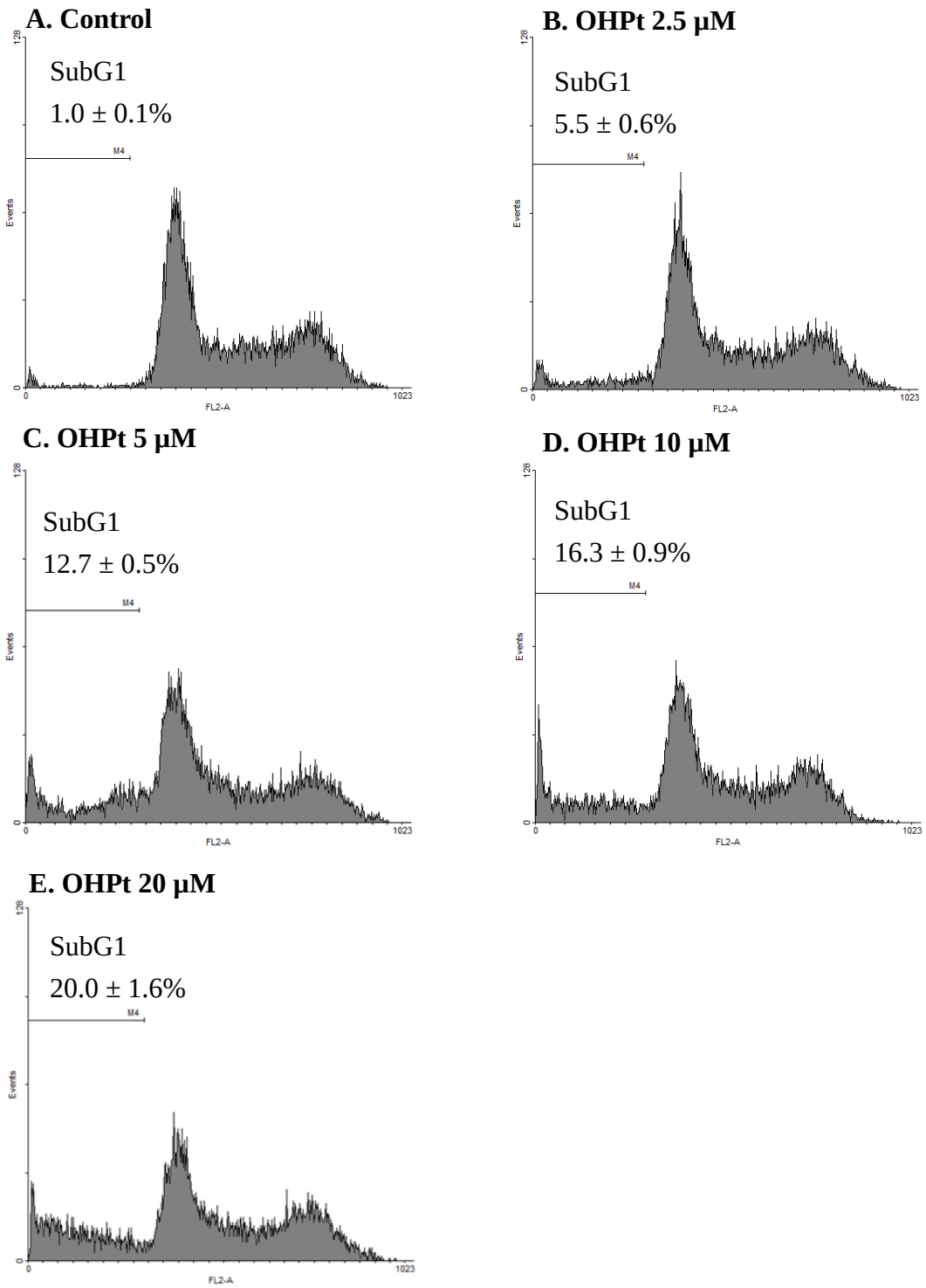

Figure 12. OHPt caused sub-G1 peak rise in PC-3 cells. Cells were treated with various concentrations of OHPt for 48 h: (A) 0.2% DMSO as control, (B) 2.5µM, (C) 5 µM, (D) 10 µM, or (E) 20 µM of OHPt. After treatment, the cells were stained with propidium iodide and analyzed by flow cytometry. The cell apoptosis% was analyzed by ModFitLT.

6.1.4 Effect of OHPt on DNA Fragmentation

DNA fragmentation is a marker of apoptosis. When the cells go through apoptosis, caspase-3 specifically activates the endonuclease CAD (Caspase-Activated DNAse), then degrades the chromosomal DNA resulting in DNA fragments of roughly 180 to 200 base pairs or multiples thereof (*52*). Furthermore, the induction of DNA fragmentation by OHPt in PC-3 cells was also assessed. Figure 13 shows that treated the PC-3 cells with 5, 10 and 20 μM OHPt for 48 h, chromatin DNA was cleaved into internucleosomal fragments, resulting in DNA ladder.

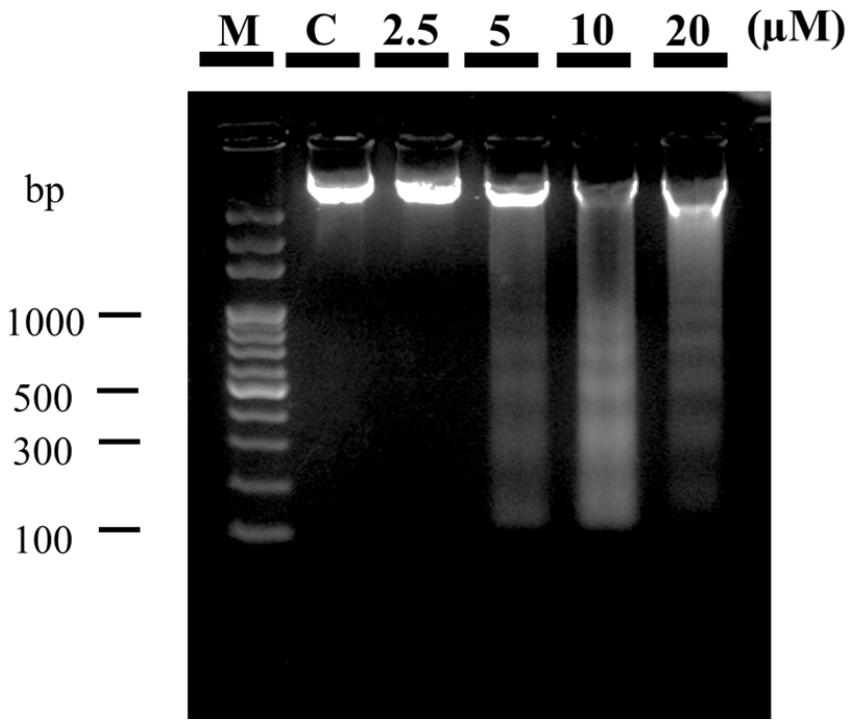

M: 100 bp DNA marker C: Control

Figure 13. Induction of DNA fragmentation by OHPt in PC-3 cells. Cells were treated with OHPt for 48 hr, and DNA fragmentation were analyzed by electrophoresis in 2.0%

agarose gel.

6.1.5 Effect of OHPt on the Apoptosis-Related Signaling Proteins

The mitochondrial outer membrane integrity is highly regulated by the interactions between pro- and anti-apoptotic members of the Bcl-2 family. The balance of pro- and anti-apoptotic Bcl-2 family proteins dictate whether a cell will die or not (*69*). In order to obtain further insights into the mechanisms of OHPt, we examined their effects on Bcl-2 family of proteins in PC-3 human prostate cancer cells. Figure 14 shows that OHPt treatment increased the protein expression of pro-apoptotic protein Bax and decreased the anti-apoptotic protein Bcl-xL in prostate cancer PC-3 cells.

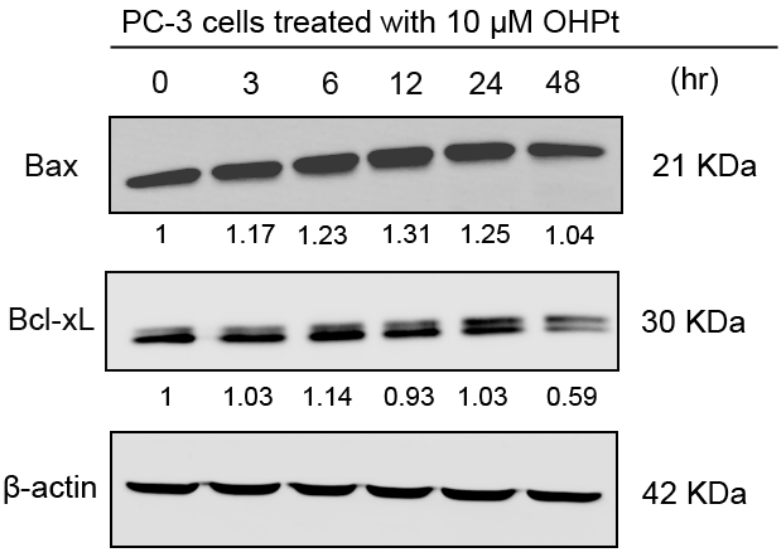

Figure 14. Bax, Bcl-xL, Actin protein expression in PC-3 cells after 10 μM OHPt treatment at different time intervals. All proteins were quantified by densitometry on immunoblots by Image J software.

6.1.6 Effect of OHPt on the Mitochondrial Membrane Potential (ΔΨ)

Increasing the mitochondrial outer membrane permeability is crucial to intrinsic apoptotic cell death, since it leads to the release of several apoptogenic factors, such as cytochrome c and Smac, into the cytoplasm that activate downstream death signalings (*66*). To further examine whether OHPt-induced cell death caused by intrinsic apoptotic pathway, PC-3 human prostate cancer cells were treated with various concentrations of OHPt (2.5, 5, 10, and 20 μM) and the mitochondrial membrane potential (ΔΨ) was measured by flow cytometry after incubating the cells with the cationic lipophilic fluorochrome $DiOC_6$. The results showed that OHPt treatment were capable of reducing the mitochondrial membrane potential in a dose-dependent manner (Figure 15), which meant that OHPt could disrupt the mitochondrial outer membrane integrity and release apoptogenic factors into cytoplasm to activate downstream caspases. Besides, OHPt strongly reduced the mitochondrial membrane potential than that of Pt.

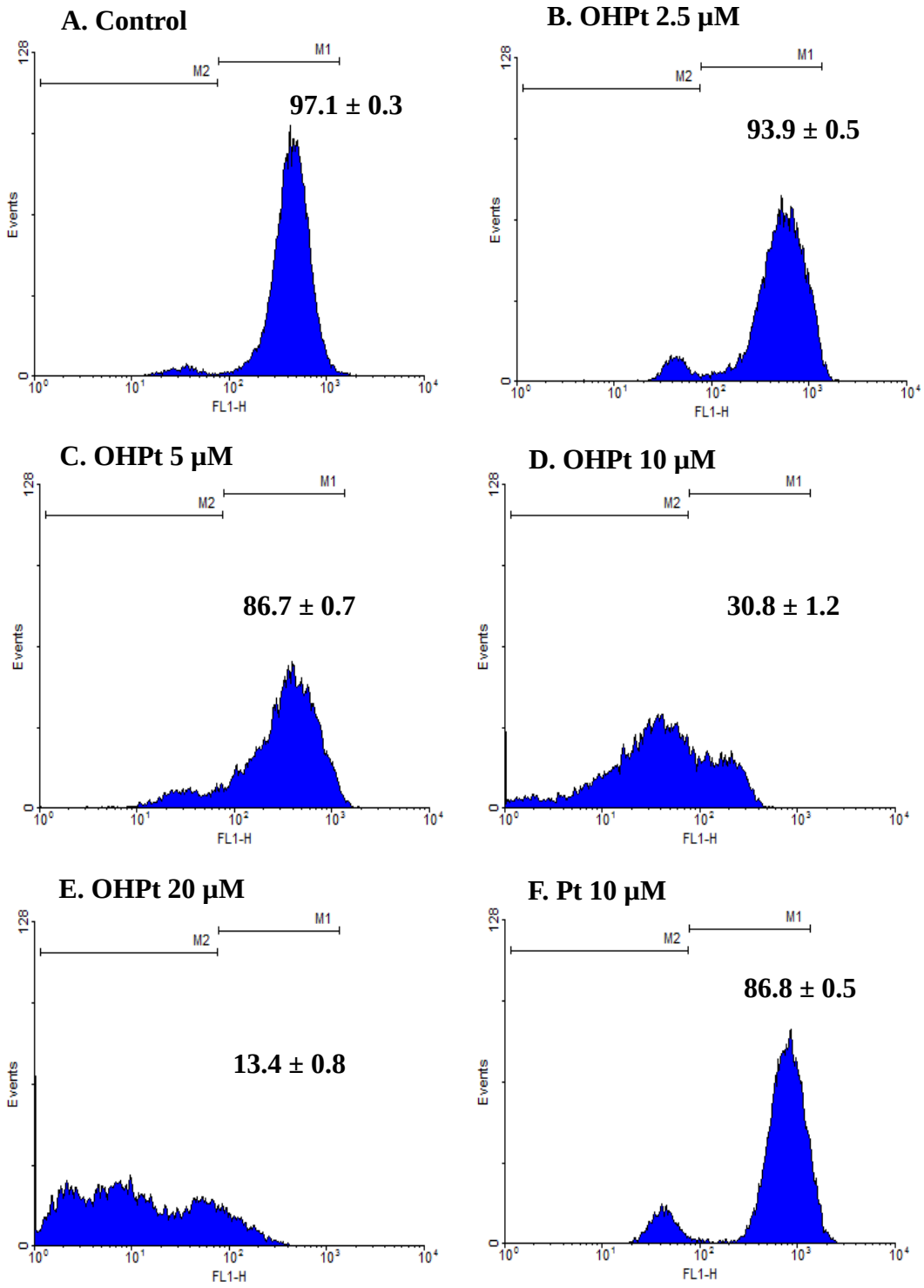

Figure 15. Effects of OHPt and Pt on the mitochondrial membrane potential in PC-3 cells for 48 hr. PC-3 cells were cultured in serum-free RPMI containing various concentrations of OHPt and Pt for 48 hr. Then, cells were stained with $DiOC_6$ and analyzed by flow cytometry. Cells with depolarization of mitochondrial membrane showed a lower

fluorescence compared with the control. The M1 and M2 gates standardize cell population with normal ΔΨ or with disrupted ΔΨ, respectively.

6.1.7 Effects of OHPt on the Caspase-9 and Caspase-3 Activity

The disruption in ΔΨ causes the release of proapoptotic factors (such as cytochrome c, Smac/DIABLO and Omi/HtrA2) from the mitochondria which activate caspase-9. Caspase-9 is an initiator of the cytochrome c-dependent caspase cascade, then activates caspase-3 (*52, 58*). Substantial researches demonstrate that caspase-3 is the most important of the executioner caspase (*10, 144*). Thus, we evaluated the effects of OHPt on caspase-9 and caspase-3 activity. The results indicated that treatment with OHPt at various concentration (2.5, 5, 10, and 20 μM) increased the caspase-9 and caspase-3 activity in a dose-dependent manner (Figure 16 and 17), demonstrating that OHPt induced cell death via intrinsic apoptotic pathway. Besides, compared to Pt, OHPt strongly increased the caspase-9 and caspase-3 activity.

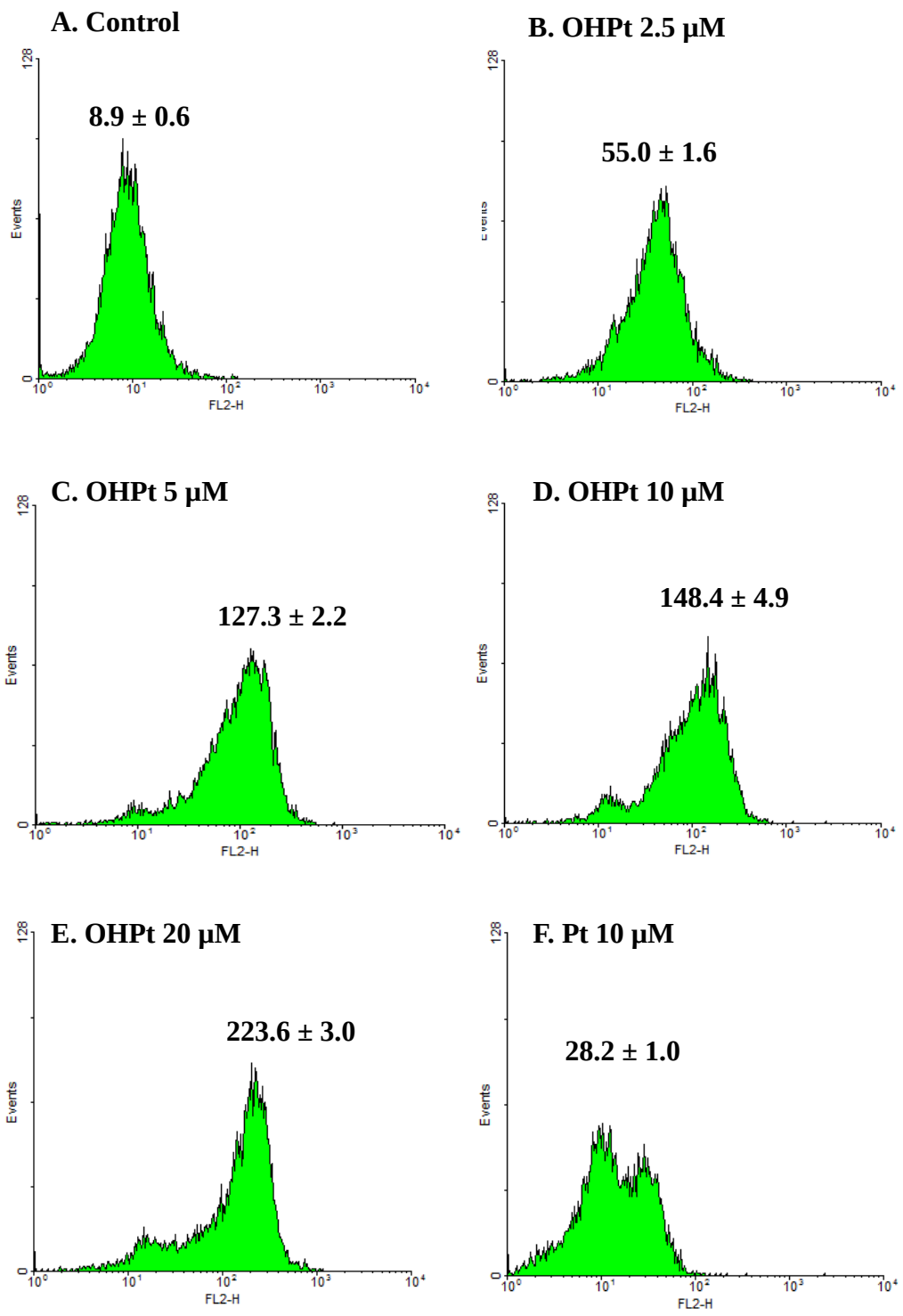

Figure 16. Effects of OHPt and Pt on the activity of caspase-9 in PC-3 cells for 48 hr. PC-3 cells were cultured in serum-free RPMI containing various concentrations of OHPt and Pt for 48 hr. Then, cells were stained with caspase-9 kit and analyzed by flow cytometry.

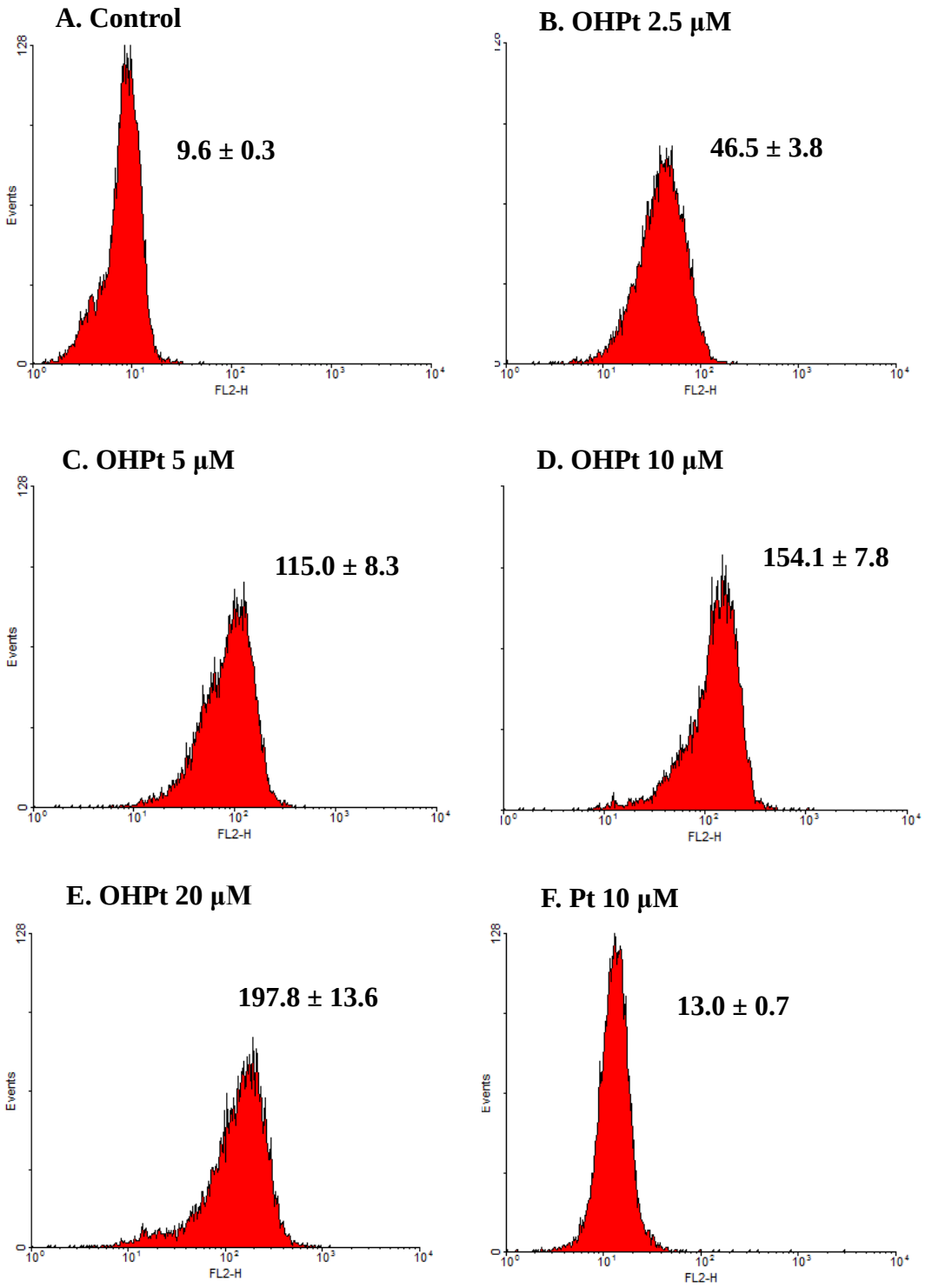

Figure 17. Effects of OHPt and Pt on the activity of caspase-3 in PC-3 cells for 48 hr. PC-3 cells were cultured in serum-free RPMI containing various concentrations of OHPt and Pt for 48 hr. Then, cells were stained with caspase-3 kit and analyzed by flow cytometry.

6.1.8 Effects of OHPt on the Caspase-8 Activity

The extrinsic apoptotic pathway is mediated by the activation of death receptors such as FAS, TNFR and TRAIL, directly activates caspase-8 (*68, 69*). In this study, to determine whether OHPt-induced cell death caused by extrinsic apoptotic pathway, PC-3 human prostate cancer cells were treated with various concentrations of OHPt and the activity of caspase-8 was evaluated. The results showed that treatment with OHPt at various concentrations (2.5, 5, 10, and 20 μM) increased the caspase-8 activity in a dose dependent manner, indicating that the OHPt-induced cell death also underwent extrinsic apoptotic pathway (Figure 18).

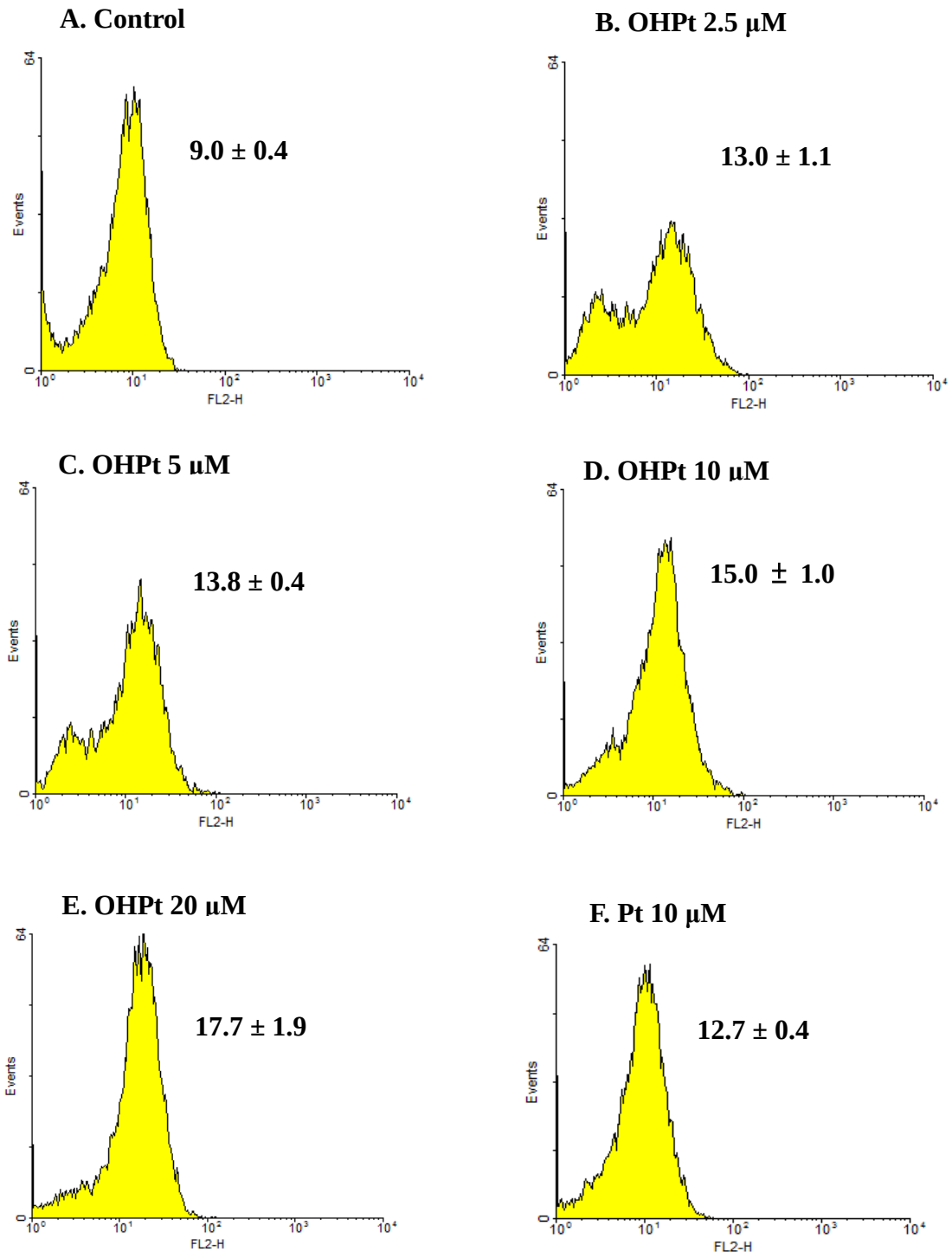

Figure 18. Effects of OHPt and Pt on the activity of caspase-8 in PC-3 cells for 48 hr. PC-3 cells were cultured in serum-free RPMI containing various concentrations of OHPt and Pt for 48 hr. Then, cells were stained with caspase-8 kit and analyzed by flow cytometry.

6.1.9 Effect of OHPt on Autophagic Protein Beclin-1

Beclin-1 is key regulators of autophagy and tumor suppression protein. Overexpression of Beclin-1 induced autophagy (*145-147*). In this study, in order to evaluate the hypothesis that OHPt induced cell death went through autophagic cell death, we examined the expression of Beclin-1. Our results showed that treatment with OHPt 10 μM induced autophagy by increasing the expression of autophagic protein Beclin-1 by approximately 2-folds (Figure 19).

6.1.10 Effect of OHPt on Autophagic Protein LC3

The LC3 protein plays a critical role in autophagy. Typically LC3 protein presents in the cytosol, but undergoes cleavage and conjugation with phosphatidylethanolamine, LC3 associates with the autophagic membrane (*148*) . The conversion of LC3-I (14 kDa cytosolic free form) to LC3-II (16 kDa PE-conjugated form) is a key marker for autophagosome formation (*13, 148*). We next determined the expression of LC3 protein by western blotting. The induction of LC3-II was revealed in PC-3 human prostate cancer cells (Figure 19). Treatment with 10 μM OHPt for 24 and 48 hrs significantly induced LC3-II expression, approximately increased 48- and 100-fold, respectively. This result represented that OHPt induced autophagy tremendously.

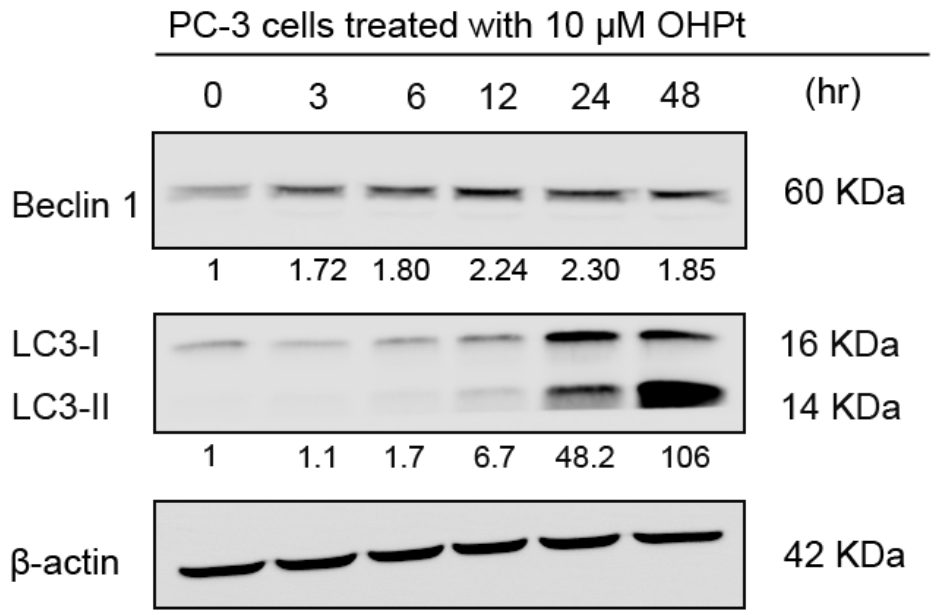

Figure 19. Beclin-1, LC3-I, LC3- II, Actin protein expression in PC-3 cells after 10 μM OHPt treatment at different time intervals. All proteins were quantified by densitometry on immunoblots by Image J software.

6.1.11 Effect of OHPt on Autophagosome Formation

LC3 is involved in the formation of autophagosomes and autophagolysosomes, which are usually characterized and monitored by fluorescence microscopy using green fluorescent protein with LC3 (GFP-LC3) (*73*, *103*, *148*). As shown in Figure 20, the numbers of GFP-LC3-labeled-puncta in cytosol were markedly increased in the OHPt group than in the control group. The results indicated that OHPT induced autophagy by increasing the formation of autophagosomes and autophagolysosomes in PC-3 human

prostate cancer cells.

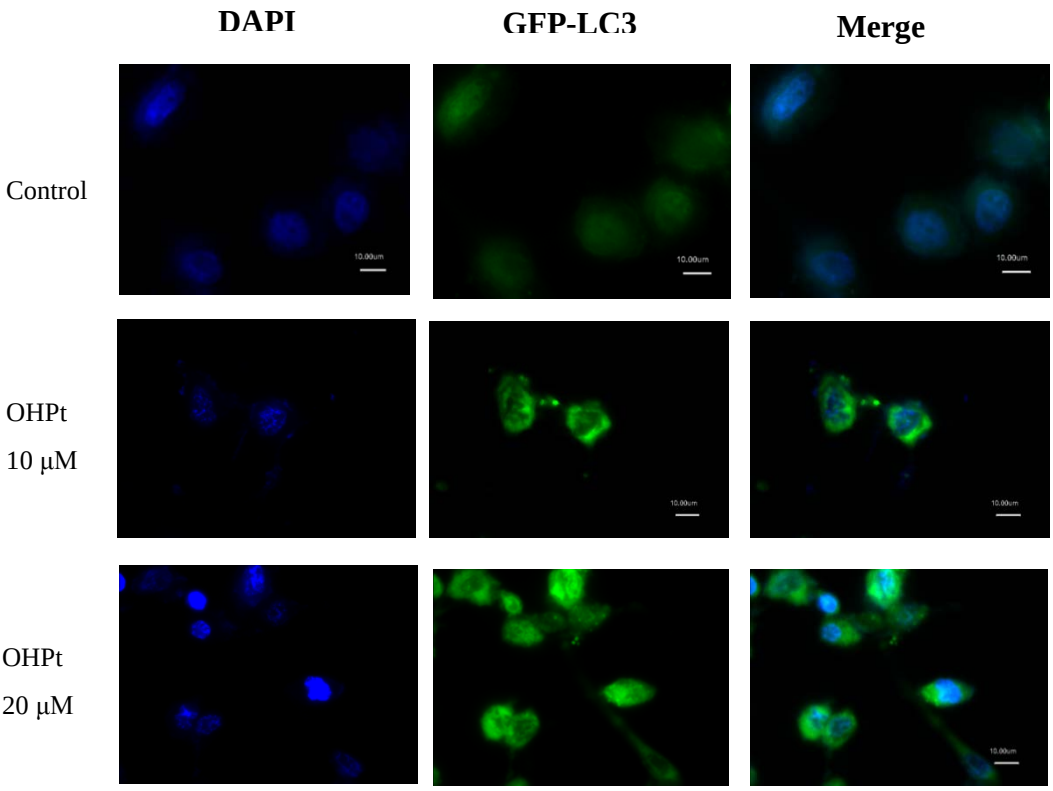

Figure 20. Confocal fluorescence microscopy to detect GFP-LC3 in OHPt-treated PC-3 cells. The cells were transfected with GFP-LC3, then treated with 10 or 20 μM OHPt for 18 hrs and compared with untreated controls. Nuclei were stained with DAPI (blue).

6.2 Human Prostate Cancer LNCaP Cell Line Experiment

In this part of study, we aim to investigate the growth inhibitory effect of OHPt on p53 wild type prostate cancer LNCaP cells, and to compare the molecular mechanisms induced by OHPt between PC-3 and LNCaP cells, including cell viability, cell cycle distribution, expression of apoptosis- and autophagy-related proteins, and autophagosome formation. Our MTT results showed that Pt and OHPt treatments significantly decreased cell viability of LNCaP cells in a dose-dependent manner (Figure 21). After 48 h treatment, the IC_{50} values of Pt and OHPt for LNCaP cells are 14.4 μM and 2.4 μM, respectively (Table 6). OHPt showed much stronger anti-proliferation activity than its parent compound Pt against LNCaP cells. These results obtained in LNCaP cells were similar to those observed in PC-3 cells in our previous study.

6.2.1 Effects of OHPt on the Cell Viability

LNCaP cells were treated with various concentrations (2.5, 5, 10, and 20 μM) of OHPt for 24, 48, and 72 h, and the results indicated that OHPt markedly inhibited cell viability of LNCaP in a dose-dependent manner (Figure 22). Besides, a time-dependent decrease in the cell viability of LNCaP was also determined, and the IC_{50} values of OHPt against LNCaP cells treated for 24, 48, and 72 h were 5.7, 2.4, and 2.0 μM, respectively

(Table 7).

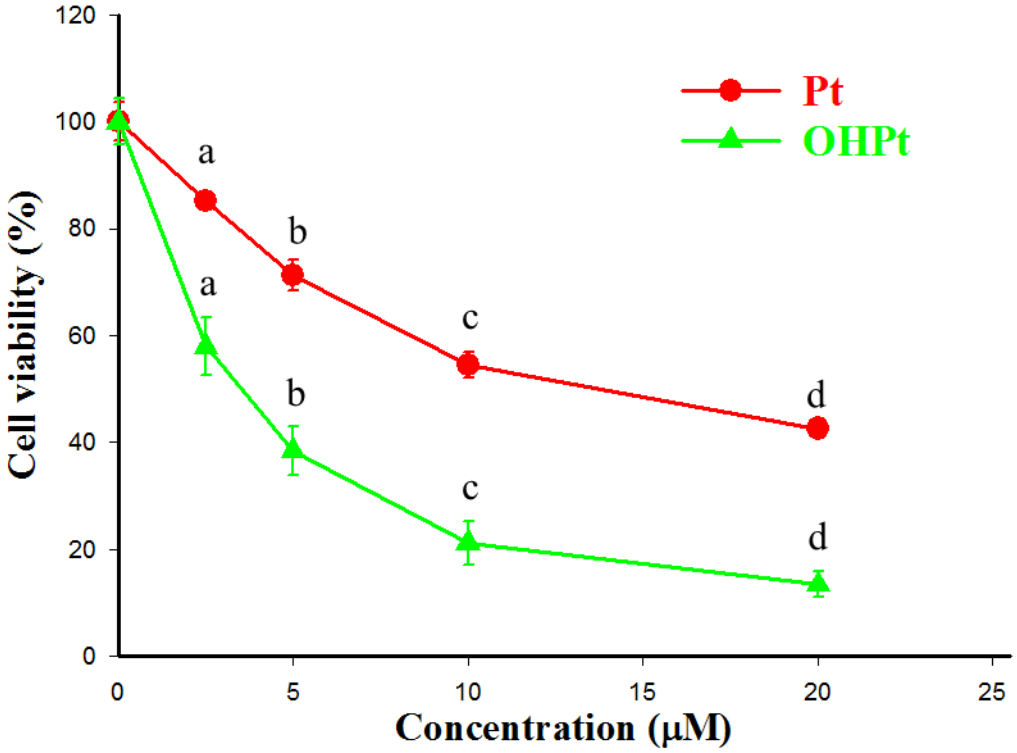

Figure 21. Effects of Pt and OHPt on the cell viability of LNCaP cells. Cells were treated various concentrations of Pt and OHPt for 48 h.

Table 6. Effect of pterostilbene and 3'-hyroxypterostilbene on the cell viability of human prostate cancer LNCaP cells

Concentration (μM)	Cell viability (% of control)[1,2,3]	
	Pterostilbene	3'-hyroxypterostilbene
2.5	85.3 ± 1.1 [a]	58.0 ± 5.4 [a]
5	71.3 ± 2.8 [b]	38.4 ± 4.5 [b]
10	54.5 ± 2.4 [c]	21.2 ± 4.1 [c]
20	42.6 ± 1.8 [d]	13.4 ± 2.4 [d]
IC_{50}	14.4	2.4

[1] LNCaP cells were treated with pterostilbene or 3'-hyroxypterostilbene for 48 hours.

[2] Each data represents mean ± SD (n=3).

[3] Data with different superscripts in the column were significantly different (p<0.05).

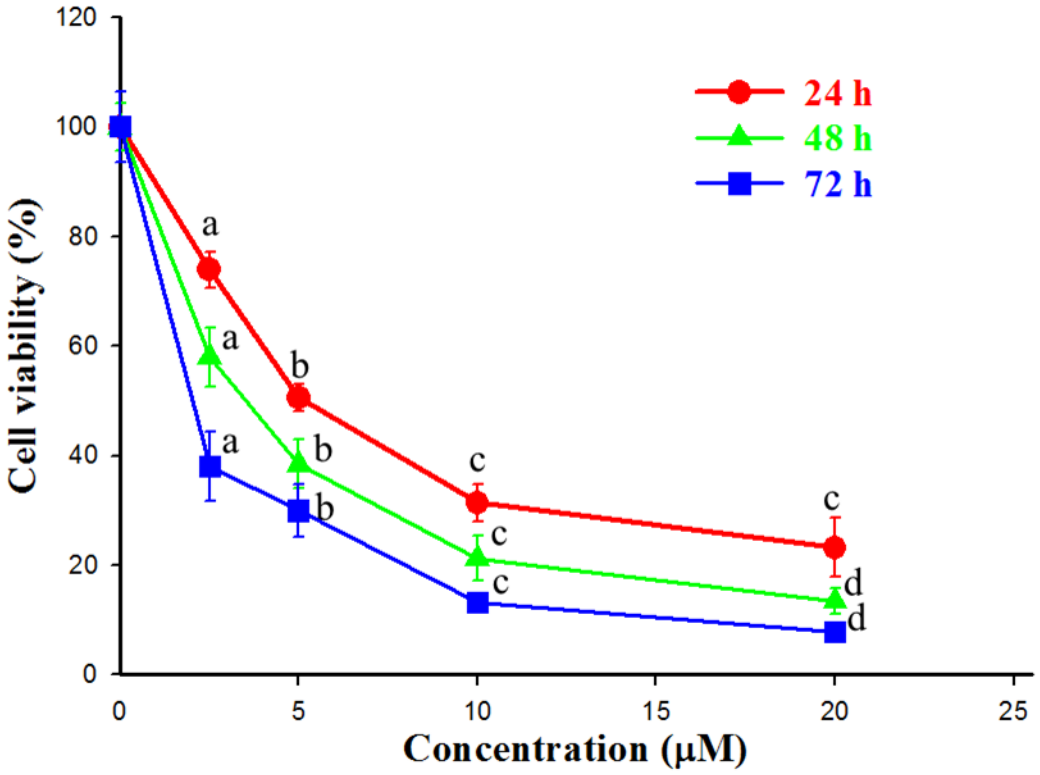

Figure 22. Effect of OHPt on the cell viability of LNCaP cells. Cells were treated various concentrations of OHPt for 24, 48, and 72 h.

Table 7. Effect of 3'-hyroxypterostilbene on the cell viability of human prostate cancer LNCaP cells

Concentration	Cell viability (% of control)[1,2,3]		
(μM)	24	48	72
2.5	73.9 ± 3.3 [a]	58.0 ± 5.4 [a]	38.0 ± 6.3 [a]
5	50.5 ± 2.4 [b]	38.4 ± 4.5 [b]	30.0 ± 4.7 [b]
10	31.4 ± 3.4 [c]	21.2 ± 4.1 [c]	13.3 ± 1.5 [c]
20	23.2 ± 5.4 [c]	13.4 ± 2.4 [d]	7.9 ± 1.6 [d]
IC_{50}	5.7	2.4	2.0

[1]LNCaP cells were treated with 3'-hyroxypterostilbene for 24, 48, or 72 hours.

[2] Each data represents mean ± SD (n=3).

[3] Data with different superscripts in the column were significantly different (p<0.05).

6.2.2 Effects of OHPt on Morphology Changes

OHPt-induced morphological changes in LNCaP cells which was observed under a phase-contrast microscope. As shown in Figure 23A, normal prostate cancer LNCaP cells attached on the plate uniformly with compressed shaped. When exposed to various concentrations of OHPt (2.5, 5, 10, and 20 μM) for 48 hr, the LNCaP cells appeared obviously morphological changes, became shrinkage with much smaller size and suspended in the culture medium in a dose-dependent manner, indicating that OHPt induced the human prostate cancer LNCaP cells death (Figure 23B-E).

6.2.3 Effect of OHPt on Cell Cycle Distribution

In order to evaluate the influence of OHPt on cell cycle distribution, we treated LNCaP cells with different concentrations of OHPt for 48 h and quantified the percentage of cells in different cell cycle phases. As shown in Figure 24, the percentage of sub-G1 cells (DNA content less than 2N) had significantly increased by OHPt treatment in a dose-dependent manner, indicating that OHPt induced DNA damage. Therefore, it was clear evidence that OHPt induced apoptosis in LNCaP cells. The results of cell cycle distribution observed in LNCaP cells were similar to those observed in PC-3 cells in our previous study.

A. Control

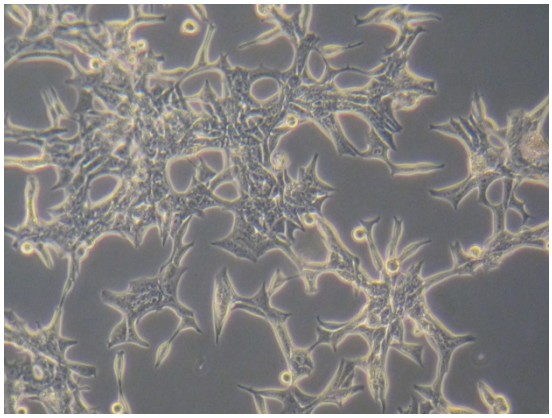

B. 2.5 μM OHPt

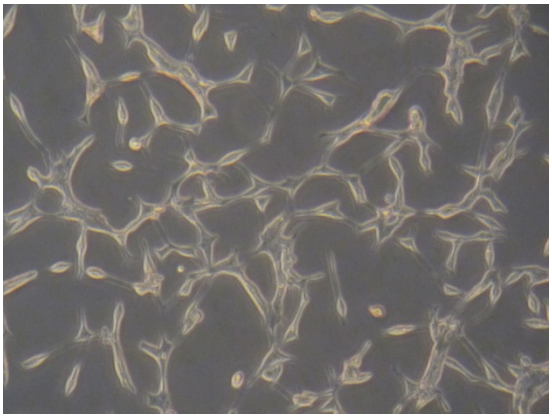

C. 5 μM OHPt

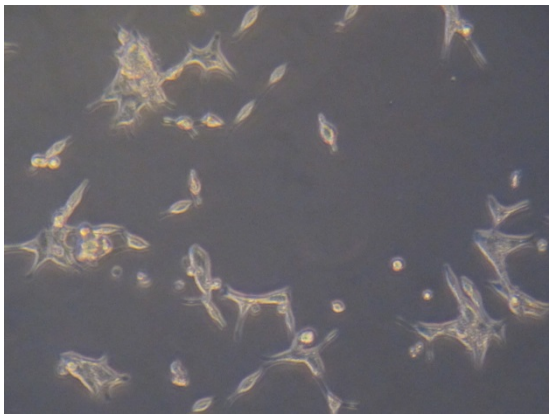

D. 10 μM OHPt

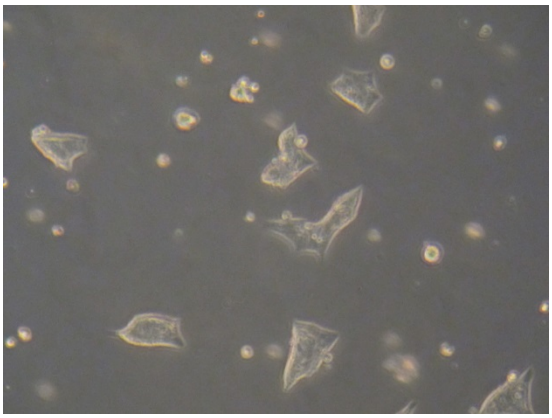

E. 20 μM OHPt

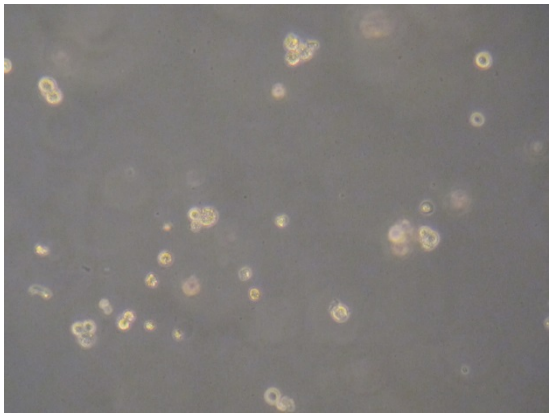

Figure 23. Morphology changes of LNCaP cells treated with various concentrations of OHPt for 48 hr. (100X under inverted stage microscope equipped with phase contrast)

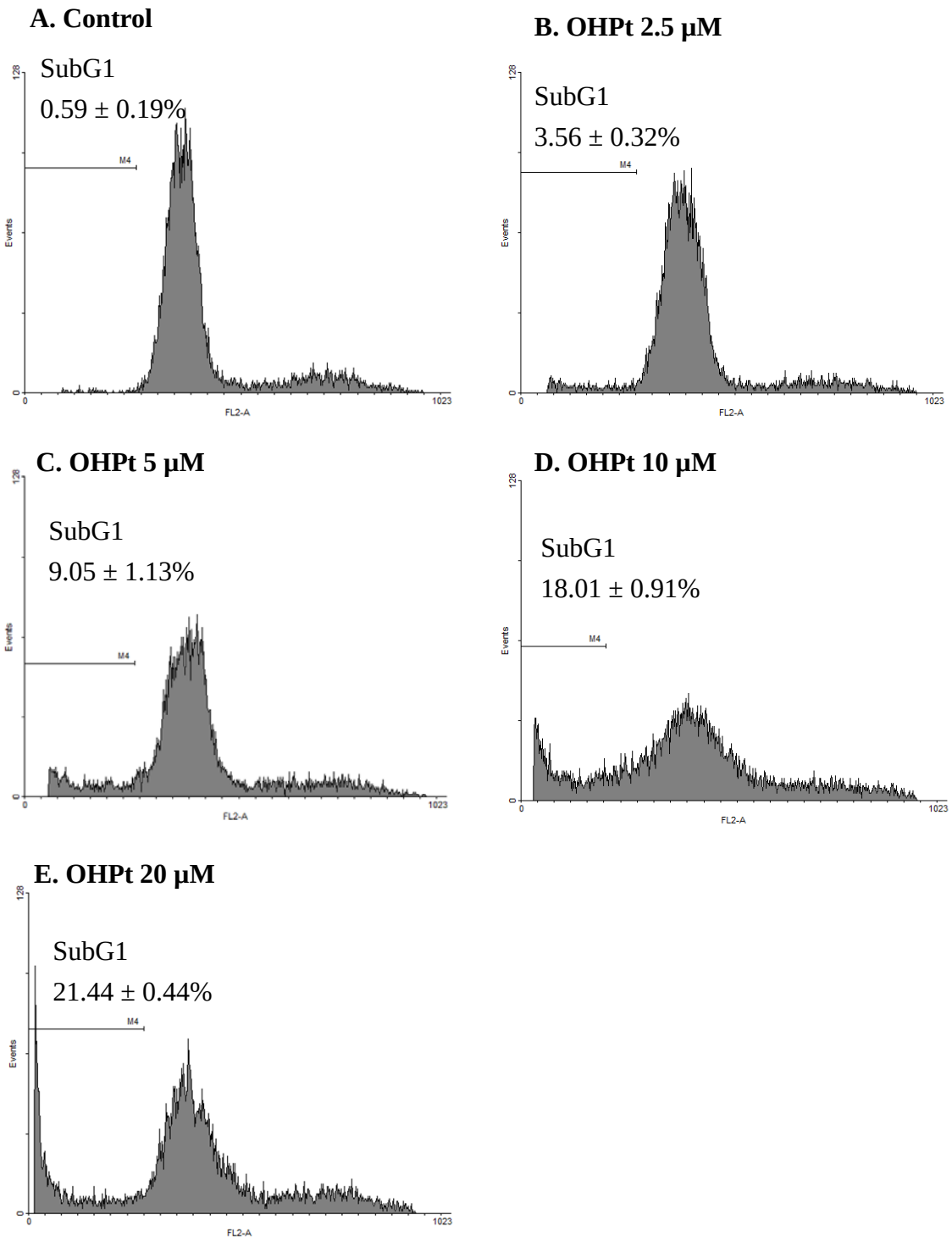

Figure 24. OHPt caused sub-G1 peak rise in LNCaP cells. Cells were treated with various concentrations of OHPt for 48 h: (A) 0.2% DMSO as control, (B) 2.5µM, (C) 5 µM, (D) 10 µM, or (E) 20 µM of OHPt. After treatment, the cells were stained with propidium iodide and analyzed by flow cytometry.

6.2.5 Effect of OHPt on the Apoptosis-Related Signaling Proteins

Apoptosis is highly regulated by the interactions between pro-apoptotic protein (Bax) and anti-apoptotic protein (Bcl-xL) (*69*). In order to obtain further insights into the molecular mechanisms induced by OHPt in LNCaP human prostate cancer cells, we investigate its effects on Bcl-2 family of proteins. As shown in Figure 25, OHPt treatment significantly increased the Bax/Bcl-xL ratio in LNCaP human prostate cancer cells.

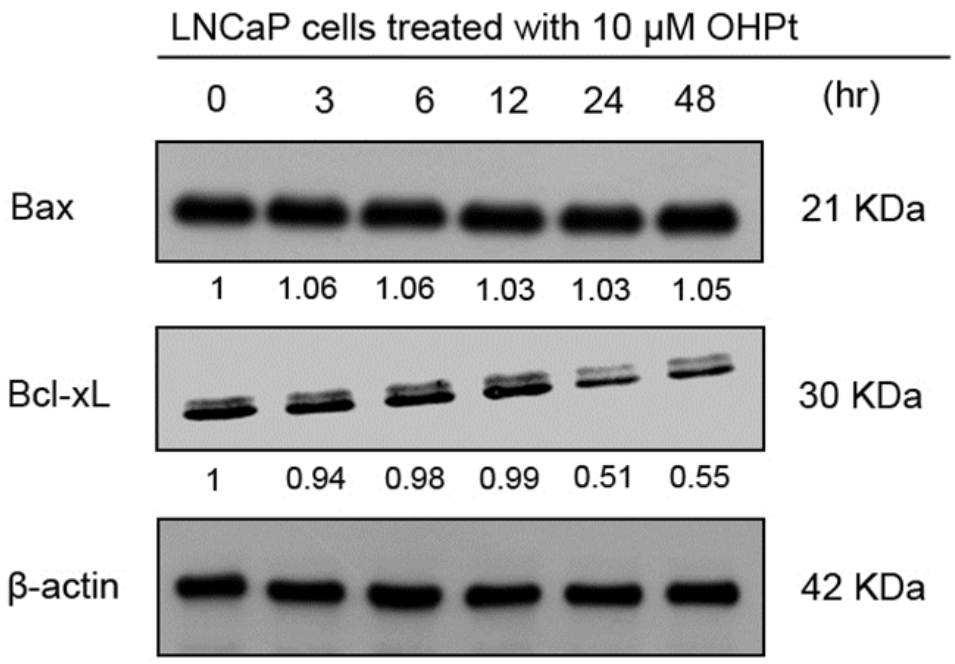

Figure 25. Bax, Bcl-xL, Actin protein expression in LNCaP cells after 10 μM OHPt treatment at different time intervals. All proteins were quantified by densitometry on immunoblots by Image J software.

6.2.6 Effect of OHPt on the Mitochondrial Membrane Potential (ΔΨ)

Mitochondrial membrane potential is an important marker of mitochondrial function. Reduction of mitochondrial membrane potential indicates that the loss of mitochondrial membrane integrity which will release several apoptogenic factors to induce intrinsic apoptotic signaling pathway (*66*). To further examine whether OHPt-induced cell death caused by intrinsic apoptotic pathway, LNCaP human prostate cancer cells were treated with various concentrations of OHPt (2.5, 5, 10, and 20 μM) for 48 hrs and the mitochondrial membrane potential was measured. As shown in Figure 26, treatment with various concentrations of OHPt markedly collapsed the mitochondrial membrane potential in a dose-dependent manner in LNCaP human prostate cancer cells, indicating that OHPt could disrupt the mitochondrial outer membrane integrity and release apoptogenic factors into cytoplasm to activate downstream caspases. Besides, OHPt strongly reduced the mitochondrial membrane potential than that of Pt. The results of mitochondrial membrane potential observed in LNCaP cells were similar to that obtained in PC-3 cells.

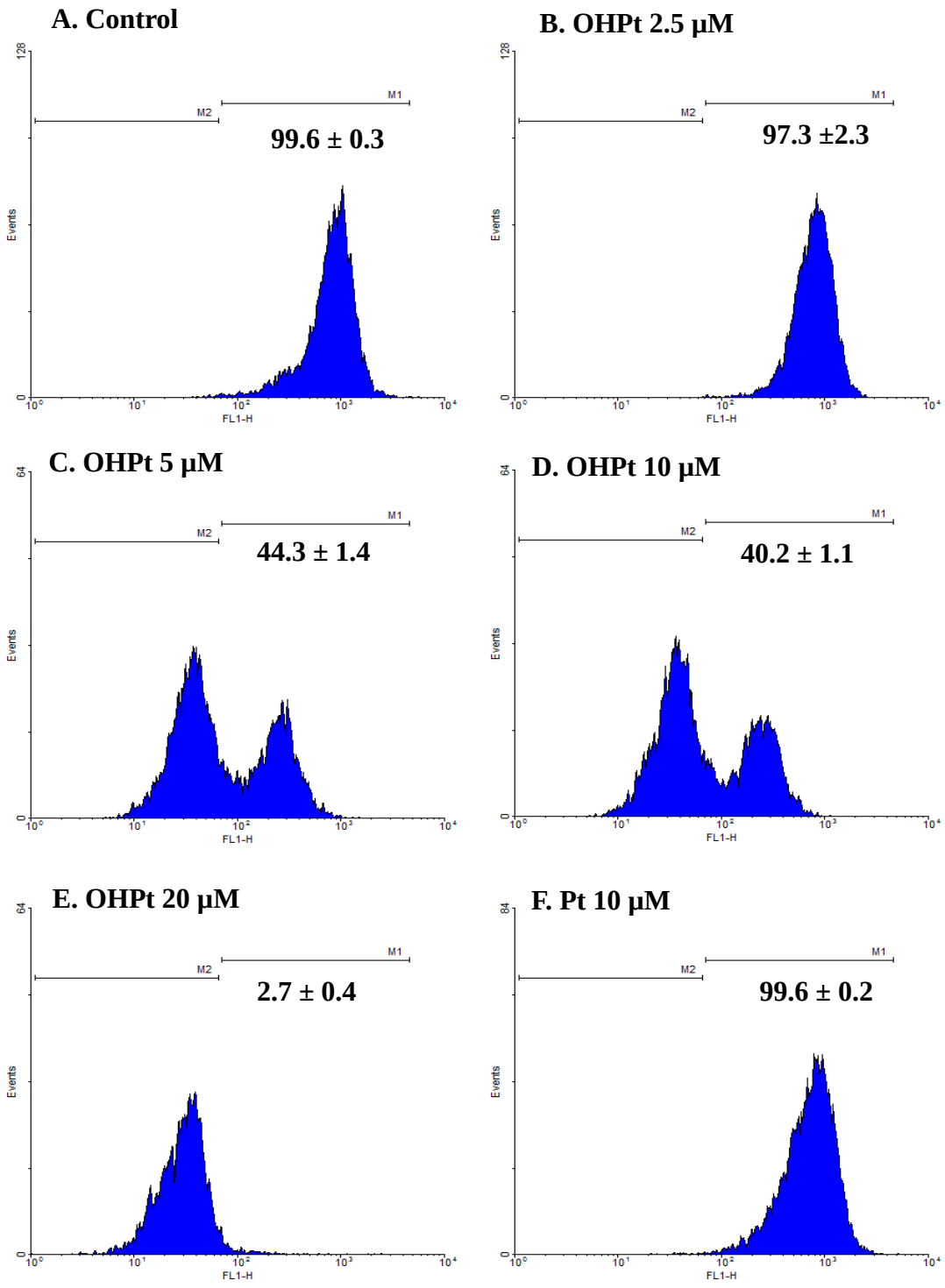

Figure 26. Effects of OHPt and Pt on the mitochondrial membrane potential in LNCaP cells for 48 hr. LNCaP cells were cultured in serum-free RPMI containing various concentrations of OHPt and Pt for 48 hr, respectively. Then, cells were stained with $DiOC_6$ and analyzed by flow cytometry. Cells with depolarization of mitochondrial membrane

showed a lower fluorescence compared with the control. The M1 and M2 gates standardize cell population with normal $\Delta\Psi$ or with disrupted $\Delta\Psi$, respectively.

6.2.7 Effects of OHPt on the Caspase-9 and Caspase-3 Activity

The disruption of mitochondrial membrane integrity causes the release of proapoptotic factors, such as cytochrome c, Smac/DIABLO and Omi/HtrA2, followed by activation of caspase-9 and caspase-3 and lead to intrinsic apoptotic cell death (*52*, *58*). To examine this, we evaluated the effects of OHPt on caspase-9 and caspase-3 activity. The results indicated that treatment with OHPt at various concentration (2.5, 5, 10, and 20 μM) increased the caspase-9 and caspase-3 activity in a dose-dependent manner in LNCaP cells (Figure 27 and 28), demonstrating that OHPt induced prostate cancer cell death via intrinsic apoptotic pathway. Besides, compared to Pt, OHPt strongly increased the caspase-9 and caspase-3 activity in LNCaP cells. These findings were similar to those obtained in PC-3 cells.

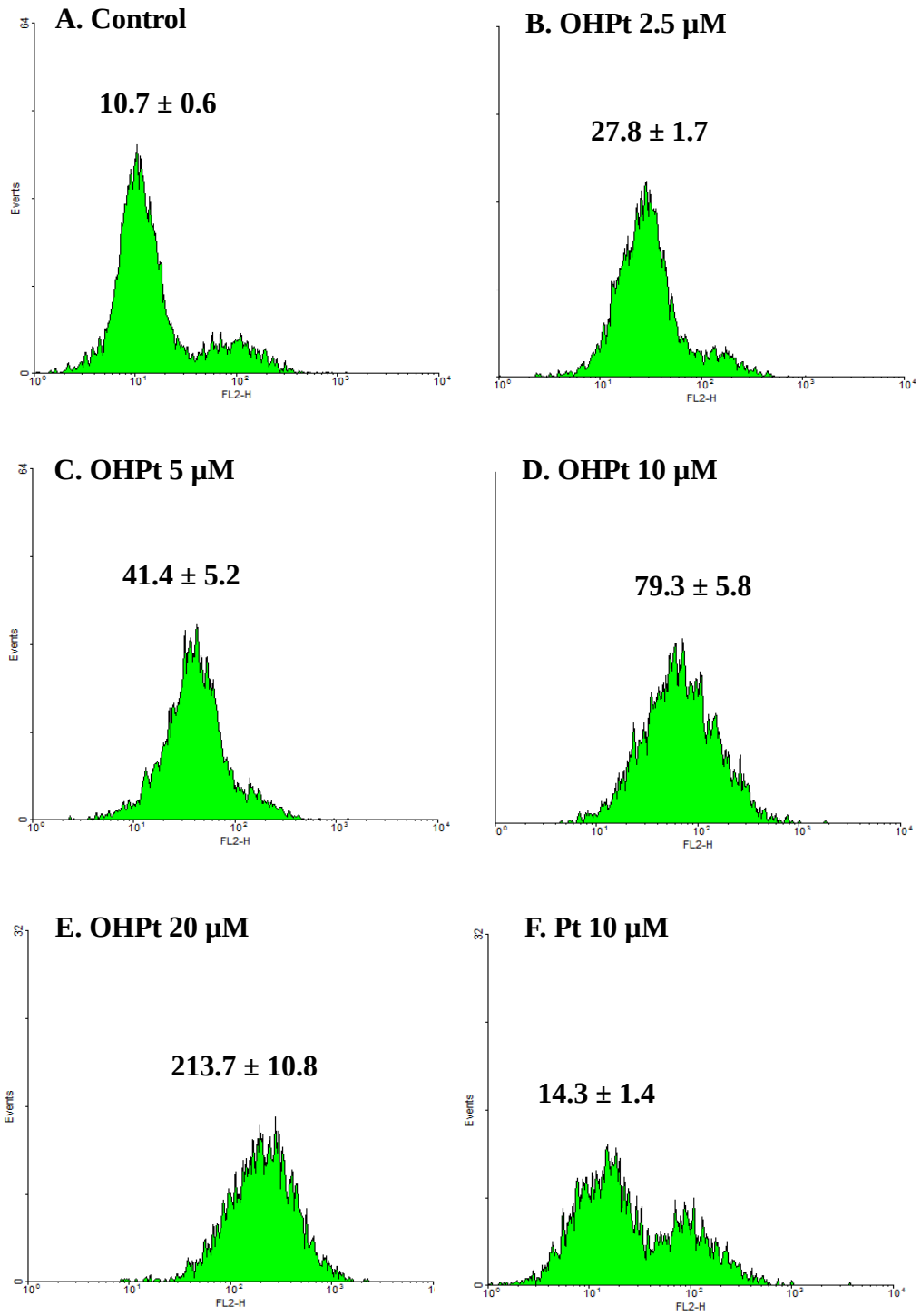

Figure 27. Effects of OHPt and Pt on the activity of caspase-9 in LNCaP cells for 48 hr. LNCaP cells were cultured in serum-free RPMI containing various concentrations of OHPt and Pt for 48 hr. Then, cells were stained with caspase-9 kit and analyzed by flow cytometry.

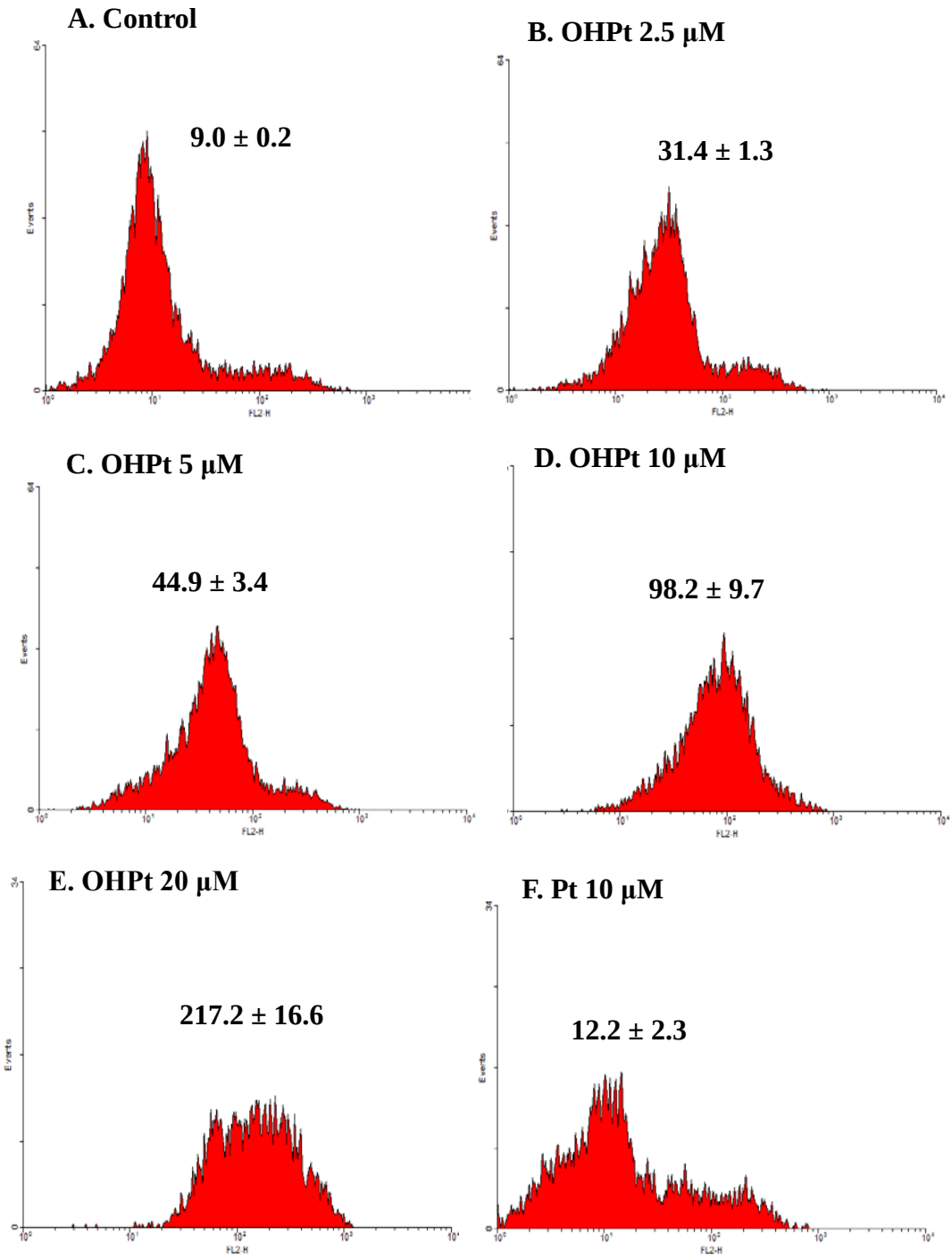

Figure 28. Effects of OHPt and Pt on the activity of caspase-3 in LNCaP cells for 48 hr. LNCaP cells were cultured in serum-free RPMI containing various concentrations of OHPt and Pt for 48 hr. Then, cells were stained with caspase-3 kit and analyzed by flow cytometry.

6.2.8 Effects of OHPt on the Caspase-8 Activity

The extrinsic apoptotic pathway is mediated by the activation of death receptors such as FAS, TNFR and TRAIL, directly activates caspase-8 (*68, 69*). In this study, to determine whether OHPt-induced cell death caused by extrinsic apoptotic pathway, LNCaP human prostate cancer cells were treated with various concentrations of OHPt and the activity of caspase-8 was evaluated. The results showed that treatment with OHPt at various concentrations (2.5, 5, 10, and 20 μM) increased the caspase-8 activity in a dose dependent manner, indicating that the OHPt-induced cell death also underwent extrinsic apoptotic pathway in LNCaP cells (Figure 29). Besides, compared to Pt, OHPt strongly increased the caspase-8 activity in LNCaP cells. The result was similar to that observed in PC-3 cells.

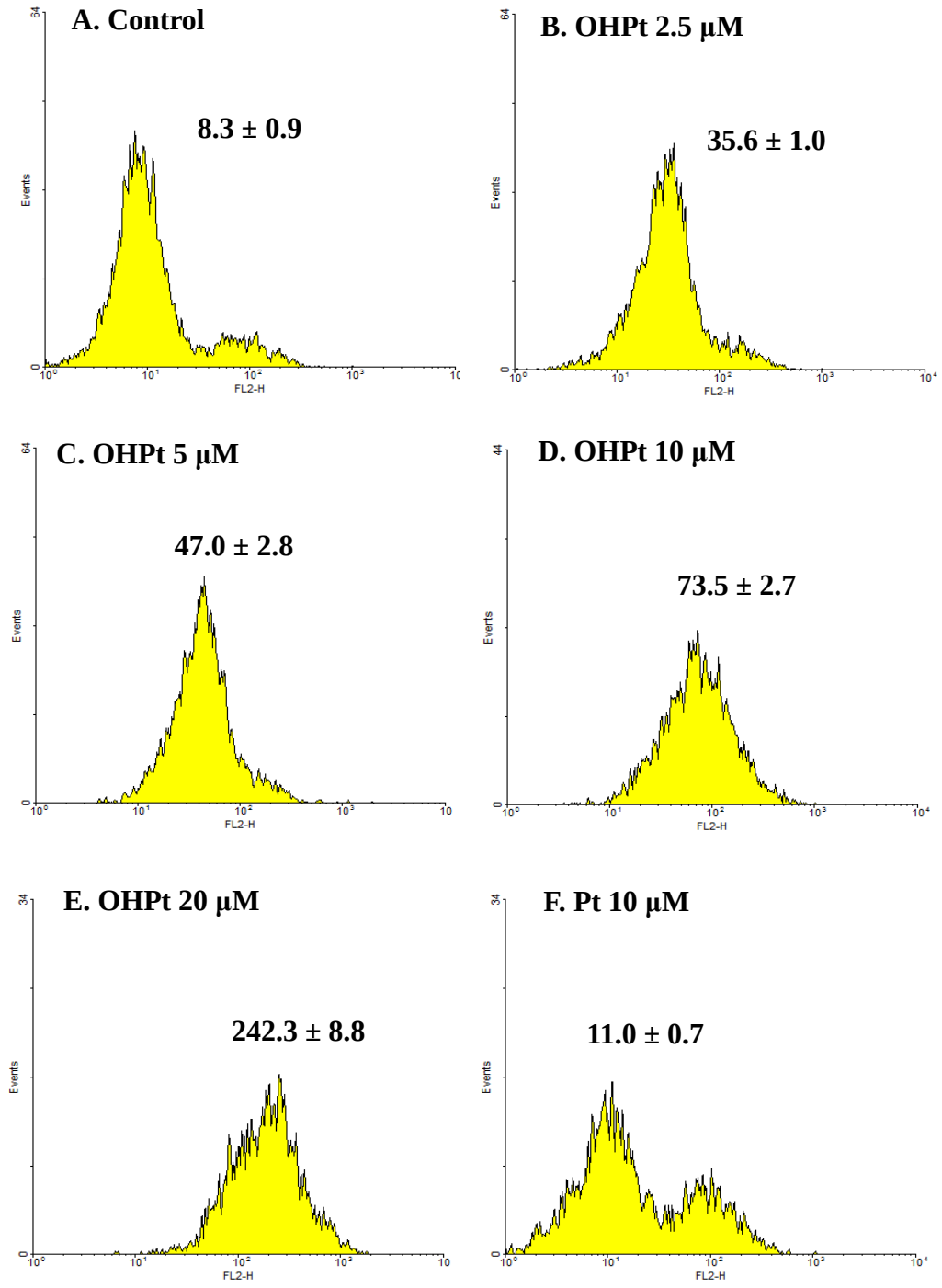

Figure 29. Effects of OHPt and Pt on the activity of caspase-8 in LNCaP cells for 48 hr. LNCaP cells were cultured in serum-free RPMI containing various concentrations of OHPt and Pt for 48 hr, respectively. Then, cells were stained with caspase-8 kit and analyzed by flow cytometry.

6.2.9 Effect of OHPt on Autophagic Protein Beclin-1

Beclin-1 is an important initiator of autophagy during the autophagosome nucleation (*149*). In this study, in order to evaluate whether OHPt induced autophagy in LNCaP cells, we examined the expression of Beclin-1. Our results showed that treatment with 10 μM OHPt could increase the level of autophagic protein Beclin-1 by approximately 30 % (Figure 30).

6.2.10 Effect of OHPt on Autophagic Protein LC3

The LC3 protein plays a critical role in autophagosome formation. Typically, LC3 protein presents in the cytosol, but undergoes cleavage and conjugation with phosphatidylethanolamine, LC3 associates with the autophagic membrane (*148*) . The conversion of LC3-I (14 kDa cytosolic free form) to LC3-II (16 kDa PE-conjugated form) is a key marker for autophagosome formation (*13, 148*). We next determined the expression of LC3B protein by western blotting. The induction of LC3-II was revealed in LNCaP human prostate cancer cells (Figure 30). Treatment with 10 μM OHPt significantly increased LC3-II expression by approximately 3 fold. This result indicated that OHPt induced autophagy tremendously in LNCaP cells.

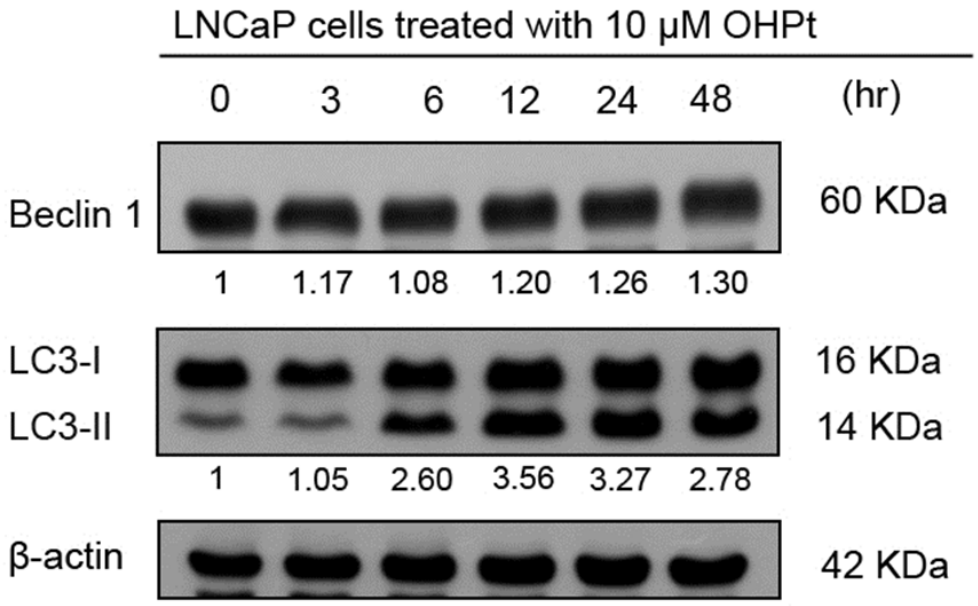

Figure 30. Beclin-1, LC3-I, LC3- II, Actin protein expression in LNCaP cells after 10 µM OHPt treatment at different time intervals. All proteins were quantified by densitometry on immunoblots by Image J software.

6.2.11 Effect of OHPt on Autophagosome Formation

LC3 is involved in the formation of autophagosomes and autophagolysosomes, which are usually characterized and monitored by fluorescence microscopy using green fluorescent protein with LC3 (GFP-LC3) (*73*, *103*, *148*). As shown in Figure 31, the numbers of GFP-LC3-labeled-puncta in cytosol were markedly increased in the OHPt-treated group in comparison with control group. The results indicated that OHPT induced autophagy by increasing the formation of autophagosomes and

autophagolysosomes in LNCaP human prostate cancer cells.

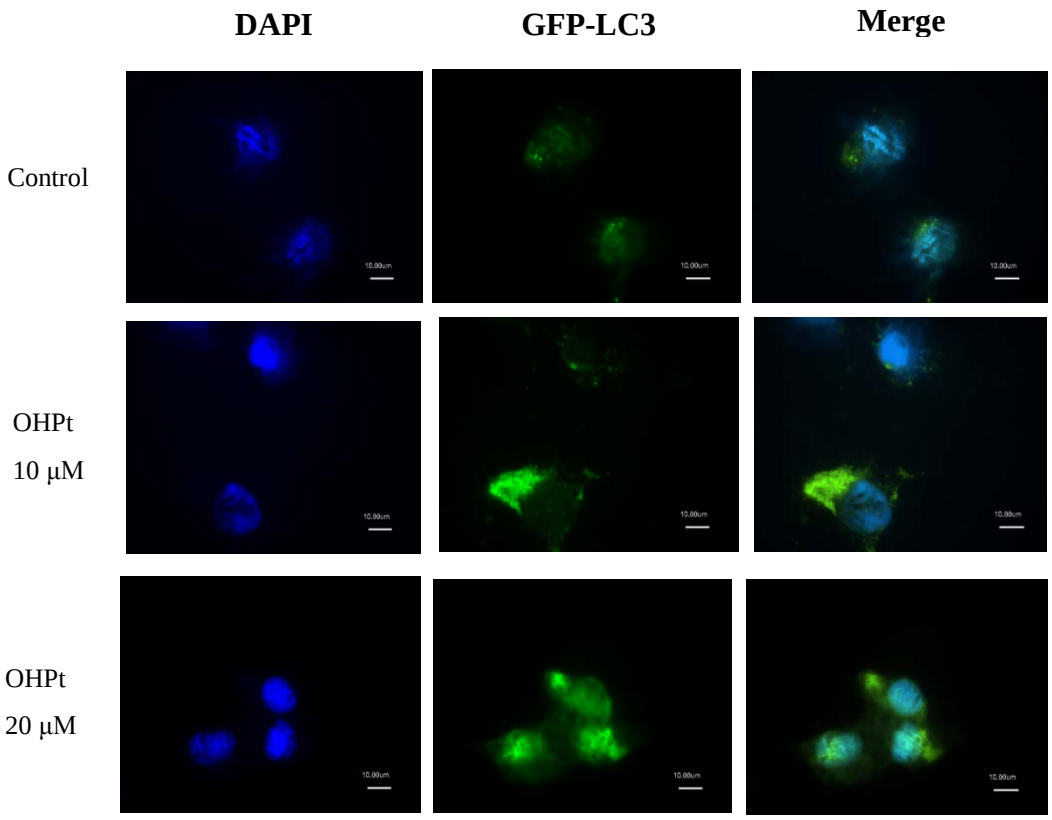

Figure 31. Confocal fluorescence microscopy to detect GFP-LC3 in OHPt-treated LNCaP cells. The cells were transfected with GFP-LC3, then treated with 10 or 20 μM OHPt for 18 hrs and compared with untreated controls. Nuclei were stained with DAPI (blue).

6.3 PC-3 Xenograft Nude Mice Model

Inhibition of human prostate cancer PC-3 cells growth by OHPt provided the important message that treatment with OHPt may be a promising strategy for the management of prostate cancer *in vivo*. To examine this, we performed a PC-3 tumor xenograft study in athymic nude mice. Nude mice bearing PC-3 tumors were orally administrated with OHPt at different dosages (5, 25, 50 mg/kg) and Pt (25 mg/kg) once a day for 4 weeks. The tumor size was analyzed once or twice per week and at the end of the study, the body weight, organ weight and tumor weight were measured.

6.3.1 Effects of OHPt and Pt on the body weight and organ weight in a PC-3 xenograft model

In order to investigate any adverse effects caused by OHPt or Pt treatment, all mice were monitored throughout the study. During the experiment, all treated mice remained alive and without producing any side effects or toxicity by oral administration of OHPt and Pt in any of the doses. As shown in Table 8, the body weight and organ weight did not show any significant difference between each group. Moreover, after treatment with different dosages of OHPt or Pt for 4 weeks, no gross abnormalities were observed in various individual organs.

Table 8. Effects of OHPt and Pt administration on the body weight and relative organ weights in a PC-3 xenograft model

	Body weight (g)	Relative organ weight (mg/g)			
		Liver	Lung	Kidney	Spleen
Control	21.3 ± 3.2	39.3 ± 12.3	6.7 ± 1.6	14.8 ± 1.5	3.6 ± 1.6
OHPt-L	22.5 ± 3.8	43.8 ± 4.6	6.2 ± 1.0	15.8 ± 2.1	2.9 ± 0.5
OHPt-M	24.2 ± 1.6	42.3 ± 5.4	6.1 ± 0.7	16.4 ± 3.1	3.8 ± 1.3
OHPt-H	24.6 ± 1.3	45.6 ± 5.5	5.9 ± 1.8	17.6 ± 2.9	3.7 ± 0.4
Pt-M	21.9 ± 3.3	41.6 ± 5.4	6.7 ± 1.1	16.1 ± 1.6	3.4 ± 0.8

Values are shown as mean ± SD (n=6).

6.3.2 Effects of OHPt and Pt on the tumor weight and tumor volume in a PC-3 xenograft model

Next, we determined whether OHPt and Pt would reduce the growth rate of prostate tumor *in vivo*. As shown in Figure 32, OHPt and Pt significantly decreased the prostate tumors volume during the experiment. Moreover, the tumor volume in OHPt-M group was strongly inhibited in comparison with the Pt-M-treated mice. At the end of the study, the tumors were excised and weighed. The photograph of xenograft tumors developed in each group is shown in Figure 33. Treated with OHPt and Pt could reduce the tumor weight compared with the control group (Tumor weight: Control 2.59 ± 0.38g; OHPt-L 1.09 ± 0.37g; OHPt-M 0.75 ± 0.34g; OHPt-H 0.32 ± 0.21g; Pt-M 1.87 ± 0.18g) (Figure

34). Furthermore, OHPt-M significantly inhibited tumor weight by about 71% compared to control tumors; whereas Pt-M inhibited tumor weight by about 25%. Apparently, the anti-tumor effect of OHPt was more potent than that of Pt in PC-3 xenograft nude mice.

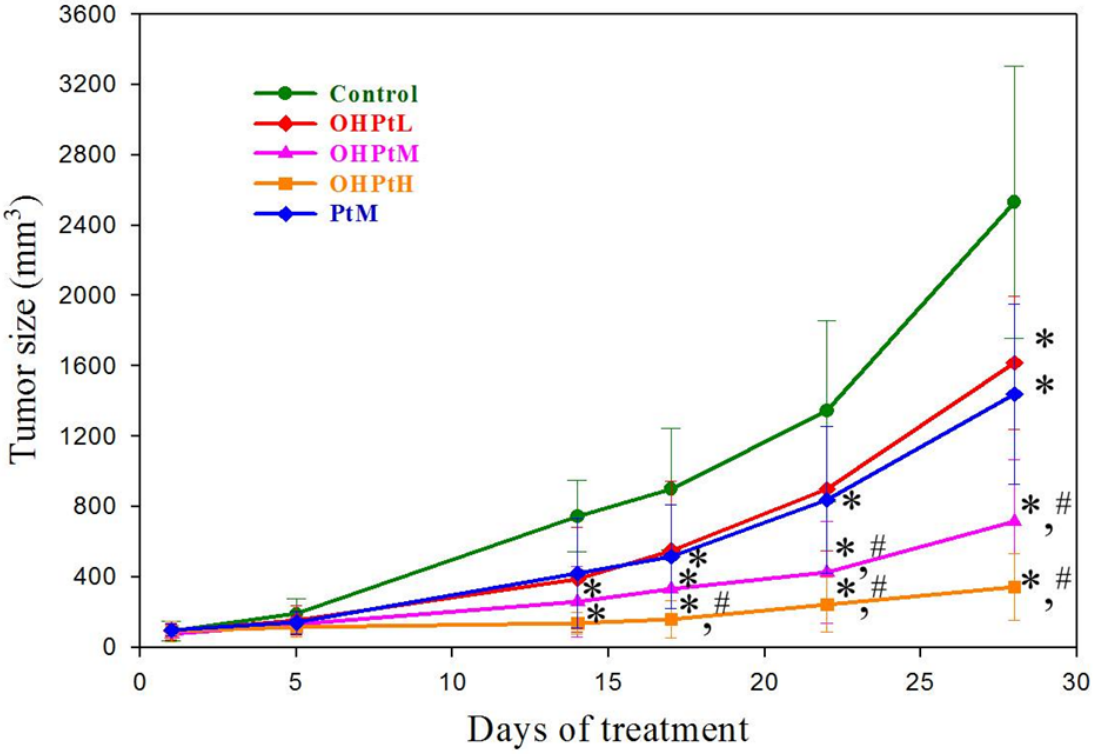

Figure 32. Effects of OHPt or Pt on the tumor volume in xenografted nude mice. The tumor volume was determined by measuring the tumor with external calipers once or twice a week in each mouse. Values are shown as mean ± SD (n=6). *p<0.05 compared with control group. #p<0.05 compared with Pt group.

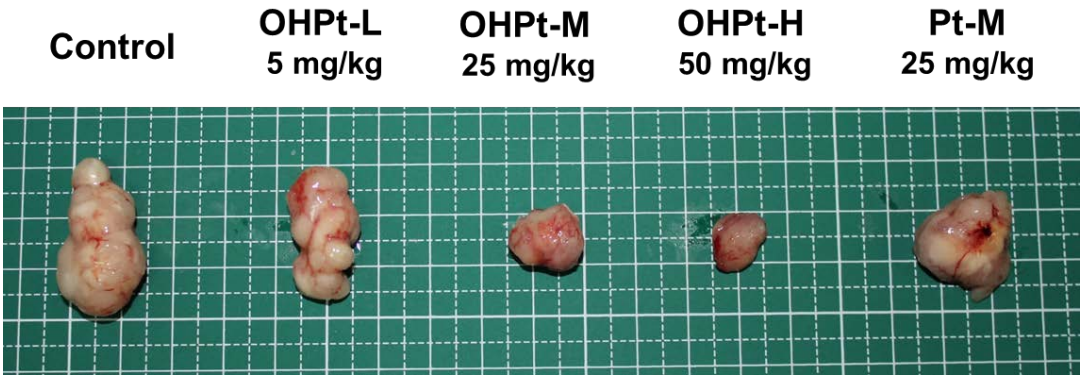

Figure 33. Photograph of xenograft tumors developed in each group is shown at the end of the experiment.

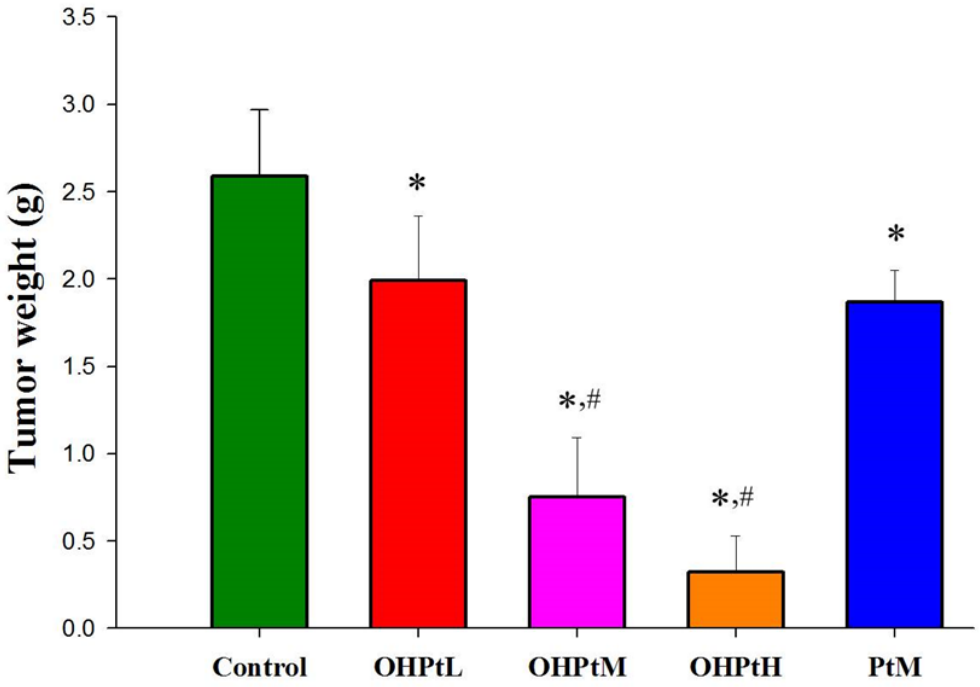

Figure 34. Effects of OHPt or Pt on the tumor weight in xenografted nude mice. Tumor weight was measured at the end of the experiment after excision of the tumor from the euthanized mouse. Values are shown as mean ± SD (n=6). *$p<0.05$ compared with control group. #$p<0.05$ compared with Pt group.

CHAPTER 7. DISCUSSION

Pterostilbene, the 3,5-dimethoxy motif at the A-phenyl ring of resveratrol, has recently received tremendous attention due to its possess potential chemopreventive and chemotherapeutic properties on various cancer types. (*24, 122-130*). Due to this structural characteristic, pterostilbene was found to be more lipophilic and exhibit much better bioavailability and more biologically active than resveratrol (*137*). In present study, we are highly interested in its hydroxyl structural analog, 3'-hydroxypterostilbene, which also contains 3,5-dimethoxy motif at the A-phenyl ring but with an additional hydroxyl group on 3' position. Our present results showed that treatment with Pt or OHPt significantly inhibited the viability of PC-3 and LNCaP cells in a dose-dependent manner. After 48 hrs treatment, the IC_{50} of Pt and OHPt for PC-3 cells are >20 μM and 5 μM, respectively; whereas the IC_{50} of Pt and OHPt for LNCaP cells are 14.4 μM and 2.4 μM, respectively. OHPt showed much stronger inhibitory effects on the growth of the prostate cancer cells in comparison with its parent compound Pt. These results suggested that addition of an OH group to the 3'-position of Pt ameliorated its anti-cancer property. From the chemical structure point of view, OHPt contains a catechol group (3',4'-dihydroxybenzene), while Pt contains a phenol group (4'-hydroxybenzene). In

different publications, multiple catechol and phenol based compounds are reported to have antioxidant and anti-cancer activities (*26, 27, 150*). In a study conducted by Giante *et al*. showed that catechols from abietic acid exhibited various biological activities namely, antifungal, antitumoral, antimutagenic, antiviral and inhibition of nitric oxide production (*151*). Other research group isolated the catechol compound from *Semecarpus anacardium* and demonstrated that this catechol derivative can be developed as an effective anticancer agent in human leukemia, colon carcinoma, breast cancer cells (*27*). Ali *et al*. indicated that several pyridine-amide compounds appended with phenol or catechol groups significantly inhibited the lung, brain, and thyroid malignant cells growth ~~a~~nd increased cellular caspase-3 and caspase-7 activities (*26*). Moreover, in a study by Cai *et al.* showed that the analogs of trans-resveratrol containing 3,4-dihydroxyl groups (catechol groups) had significantly higher antioxidant and apoptotic activities than those of the other analogs containing phenol groups (*150*). In our study, similar results were observed among Pt and OHPt. OHPt containing catechol group possessed much stronger inhibitory effects on the prostate cancer cells growth in comparison with Pt which contains phenol group. Thus, we postulated that OHPt could possess much better anti-cancer activities than Pt might due to its catechol structure. The 3',4'-dihydroxyl groups are important for OHPt to exhibit higher anti-cancer activities.

Next, in order to gain mechanistic information on how OHPt can lead to inhibition of prostate cancer cells growth, we further elucidate the molecular mechanisms of apoptosis and autophagy induced by OHPt on p53 null type PC-3 and p53 wild type LNCaP human prostate cancer cells. The molecular mechanisms of growth inhibitory effects of OHPt on human prostate cancer cells are shown in Figure 35.

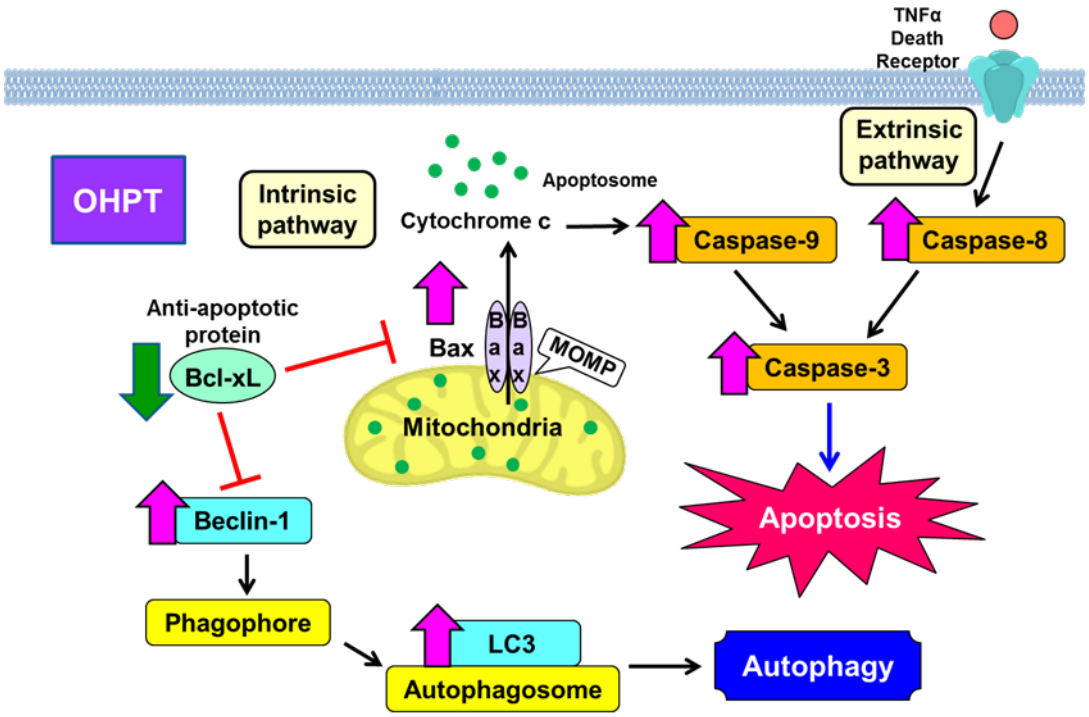

Figure 35. Molecular mechanisms of anti-cancer activity of OHPt on human prostate cancer cells.

The results presented in this study demonstrated that OHPt showed significant growth inhibition effects in both PC-3 and LNCaP human prostate cancer cells.

Treatment with OHPt could promote apoptosis via inducing the mitochondrial outer membrane permeabilization (MOMP) in both PC-3 and LNCaP cancer cells. Disruption of mitochondrial outer membrane integrity is a hallmark of intrinsic apoptotic cell death, since it leads to the release of several apoptogenic factors, such as cytochrome c, into the cytoplasm followed by the activation of downstream death signaling proteins, such as caspase-9 and caspase-3, to execute apoptosis (*66*). In our studies, the intrinsic initiator caspase-9 and the effector caspase-3 were all activated in OHPt-treated prostate cancer cells. Besides, OHPt also induced extrinsic apoptotic pathway by activating caspase-8. The extrinsic apoptotic pathway is mediated by the activation of death receptors belonging to the tumor necrosis factor-α receptor (TNF-R) family, such as FAS/CD95, TNFR and TRAIL, directly activates caspase-8 (*68*, *69*). Once caspase-8 is activated, the execution phase of apoptosis is triggered that activates downstream caspase-3, which leads to apoptotic cell death (*70*). Moreover, OHPt increased the expression of pro-apototic protein Bax and decreased the anti-apoptotic Bcl-2 family protein, Bcl-xL. The pro-apoptotic protein, Bax, plays an important role in inducing MOMP, increasing the release of cytochrome c and subsequently activate the apoptotic caspase cascades (*58*, *63*, *96*, *99*). The anti-apoptotic Bcl-2 family proteins, Bcl-xL, can antagonize pro-apoptotic proteins Bax and inhibit the activator BH3-only protein Bid, Puma and Bim,

thus prevent apoptosis (*58, 63, 96, 99*). In addition, recent newly studies indicated that the anti-apoptotic Bcl-2 family proteins can also inhibit autophagy by interacting with Beclin-1 which can sequester Beclin-1 from binding to Vps34 and prevent its association to Class III PI3K to initiate autophagy (*96, 100*). Thus, the dual function of anti-apoptotic protein Bcl-xL in inhibiting both apoptosis and autophagy makes it as an ideal target for chemotherapy. In our current study, we observed that OHPt could inhibit the Bcl-xL protein levels which might significantly contribute to upregulate both apoptosis and autophagy pathway to lead the cancer cell death. Moreover, OHPt also induced autophagy by increasing the levels of Beclin-1, LC3 proteins and autophagosome formation. Beclin-1 is an initial regulator of autophagy and tumor suppression protein. Numerous studies demonstrated overexpression of Beclin-1 acts as tumor suppressor function (*152, 153*); while heterozygous disruption of Beclin-1 promotes spontaneous tumorigenesis (*154*). Thus, the increasing of Beclin-1 expression results in autophagy which may contribute to the suppression of tumorigenesis. Furthermore, the LC3 protein also plays a critical role in autophagy, which facilitates the autophagosome formation to degrade the dysfunctional and damaged constituents (*148*). Based on above results *in vitro* studies, we know that OHPt has multiple target sites to induce apoptosis and autophagy in both p53 wild type LNCaP and p53 null type PC-3 cells. The underlying

molecular mechanisms of OHPt-induced apoptosis and autophagy were similar between p53 positive and negative prostate cancer cells. These findings indicated that OHPt-induced cell death might not fully dependent on p53 of the cancer cells.

Finally, we performed a PC-3 tumor xenograft model *in vivo* to evaluate the anti-tumor effect of OHPt. Our results demonstrated that OHPt and Pt significantly inhibited tumor growth compared to control tumors. The anti-tumor effect of OHPt was more potent than that of Pt in PC-3 xenograft nude mice. Moreover, the treatment of OHPt in doses from 5 to 50 mg/kg/d for 4 weeks did not cause any deaths or clinical symptoms of toxicity in nude mice. Of note, our results showed that OHPt exhibited strong anti-tumor activities in human prostate xenograft tumors were consistent with other research conducted by Cheng *et al.* in human colon xenograft tumors (*28*). Effective therapeutic effects of OHPt were also demonstrated *in vivo* by treating nude mice bearing human colorectal carcinoma COLO 205 tumor xenografts with intravenous injection of OHPt (10 mg/kg) for 15 days (*28*).

Taken together, OHPt showed great potential as a useful agent for the treatment of human prostate cancer cells *in vitro* and also exhibited strong anti-tumor effect *in vivo*. Thus, OHPt might have significant chemotherapeutic applications for the treatment of prostate cancer.

CHAPTER 8. SUMMARY

In conclusion, our research here demonstrated that OHPt showed much stronger growh inhibitory effects on human prostate cancer cells in comparison with its parent compound Pt. OHPt exerted significant anti-proliferation effects on human prostate cancer PC-3 and LNCaP cells by simultaneously promoting apoptosis and autophagy. Treatment with OHPt triggered apoptosis by disruption of mitochondrial membrane integrity and activation of caspase-8, caspase-9 and caspase-3 in both PC-3 and LNCaP cells. Moreover, OHPt elevated the ratio of pro-apototic Bax to anti-apoptotic Bcl-xL members. These results indicated that OHPt could induce apoptosis via both intrinsic and extrinsic apoptotic pathways. Besides, OHPt enhanced autophagic cell death by upregulating the expression of Beclin-1, LC3 proteins and autophagosome formation. Furthermore, *in vivo* study, OHPt showed potent anti-tumor effects in PC-3 xenograft nude mice. Taken together, our findings provide insight that OHPt might have great potential as a novel and useful agent for the treatment and prevention of human prostate cancer.

REFERENCES

1. Jemal, A.; Siegel, R.; Xu, J.; Ward, E., Cancer statistics, 2010. *CA: a cancer journal for clinicians* **2010,** *60*, 277-300.

2. Ru, P.; Steele, R.; Nerurkar, P. V.; Phillips, N.; Ray, R. B., Bitter melon extract impairs prostate cancer cell-cycle progression and delays prostatic intraepithelial neoplasia in TRAMP model. *Cancer prevention research* **2011,** *4*, 2122-2130.

3. Feldman, B. J.; Feldman, D., The development of androgen-independent prostate cancer. *Nature Reviews Cancer* **2001,** *1*, 34-45.

4. Nixon, R. A., Autophagy in neurodegenerative disease: friend, foe or turncoat? *Trends in neurosciences* **2006,** *29*, 528-535.

5. Bold, R. J.; Termuhlen, P. M.; McConkey, D. J., Apoptosis, cancer and cancer therapy. *Surgical oncology* **1997,** *6*, 133-142.

6. Lockshin, R. A.; Zakeri, Z., Apoptosis, autophagy, and more. *The international journal of biochemistry & cell biology* **2004,** *36*, 2405-2419.

7. Rubinsztein, D. C.; Codogno, P.; Levine, B., Autophagy modulation as a potential therapeutic target for diverse diseases. *Nature reviews Drug discovery* **2012,** *11*, 709-730.

8. Shimizu, S.; Yoshida, T.; Tsujioka, M.; Arakawa, S., Autophagic cell death and cancer. *International journal of molecular sciences* **2014,** *15*, 3145-53.

9. Ouyang, L.; Shi, Z.; Zhao, S.; Wang, F. T.; Zhou, T. T.; Liu, B.; Bao, J. K., Programmed cell death pathways in cancer: a review of apoptosis, autophagy and programmed necrosis. *Cell proliferation* **2012,** *45*, 487-98.

10. Lawen, A., Apoptosis-an introduction. *BioEssays : news and reviews in molecular, cellular and developmental biology* **2003,** *25*, 888-96.

11. Patel, A. S.; Lin, L.; Geyer, A.; Haspel, J. A.; An, C. H.; Cao, J.; Rosas, I. O.; Morse,

D., Autophagy in idiopathic pulmonary fibrosis. *PloS one* **2012,** *7*, e41394.

12. Bincoletto, C.; Bechara, A.; Pereira, G.; Santos, C.; Antunes, F.; Peixoto da-Silva, J.; Muler, M.; Gigli, R.; Monteforte, P.; Hirata, H., Interplay between apoptosis and autophagy, a challenging puzzle: new perspectives on antitumor chemotherapies. *Chemico-biological interactions* **2013,** *206*, 279-288.

13. Choi, A. M.; Ryter, S. W.; Levine, B., Autophagy in human health and disease. *The New England journal of medicine* **2013,** *368*, 1845-6.

14. Yao, Q.; Chen, J.; Lv, Y.; Wang, T.; Zhang, J.; Fan, J.; Wang, L., The significance of expression of autophagy-related gene Beclin, Bcl-2, and Bax in breast cancer tissues. *Tumor Biology* **2011,** *32*, 1163-1171.

15. Scarlatti, F.; Maffei, R.; Beau, I.; Codogno, P.; Ghidoni, R., Role of non-canonical Beclin 1-independent autophagy in cell death induced by resveratrol in human breast cancer cells. *Cell Death & Differentiation* **2008,** *15*, 1318-1329.

16. Seong, Y.-A.; Shin, P.-G.; Yoon, J.-S.; Yadunandam, A. K.; Kim, G.-D., Induction of the endoplasmic reticulum stress and autophagy in human lung carcinoma A549 cells by anacardic acid. *Cell biochemistry and biophysics* **2014,** *68*, 369-377.

17. Surh, Y.-J., Cancer chemoprevention with dietary phytochemicals. *Nature Reviews Cancer* **2003,** *3*, 768-780.

18. Lin, V. C.; Tsai, Y. C.; Lin, J. N.; Fan, L. L.; Pan, M. H.; Ho, C. T.; Wu, J. Y.; Way, T. D., Activation of AMPK by pterostilbene suppresses lipogenesis and cell-cycle progression in p53 positive and negative human prostate cancer cells. *Journal of agricultural and food chemistry* **2012,** *60*, 6399-407.

19. Roupe, K. A.; Remsberg, C. M.; Yáñez, J. A.; Davies, N. M., Pharmacometrics of stilbenes: seguing towards the clinic. *Current clinical pharmacology* **2006,** *1*, 81-101.

20. Ma, Z.-j.; Li, X.; Li, N.; Wang, J.-h., Stilbenes from< i> Sphaerophysa salsula</i>. *Fitoterapia* **2002,** *73*, 313-315.

21. McCormack, D.; McFadden, D., Pterostilbene and cancer: current review. *The Journal of surgical research* **2012,** *173*, e53-61.

22. Wang, T. T.; Schoene, N. W.; Kim, Y. S.; Mizuno, C. S.; Rimando, A. M., Differential effects of resveratrol and its naturally occurring methylether analogs on cell cycle and apoptosis in human androgen-responsive LNCaP cancer cells. *Molecular nutrition & food research* **2010,** *54*, 335-44.

23. Chakraborty, A.; Gupta, N.; Ghosh, K.; Roy, P., In vitro evaluation of the cytotoxic, anti-proliferative and anti-oxidant properties of pterostilbene isolated from Pterocarpus marsupium. *Toxicology in vitro : an international journal published in association with BIBRA* **2010,** *24*, 1215-28.

24. Lin, V. C.-H.; Tsai, Y.-C.; Lin, J.-N.; Fan, L.-L.; Pan, M.-H.; Ho, C.-T.; Wu, J.-Y.; Way, T.-D., Activation of AMPK by pterostilbene suppresses lipogenesis and cell-cycle progression in p53 positive and negative human prostate cancer cells. *Journal of agricultural and food chemistry* **2012,** *60*, 6399-6407.

25. Tolomeo, M.; Grimaudo, S.; Di Cristina, A.; Roberti, M.; Pizzirani, D.; Meli, M.; Dusonchet, L.; Gebbia, N.; Abbadessa, V.; Crosta, L.; Barucchello, R.; Grisolia, G.; Invidiata, F.; Simoni, D., Pterostilbene and 3'-hydroxypterostilbene are effective apoptosis-inducing agents in MDR and BCR-ABL-expressing leukemia cells. *The international journal of biochemistry & cell biology* **2005,** *37*, 1709-26.

26. Ali, A.; Bansal, D.; Kaushik, N. K.; Kaushik, N.; Choi, E. H.; Gupta, R., Syntheses, characterization, and anti-cancer activities of pyridine-amide based compounds containing appended phenol or catechol groups. *Journal of Chemical Sciences* **2014,** *126*, 1091-1105.

27. Nair, P. R.; Melnick, S. J.; Wnuk, S. F.; Rapp, M.; Escalon, E.; Ramachandran, C., Isolation and characterization of an anticancer catechol compound from Semecarpus anacardium. *Journal of ethnopharmacology* **2009,** *122*, 450-456.

28. Cheng, T.-C.; Lai, C.-S.; Chung, M.-C.; Kalyanam, N.; Majeed, M.; Ho, C.-T.; Ho, Y.-S.; Pan, M.-H., Potent Anti-Cancer Effect of 3′-Hydroxypterostilbene in Human Colon Xenograft Tumors. **2014**.

29. Krumwiede, K. A.; Krumwiede, N. In *The lived experience of men diagnosed with prostate cancer*, Oncology nursing forum, 2012; Onc Nurs Society: 2012; pp E443-E450.

30. Schröder, F.; Hermanek, P.; Denis, L.; Fair, W.; Gospodarowicz, M.; Pavone-Macaluso, M., The TNM classification of prostate cancer. *The Prostate* **1992,** *21*, 129-138.

31. Ohori, M.; Wheeler, T. M.; Scardino, P. T., The new American joint committee on cancer and international union against cancer TNM classification of prostate cancer. *Cancer* **1994,** *74*, 104-114.

32. Edge, S. B.; Compton, C. C., The American Joint Committee on Cancer: the 7th edition of the AJCC cancer staging manual and the future of TNM. *Annals of surgical oncology* **2010,** *17*, 1471-1474.

33. Scherr, D.; Swindle, P. W.; Scardino, P. T., National Comprehensive Cancer Network guidelines for the management of prostate cancer. *Urology* **2003,** *61*, 14-24.

34. Partin, A.; Yoo, J.; Carter, H. B.; Pearson, J.; Chan, D.; Epstein, J.; Walsh, P., The use of prostate specific antigen, clinical stage and Gleason score to predict pathological stage in men with localized prostate cancer. *The Journal of urology* **1993,** *150*, 110-114.

35. Partin, A. W.; Kattan, M. W.; Subong, E. N.; Walsh, P. C.; Wojno, K. J.; Oesterling, J. E.; Scardino, P. T.; Pearson, J., Combination of prostate-specific antigen, clinical stage, and Gleason score to predict pathological stage of localized prostate cancer: a multi-institutional update. *Jama* **1997,** *277*, 1445-1451.

36. Thomas, L. N.; Douglas, R. C.; Lazier, C. B.; Too, C. K.; Rittmaster, R. S.; Tindall, D. J., Type 1 and type 2 5α-reductase expression in the development and progression of prostate cancer. *European urology* **2008,** *53*, 244-252.

37. Hurwitz, A. A.; Foster, B. A.; Allison, J. P.; Greenberg, N. M.; Kwon, E. D., The TRAMP mouse as a model for prostate cancer. *Current protocols in immunology* **2001**, 20.5. 1-20.5. 23.

38. Lee, S.-C.; Chan, W.-K.; Lee, T.-W.; Lam, W.-H.; Wang, X.; Chan, T.-H.; Wong,

Y.-C., Effect of a prodrug of the green tea polyphenol (-)-epigallocatechin-3-gallate on the growth of androgen-independent prostate cancer in vivo. *Nutrition and cancer* **2008,** *60*, 483-491.

39. Arnold, J.; Isaacs, J., Mechanisms involved in the progression of androgen-independent prostate cancers: it is not only the cancer cell's fault. *Endocrine-related cancer* **2002,** *9*, 61-73.

40. Miyamoto, H.; Messing, E. M.; Chang, C., Androgen deprivation therapy for prostate cancer: current status and future prospects. *The Prostate* **2004,** *61*, 332-353.

41. Nesslinger, N. J.; Shi, X.-B.; deVere White, R. W., Androgen-independent growth of LNCaP prostate cancer cells is mediated by gain-of-function mutant p53. *Cancer research* **2003,** *63*, 2228-2233.

42. Heidenberg, H. B.; Sesterhenn, I. A.; Gaddipati, J. P.; Weghorst, C. M.; Buzard, G. S.; Moul, J. W., Alteration of the tumor suppressor gene p53 in a high fraction of hormone refractory prostate cancer. *The Journal of urology* **1995,** *154*, 414-421.

43. Horoszewicz, J. S.; Leong, S. S.; Kawinski, E.; Karr, J. P.; Rosenthal, H.; Chu, T. M.; Mirand, E. A.; Murphy, G. P., LNCaP model of human prostatic carcinoma. *Cancer research* **1983,** *43*, 1809-1818.

44. Thalmann, G. N.; Anezinis, P. E.; Chang, S.-M.; Zhau, H. E.; Kim, E. E.; Hopwood, V. L.; Pathak, S.; von Eschenbach, A. C.; Chung, L. W., Androgen-independent cancer progression and bone metastasis in the LNCaP model of human prostate cancer. *Cancer research* **1994,** *54*, 2577-2581.

45. Ringer, L.; Sirajuddin, P.; Tricoli, L.; Waye, S.; Choudhry, M. U.; Parasido, E.; Sivakumar, A.; Heckler, M.; Naeem, A.; Abdelgawad, I., The induction of the p53 tumor suppressor protein bridges the apoptotic and autophagic signaling pathways to regulate cell death in prostate cancer cells. *Oncotarget* **2014,** *5*, 10678.

46. Wu, X.; Gong, S.; Roy-Burman, P.; Lee, P.; Culig, Z., Current mouse and cell models in prostate cancer research. *Endocrine-related cancer* **2013,** *20*, R155-R170.

47. Aalinkeel, R.; Nair, M. P.; Sufrin, G.; Mahajan, S. D.; Chadha, K. C.; Chawda, R. P.; Schwartz, S. A., Gene expression of angiogenic factors correlates with metastatic potential of prostate cancer cells. *Cancer research* **2004,** *64*, 5311-5321.

48. Lim, D. J.; Liu, X. L.; Sutkowski, D. M.; Braun, E. J.; Lee, C.; Kozlowski, J. M., Growth of an androgen-sensitive human prostate cancer cell line, LNCaP, in nude mice. *The Prostate* **1993,** *22*, 109-118.

49. Taylor, R. C.; Cullen, S. P.; Martin, S. J., Apoptosis: controlled demolition at the cellular level. *Nature reviews Molecular cell biology* **2008,** *9*, 231-241.

50. Leist, M.; Jäättelä, M., Four deaths and a funeral: from caspases to alternative mechanisms. *Nature Reviews Molecular Cell Biology* **2001,** *2*, 589-598.

51. Ouyang, L.; Shi, Z.; Zhao, S.; Wang, F. T.; Zhou, T. T.; Liu, B.; Bao, J. K., Programmed cell death pathways in cancer: a review of apoptosis, autophagy and programmed necrosis. *Cell proliferation* **2012,** *45*, 487-498.

52. Elmore, S., Apoptosis: a review of programmed cell death. *Toxicologic pathology* **2007,** *35*, 495-516.

53. Reed, J. C., Apoptosis-based therapies. *Nature reviews. Drug discovery* **2002,** *1*, 111-21.

54. Yuan, J.; Yankner, B. A., Apoptosis in the nervous system. *Nature* **2000,** *407*, 802-9.

55. Hengartner, M. O., The biochemistry of apoptosis. *Nature* **2000,** *407*, 770-776.

56. Saraste, A.; Pulkki, K., Morphologic and biochemical hallmarks of apoptosis. *Cardiovascular research* **2000,** *45*, 528-537.

57. Kurosaka, K.; Takahashi, M.; Watanabe, N.; Kobayashi, Y., Silent cleanup of very early apoptotic cells by macrophages. *The Journal of Immunology* **2003,** *171*, 4672-4679.

58. Garrido, C.; Galluzzi, L.; Brunet, M.; Puig, P.; Didelot, C.; Kroemer, G., Mechanisms of cytochrome c release from mitochondria. *Cell Death & Differentiation*

2006, *13*, 1423-1433.

59. Du, C.; Fang, M.; Li, Y.; Li, L.; Wang, X., Smac, a mitochondrial protein that promotes cytochrome c–dependent caspase activation by eliminating IAP inhibition. *cell* **2000,** *102*, 33-42.

60. Fadeel, B.; Ottosson, A.; Pervaiz, S., Big wheel keeps on turning: apoptosome regulation and its role in chemoresistance. *Cell Death & Differentiation* **2007,** *15*, 443-452.

61. Hill, M. M.; Adrain, C.; Duriez, P. J.; Creagh, E. M.; Martin, S. J., Analysis of the composition, assembly kinetics and activity of native Apaf-1 apoptosomes. *The EMBO journal* **2004,** *23*, 2134-2145.

62. Schimmer, A. D., Inhibitor of apoptosis proteins: translating basic knowledge into clinical practice. *Cancer research* **2004,** *64*, 7183-7190.

63. Tait, S. W.; Green, D. R., Mitochondria and cell death: outer membrane permeabilization and beyond. *Nature reviews Molecular cell biology* **2010,** *11*, 621-632.

64. Rudner, J.; Elsaesser, S. J.; Jendrossek, V.; Huber, S. M., Anti-apoptotic Bcl-2 fails to form efficient complexes with pro-apoptotic Bak to protect from Celecoxib-induced apoptosis. *Biochemical pharmacology* **2011,** *81*, 32-42.

65. Cory, S.; Adams, J. M., The Bcl2 family: regulators of the cellular life-or-death switch. *Nature Reviews Cancer* **2002,** *2*, 647-656.

66. Tsujimoto, Y., Cell death regulation by the Bcl-2 protein family in the mitochondria. *Journal of cellular physiology* **2003,** *195*, 158-167.

67. Haupt, S.; Berger, M.; Goldberg, Z.; Haupt, Y., Apoptosis-the p53 network. *Journal of cell science* **2003,** *116*, 4077-4085.

68. Ashkenazi, A., Targeting death and decoy receptors of the tumour-necrosis factor superfamily. *Nature Reviews Cancer* **2002,** *2*, 420-430.

69. Koehler, B. C.; Jäger, D.; Schulze-Bergkamen, H., Targeting cell death signaling in colorectal cancer: Current strategies and future perspectives. *World journal of gastroenterology: WJG* **2014,** *20*, 1923.

70. Locksley, R. M.; Killeen, N.; Lenardo, M. J., The TNF and TNF receptor superfamilies-integrating mammalian biology. *Cell* **2001,** *104*, 487-501.

71. Kaufmann, T.; Strasser, A.; Jost, P., Fas death receptor signalling: roles of Bid and XIAP. *Cell Death & Differentiation* **2011,** *19*, 42-50.

72. Gross, A., BID as a double agent in cell life and death. *Cell cycle* **2006,** *5*, 582-584.

73. Levine, B.; Kroemer, G., Autophagy in the pathogenesis of disease. *Cell* **2008,** *132*, 27-42.

74. Mizushima, N.; Komatsu, M., Autophagy: renovation of cells and tissues. *Cell* **2011,** *147*, 728-741.

75. Mizushima, N.; Levine, B.; Cuervo, A. M.; Klionsky, D. J., Autophagy fights disease through cellular self-digestion. *Nature* **2008,** *451*, 1069-1075.

76. Sengupta, S.; Peterson, T. R.; Sabatini, D. M., Regulation of the mTOR complex 1 pathway by nutrients, growth factors, and stress. *Molecular cell* **2010,** *40*, 310-322.

77. Hosokawa, N.; Hara, T.; Kaizuka, T.; Kishi, C.; Takamura, A.; Miura, Y.; Iemura, S.-i.; Natsume, T.; Takehana, K.; Yamada, N., Nutrient-dependent mTORC1 association with the ULK1–Atg13–FIP200 complex required for autophagy. *Molecular biology of the cell* **2009,** *20*, 1981-1991.

78. Ganley, I. G.; Lam, D. H.; Wang, J.; Ding, X.; Chen, S.; Jiang, X., ULK1· ATG13· FIP200 complex mediates mTOR signaling and is essential for autophagy. *Journal of Biological Chemistry* **2009,** *284*, 12297-12305.

79. Liang, C., Negative regulation of autophagy. *Cell Death & Differentiation* **2010,** *17*, 1807-1815.

80. Lum, J. J.; Bauer, D. E.; Kong, M.; Harris, M. H.; Li, C.; Lindsten, T.; Thompson, C. B., Growth factor regulation of autophagy and cell survival in the absence of apoptosis. *Cell* **2005,** *120*, 237-248.

81. Wang, R. C.; Wei, Y.; An, Z.; Zou, Z.; Xiao, G.; Bhagat, G.; White, M.; Reichelt, J.; Levine, B., Akt-mediated regulation of autophagy and tumorigenesis through Beclin 1 phosphorylation. *Science* **2012,** *338*, 956-959.

82. Axe, E. L.; Walker, S. A.; Manifava, M.; Chandra, P.; Roderick, H. L.; Habermann, A.; Griffiths, G.; Ktistakis, N. T., Autophagosome formation from membrane compartments enriched in phosphatidylinositol 3-phosphate and dynamically connected to the endoplasmic reticulum. *The Journal of cell biology* **2008,** *182*, 685-701.

83. Wei, Y.; Sinha, S.; Levine, B., Dual role of JNK1-mediated phosphorylation of Bcl-2 in autophagy and apoptosis regulation. *Autophagy* **2008,** *4*, 949-951.

84. Mizushima, N.; Yoshimori, T.; Ohsumi, Y., The role of Atg proteins in autophagosome formation. *Annual review of cell and developmental biology* **2011,** *27*, 107-132.

85. Ohsumi, Y.; Mizushima, N. In *Two ubiquitin-like conjugation systems essential for autophagy*, Seminars in cell & developmental biology, 2004; Academic Press: 2004; pp 231-236.

86. Geng, J.; Klionsky, D. J., The Atg8 and Atg12 ubiquitin-like conjugation systems in macroautophagy. *EMBO reports* **2008,** *9*, 859-864.

87. Yorimitsu, T.; Klionsky, D. J., Autophagy: molecular machinery for self-eating. *Cell Death & Differentiation* **2005,** *12*, 1542-1552.

88. Hanada, T.; Noda, N. N.; Satomi, Y.; Ichimura, Y.; Fujioka, Y.; Takao, T.; Inagaki, F.; Ohsumi, Y., The Atg12-Atg5 conjugate has a novel E3-like activity for protein lipidation in autophagy. *Journal of Biological Chemistry* **2007,** *282*, 37298-37302.

89. Mizushima, N.; Yoshimori, T.; Levine, B., Methods in mammalian autophagy research. *Cell* **2010,** *140*, 313-326.

90. Satoo, K.; Noda, N. N.; Kumeta, H.; Fujioka, Y.; Mizushima, N.; Ohsumi, Y.; Inagaki, F., The structure of Atg4B–LC3 complex reveals the mechanism of LC3 processing and delipidation during autophagy. *The EMBO Journal* **2009,** *28*, 1341-1350.

91. Bergmann, A., Autophagy and cell death: no longer at odds. *Cell* **2007,** *131*, 1032-1034.

92. Gordy, C.; He, Y.-W., The crosstalk between autophagy and apoptosis: where does this lead? *Protein & cell* **2012,** *3*, 17-27.

93. Maiuri, M. C.; Zalckvar, E.; Kimchi, A.; Kroemer, G., Self-eating and self-killing: crosstalk between autophagy and apoptosis. *Nature reviews Molecular cell biology* **2007,** *8*, 741-752.

94. Eisenberg-Lerner, A.; Bialik, S.; Simon, H.; Kimchi, A., Life and death partners: apoptosis, autophagy and the cross-talk between them. *Cell Death & Differentiation* **2009,** *16*, 966-975.

95. Zhou, F.; Yang, Y.; Xing, D., Bcl-2 and Bcl-xL play important roles in the crosstalk between autophagy and apoptosis. *FEBS journal* **2011,** *278*, 403-413.

96. Wu, H.-J.; Pu, J.-L.; Krafft, P. R.; Zhang, J.-M.; Chen, S., The molecular mechanisms between autophagy and apoptosis: Potential role in central nervous system disorders. *Cellular and molecular neurobiology* **2014**, 1-15.

97. Djavaheri-Mergny, M.; Maiuri, M.; Kroemer, G., Cross talk between apoptosis and autophagy by caspase-mediated cleavage of Beclin 1. *Oncogene* **2010,** *29*, 1717-1719.

98. Maiuri, M. C.; Criollo, A.; Kroemer, G., Crosstalk between apoptosis and autophagy within the Beclin 1 interactome. *EMBO Journal* **2010,** *29*, 515.

99. Green, D. R.; Evan, G. I., A matter of life and death. *Cancer cell* **2002,** *1*, 19-30.

100. Marquez, R. T.; Xu, L., Bcl-2: Beclin 1 complex: multiple, mechanisms regulating autophagy/apoptosis toggle switch. *American journal of cancer research* **2012,** *2*, 214.

101. Wirawan, E.; Walle, L. V.; Kersse, K.; Cornelis, S.; Claerhout, S.; Vanoverberghe, I.; Roelandt, R.; De Rycke, R.; Verspurten, J.; Declercq, W., Caspase-mediated cleavage of Beclin-1 inactivates Beclin-1-induced autophagy and enhances apoptosis by promoting the release of proapoptotic factors from mitochondria. *Cell death & disease* **2010,** *1*, e18.

102. Fimia, G. M.; Piacentini, M., Regulation of autophagy in mammals and its interplay with apoptosis. *Cellular and molecular life sciences* **2010,** *67*, 1581-1588.

103. Ravikumar, B.; Sarkar, S.; Davies, J. E.; Futter, M.; Garcia-Arencibia, M.; Green-Thompson, Z. W.; Jimenez-Sanchez, M.; Korolchuk, V. I.; Lichtenberg, M.; Luo, S., Regulation of mammalian autophagy in physiology and pathophysiology. *Physiological reviews* **2010,** *90*, 1383-1435.

104.Chaabane, W.; El-Gazzah, M.; Jaksik, R.; Sajjadi, E.; Rzeszowska-Wolny, J.; Łos, M. J., Autophagy, apoptosis, mitoptosis and necrosis: interdependence between those pathways and effects on cancer. *Archivum immunologiae et therapiae experimentalis* **2013,** *61*, 43-58.

105. Lengauer, C.; Kinzler, K. W.; Vogelstein, B., Genetic instabilities in human cancers. *Nature* **1998,** *396*, 643-649.

106. Maiuri, M. C.; Galluzzi, L.; Morselli, E.; Kepp, O.; Malik, S. A.; Kroemer, G., Autophagy regulation by p53. *Current opinion in cell biology* **2010,** *22*, 181-185.

107. Chipuk, J. E.; Bouchier-Hayes, L.; Kuwana, T.; Newmeyer, D. D.; Green, D. R., PUMA couples the nuclear and cytoplasmic proapoptotic function of p53. *Science* **2005,** *309*, 1732-1735.

108. Tasdemir, E.; Maiuri, M. C.; Morselli, E.; Criollo, A.; D'Amelio, M.; Djavaheri-Mergny, M.; Cecconi, F.; Tavernarakis, N.; Kroemer, G., A dual role of p53 in the control of autophagy. *Autophagy* **2008,** *4*, 810-814.

109. Mariño, G.; Niso-Santano, M.; Baehrecke, E. H.; Kroemer, G., Self-consumption: the interplay of autophagy and apoptosis. *Nature reviews Molecular cell biology* **2014,** *15*, 81-94.

110. Levine, B.; Abrams, J., p53: The Janus of autophagy? *Nature cell biology* **2008,** *10*, 637-639.

111. Dai, C.; Gu, W., p53 post-translational modification: deregulated in tumorigenesis. *Trends in molecular medicine* **2010,** *16*, 528-536.

112. Morselli, E.; Shen, S.; Ruckenstuhl, C.; Bauer, M. A.; Mariño, G.; Galluzzi, L.; Criollo, A.; Michaud, M.; Maiuri, M. C.; Chano, T., p53 inhibits autophagy by interacting with the human ortholog of yeast Atg17, RB1CC1/FIP200. *Cell cycle* **2011,** *10*, 2763-2769.

113. Rimando, A. M.; Kalt, W.; Magee, J. B.; Dewey, J.; Ballington, J. R., Resveratrol, pterostilbene, and piceatannol in vaccinium berries. *Journal of agricultural and food chemistry* **2004,** *52*, 4713-4719.

114. Rodríguez-Bonilla, P.; López-Nicolás, J. M.; Méndez-Cazorla, L.; García-Carmona, F., Development of a reversed phase high performance liquid chromatography method based on the use of cyclodextrins as mobile phase additives to determine pterostilbene in blueberries. *Journal of Chromatography B* **2011,** *879*, 1091-1097.

115. McFadden, D., A review of pterostilbene antioxidant activity and disease modification. *Oxidative medicine and cellular longevity* **2013,** *2013*.

116. Mak, K. K.; Wu, A. T.; Lee, W. H.; Chang, T. C.; Chiou, J. F.; Wang, L. S.; Wu, C. H.; Huang, C. Y.; Shieh, Y. S.; Chao, T. Y.; Ho, C. T.; Yen, G. C.; Yeh, C. T., Pterostilbene, a bioactive component of blueberries, suppresses the generation of breast cancer stem cells within tumor microenvironment and metastasis via modulating NF-kappaB/microRNA 448 circuit. *Molecular nutrition & food research* **2013,** *57*, 1123-34.

117. Paul, S.; DeCastro, A. J.; Lee, H. J.; Smolarek, A. K.; So, J. Y.; Simi, B.; Wang, C. X.; Zhou, R.; Rimando, A. M.; Suh, N., Dietary intake of pterostilbene, a constituent of blueberries, inhibits the β-catenin/p65 downstream signaling pathway and colon carcinogenesis in rats. *Carcinogenesis* **2010,** *31*, 1272-1278.

118. Chiou, Y.-S.; Tsai, M.-L.; Wang, Y.-J.; Cheng, A.-C.; Lai, W.-M.; Badmaev, V.; Ho,

C.-T.; Pan, M.-H., Pterostilbene inhibits colorectal aberrant crypt foci (ACF) and colon carcinogenesis via suppression of multiple signal transduction pathways in azoxymethane-treated mice. *Journal of agricultural and food chemistry* **2010,** *58*, 8833-8841.

119. Rimando, A. M.; Nagmani, R.; Feller, D. R.; Yokoyama, W., Pterostilbene, a new agonist for the peroxisome proliferator-activated receptor α-isoform, lowers plasma lipoproteins and cholesterol in hypercholesterolemic hamsters. *Journal of agricultural and food chemistry* **2005,** *53*, 3403-3407.

120. Pari, L.; Satheesh, M. A., Effect of pterostilbene on hepatic key enzymes of glucose metabolism in streptozotocin-and nicotinamide-induced diabetic rats. *Life sciences* **2006,** *79*, 641-645.

121. Hsu, C.-L.; Lin, Y.-J.; Ho, C.-T.; Yen, G.-C., The inhibitory effect of pterostilbene on inflammatory responses during the interaction of 3T3-L1 adipocytes and RAW 264.7 macrophages. *Journal of agricultural and food chemistry* **2013,** *61*, 602-610.

122. Chen, R. J.; Ho, C. T.; Wang, Y. J., Pterostilbene induces autophagy and apoptosis in sensitive and chemoresistant human bladder cancer cells. *Molecular nutrition & food research* **2010,** *54*, 1819-1832.

123. Wang, Y.; Ding, L.; Wang, X.; Zhang, J.; Han, W.; Feng, L.; Sun, J.; Jin, H.; Wang, X. J., Pterostilbene simultaneously induces apoptosis, cell cycle arrest and cyto-protective autophagy in breast cancer cells. *American journal of translational research* **2012,** *4*, 44.

124. Paul, S.; Rimando, A. M.; Lee, H. J.; Ji, Y.; Reddy, B. S.; Suh, N., Anti-inflammatory action of pterostilbene is mediated through the p38 mitogen-activated protein kinase pathway in colon cancer cells. *Cancer prevention research* **2009,** *2*, 650-657.

125. Tolomeo, M.; Grimaudo, S.; Cristina, A. D.; Roberti, M.; Pizzirani, D.; Meli, M.; Dusonchet, L.; Gebbia, N.; Abbadessa, V.; Crosta, L., Pterostilbene and 3′-hydroxypterostilbene are effective apoptosis-inducing agents in MDR and BCR-ABL-expressing leukemia cells. *The international journal of biochemistry & cell biology* **2005,** *37*, 1709-1726.

126. Remsberg, C. M.; Yáñez, J. A.; Ohgami, Y.; Vega-Villa, K. R.; Rimando, A. M.; Davies, N. M., Pharmacometrics of pterostilbene: preclinical pharmacokinetics and metabolism, anticancer, antiinflammatory, antioxidant and analgesic activity. *Phytotherapy Research* **2008,** *22*, 169-179.

127. Schneider, J. G.; Alosi, J. A.; McDonald, D. E.; McFadden, D. W., Pterostilbene inhibits lung cancer through induction of apoptosis. *Journal of Surgical Research* **2010,** *161*, 18-22.

128. Ferrer, P.; Asensi, M.; Segarra, R.; Ortega, A.; Benlloch, M.; Obrador, E.; Varea, M. T.; Asensio, G.; Jordá, L.; Estrela, J. M., Association between pterostilbene and quercetin inhibits metastatic activity of B16 melanoma. *Neoplasia* **2005,** *7*, 37-47.

129. McCormack, D. E.; Mannal, P.; McDonald, D.; Tighe, S.; Hanson, J.; McFadden, D., Genomic analysis of pterostilbene predicts its antiproliferative effects against pancreatic cancer in vitro and in vivo. *Journal of Gastrointestinal Surgery* **2012,** *16*, 1136-1143.

130. Pan, M.-H.; Chang, Y.-H.; Badmaev, V.; Nagabhushanam, K.; Ho, C.-T., Pterostilbene induces apoptosis and cell cycle arrest in human gastric carcinoma cells. *J. of Agricultural and Food Chemistry* **2007,** *55*, 7777-7785.

131. Chakraborty, A.; Bodipati, N.; Demonacos, M. K.; Peddinti, R.; Ghosh, K.; Roy, P., Long term induction by pterostilbene results in autophagy and cellular differentiation in MCF-7 cells via ROS dependent pathway. *Molecular and cellular endocrinology* **2012,** *355*, 25-40.

132. Bhakkiyalakshmi, E.; Shalini, D.; Sekar, T. V.; Rajaguru, P.; Paulmurugan, R.; Ramkumar, K. M., Therapeutic potential of pterostilbene against pancreatic beta-cell apoptosis mediated through Nrf2. *British journal of pharmacology* **2014,** *171*, 1747-1757.

133. Gomez-Zorita, S.; Fernandez-Quintela, A.; Aguirre, L.; Macarulla, M.; Rimando, A.; Portillo, M., Pterostilbene improves glycaemic control in rats fed an obesogenic diet: involvement of skeletal muscle and liver. *Food & function* **2015**.

134. Satheesh, M. A.; Pari, L., Effect of pterostilbene on lipids and lipid profiles in streptozotocin–nicotinamide induced type 2 diabetes mellitus. *J Appl Biomed* **2008,** *6*,

31-37.

135. Gomez-Zorita, S.; Fernandez-Quintela, A.; Lasa, A.; Aguirre, L.; Rimando, A. M.; Portillo, M. P., Pterostilbene, a Dimethyl Ether Derivative of Resveratrol, Reduces Fat Accumulation in Rats Fed an Obesogenic Diet. *Journal of agricultural and food chemistry* **2014,** *62*, 8371-8378.

136. Rimando, A. M.; Khan, S. I.; Mizuno, C. S.; Ren, G.; Mathews, S. T.; Kim, H.; Yokoyama, W., Evaluation of PPARα activation by known blueberry constituents. *Journal of the science of food and agriculture* **2015**.

137. Kapetanovic, I. M.; Muzzio, M.; Huang, Z.; Thompson, T. N.; McCormick, D. L., Pharmacokinetics, oral bioavailability, and metabolic profile of resveratrol and its dimethylether analog, pterostilbene, in rats. *Cancer chemotherapy and pharmacology* **2011,** *68*, 593-601.

138. Perečko, T.; Drábiková, K.; Račková, L.; Číž, M.; Podborská, M.; Lojek, A.; Harmatha, J.; Šmidrkal, J.; Nosál, R.; Jančinová, V., Molecular targets of the natural antioxidant pterostilbene: effect on protein kinase C, caspase-3 and apoptosis in human neutrophils in vitro. *Neuroendocrinology Letters* **2010,** *31*, 84.

139. Alarcón de la Lastra, C.; Villegas, I., Resveratrol as an anti-inflammatory and anti-aging agent: Mechanisms and clinical implications. *Molecular nutrition & food research* **2005,** *49*, 405-430.

140. Chiou, Y.-S.; Tsai, M.-L.; Nagabhushanam, K.; Wang, Y.-J.; Wu, C.-H.; Ho, C.-T.; Pan, M.-H., Pterostilbene is more potent than resveratrol in preventing azoxymethane (AOM)-induced colon tumorigenesis via activation of the NF-E2-related factor 2 (Nrf2)-mediated antioxidant signaling pathway. *Journal of agricultural and food chemistry* **2011,** *59*, 2725-2733.

141. Nutakul, W.; Sobers, H. S.; Qiu, P.; Dong, P.; Decker, E. A.; McClements, D. J.; Xiao, H., Inhibitory effects of resveratrol and pterostilbene on human colon cancer cells: a side-by-side comparison. *Journal of agricultural and food chemistry* **2011,** *59*, 10964-10970.

142. Ma, Z.-j.; Li, X.; Li, N.; Wang, J.-h., Stilbenes from Sphaerophysa salsula. *Fitoterapia* **2002,** *73*, 313-315.

143. Takemoto, J. K.; Davies, N. M., A high-performance liquid chromatographic analysis and preliminary pharmacokinetic characterization of 3'-hydroxypterostilbene in rats. *Biomedical chromatography : BMC* **2009,** *23*, 1086-91.

144. Spierings, D.; McStay, G.; Saleh, M.; Bender, C.; Chipuk, J.; Maurer, U.; Green, D. R., Connected to death: the (unexpurgated) mitochondrial pathway of apoptosis. *Science* **2005,** *310*, 66-67.

145. Shin, J. Y.; Hong, S.-H.; Kang, B.; Minai-Tehrani, A.; Cho, M.-H., Overexpression of beclin1 induced autophagy and apoptosis in lungs of K-rasLA1 mice. *Lung cancer (Amsterdam, Netherlands)* **2013,** *81*, 362-370.

146. Liang, C.; Feng, P.; Ku, B.; Dotan, I.; Canaani, D.; Oh, B.-H.; Jung, J. U., Autophagic and tumour suppressor activity of a novel Beclin1-binding protein UVRAG. *Nature cell biology* **2006,** *8*, 688-698.

147. Yue, Z.; Jin, S.; Yang, C.; Levine, A. J.; Heintz, N., Beclin 1, an autophagy gene essential for early embryonic development, is a haploinsufficient tumor suppressor. *Proceedings of the National Academy of Sciences* **2003,** *100*, 15077-15082.

148. Mizushima, N., Methods for monitoring autophagy. *The international journal of biochemistry & cell biology* **2004,** *36*, 2491-2502.

149. Kang, R.; Zeh, H.; Lotze, M.; Tang, D., The Beclin 1 network regulates autophagy and apoptosis. *Cell Death & Differentiation* **2011,** *18*, 571-580.

150. CAI, Y.-J.; WEI, Q.-Y.; FANG, J.-G.; YANG, L.; LIU, Z.-L.; WYCHE, J. H.; HAN, Z., The 3, 4-dihydroxyl groups are important for trans-resveratrol analogs to exhibit enhanced antioxidant and apoptotic activities. *Anticancer research* **2004,** *24*, 999-1002.

151. Gigante, B.; Santos, C.; Silva, A.; Curto, M.; Nascimento, M.; Pinto, E.; Pedro, M.; Cerqueira, F.; Pinto, M.; Duarte, M., Catechols from abietic acid: synthesis and evaluation as bioactive compounds. *Bioorganic & medicinal chemistry* **2003,** *11*,

1631-1638.

152. Liang, X. H.; Jackson, S.; Seaman, M.; Brown, K.; Kempkes, B.; Hibshoosh, H.; Levine, B., Induction of autophagy and inhibition of tumorigenesis by beclin 1. *Nature* **1999,** *402*, 672-676.

153. Liang, X. H.; Yu, J.; Brown, K.; Levine, B., Beclin 1 contains a leucine-rich nuclear export signal that is required for its autophagy and tumor suppressor function. *Cancer research* **2001,** *61*, 3443-3449.

154. Qu, X.; Yu, J.; Bhagat, G.; Furuya, N.; Hibshoosh, H.; Troxel, A.; Rosen, J.; Eskelinen, E.-L.; Mizushima, N.; Ohsumi, Y., Promotion of tumorigenesis by heterozygous disruption of the< i> beclin 1</i> autophagy gene. *The Journal of clinical investigation* **2003,** *112*, 1809-1820.

APPENDIX: LIST OF ABBREVIATIONS

ACS	American Cancer Society
AJCC	American Joint Committee on Cancer
AMACR	α -Methylacyl-CoA Recemase
AMPK	AMP-Activated Protein Kinase
APAF-1	Apoptotic Protease Activating Factor-1
Beclin-1-C	C-terminal of Beclin-1 Fragment
CAD	Caspase-Activated DNAse
DAPI	40,6-Diamidino-2-Phenylindole
DRAM	Damage-Regulated Autophagy Modulator
Deptor	DEP-Domain Containing mTOR-Interacting Protein
DMSO	Dimethyl Sulfoxide
EDTA	Trypsin-Ethylenediaminetetraacetic Acid
FBS	Fetal Bovine Serum
FIP200	Focal Adhesion Kinase Family Interacting Protein of 200 kDa
GβL	G-Protein Beta-Subunit-Like Protein
HDL	High Density Lipoprotein
IGF-1	Insulin-like Growth Factor-1
IUCC	International Union for Cancer Control
LDL	Low Density Lipoprotein
MMP	Matrix Metalloproteinase 9
MOMP	Mitochondrial Outer Membrane Permeabilization

mTORC1	Mammalian Target of Rapamycin Complex 1
MTT	3-(4,5-Dimethylthiazol-2-yl)-2,5-diphenyltetrazolium bromide
Nrf-2	NF-E2-related factor 2
OHPt	3'-Hydroxypterostilbene
PCD	Programmed Cell Death
PE	Phosphatidylethanolamine
PI	Propidiumiodide
PI3K	Phosphatidylinositol-3-Kinase
PI3P	Phosphatidylinositol-3-Phosphate
PRAS40	Proline-Rich AKT Substrate 40 kDa
PSA	Prostate-Specific Antigen
Pt	Pterostilbene
Raptor	Regulatory-Associated Protein of mTOR
SD	Standard Deviation
SDS	Sodiumdodecylsulfate
tBid	Truncated Bid
TNF-R	Tumor Necrosis Factor-α Receptor
TSC	Tuberous Sclerosis Complex
ULK1/2	Unc-51-Like Kinases 1/2
XIAP	X-linked Inhibitor of Apoptosis Protein